

Aus der Klinik und Poliklinik im Dr. von Haunerschen Kinderspital  
der Ludwig-Maximilians-Universität München  
Direktor:

Professor Dr. med. Dr. sci. nat. C. Klein

Funktion und Fehlfunktion der Phenylalaninhydroxylase  
in Abhängigkeit von Genotyp, metabolischem Status und Therapie  
mit dem pharmakologischen Chaperon Tetrahydrobiopterin

Dissertation  
zum Erwerb des Doktorgrades der Medizin  
an der Medizinischen Fakultät der  
Ludwig-Maximilians-Universität zu München

vorgelegt von  
Michael Staudigl  
aus  
München  
2012

Mit Genehmigung der Medizinischen Fakultät  
der Universität München

Berichterstatter: Prof. Dr. med. Ania C. Muntau

Mitberichterstatter: Priv. Doz. Dr. Dejana Mokranjac  
Prof. Dr. Klaus Parhofer  
Priv. Doz. Dr. Tim Strom

Mitbetreuung durch den  
promovierten Mitarbeiter: Dr. med. Søren W. Gersting

Dekan: Prof. Dr. med. Dr. h.c. M. Reiser, FACR, FRCR

Tag der mündlichen Prüfung: 08.11.2012

## Inhaltsverzeichnis

1. Einleitung	
1.1. Phenylketonurie und Defekt der Phenylalaninhydroxylase	4
1.2. Die Biochemie des Phenylalanin-Stoffwechsels	5
1.3. Enzymatische Funktion und Struktur der Phenylalaninhydroxylase	6
1.4. Molekulare Mechanismen des Funktionsverlustes der PAH	8
1.5. Bestimmung der Phenylalaninhydroxylase-Aktivität – Stand der Forschung	9
2. Ziele der Arbeit	10
3. Ergebnisse eigener wissenschaftlicher Arbeiten	
3.1. Arbeiten zur kumulativen Promotionsleistung	10
3.2. Zusätzliche Arbeiten, die im Rahmen der Promotionsarbeit entstanden sind	14
4. Schlussbetrachtungen und Ausblick	15
5. Zusammenfassung	17
6. Summary	18
7. Literaturverzeichnis	19
8. Sonderdrucke der Publikationen im Rahmen der Promotionsarbeit	22
9. Danksagung	66
10. Lebenslauf	67

## 1. Einleitung

### 1.1. Phenylketonurie und Defekt der Phenylalaninhydroxylase

Die Phenylketonurie (PKU; OMIM #261600) ist mit einer Inzidenz von 1:5.062 (Nennstiel-Ratzel, U *et al.* 2010) bis heute die häufigste Aminosäure-Stoffwechselstörung der europäisch abstammenden Bevölkerung (Zschocke, J 2003). Der Erkrankung liegt eine Störung der Hydroxylierungsreaktion der essentiellen Aminosäure Phenylalanin zu Tyrosin durch die Phenylalaninhydroxylase (PAH) zu Grunde. Bereits in den 30er Jahren des vergangenen Jahrhunderts konnte Dr. Asbjørn Følling durch eine einfache Methode zum Nachweis von Ketonkörpern im Urin bei Patienten mit mentaler Entwicklungsretardierung das Ausscheidungsprodukt Phenylbrenztraubensäure nachweisen (Følling, A 1934). Hiermit wurde nicht nur eine Veränderung im Phenylalaninstoffwechsel, sondern auch die Ursache der mentalen Retardierung dieser Patienten aufgeklärt und damit die Phenylketonurie entdeckt (Jervis, GA 1953). Unbehandelt äußert sich die Erkrankung in schweren neurologischen Störungen mit psychomotorischer Retardierung, Intelligenzverlust und Autoaggression. Dr. Horst Bickel konnte 1952 zeigen, dass die Durchführung einer streng phenylalaninarmen Diät zu einer Besserung der Symptome, bzw. bei präsymptomatischer Durchführung zu einem Ausbleiben des Intelligenzverlustes führt (Bickel, H *et al.* 1953; Bickel, H *et al.* 1954). Aus dieser Beobachtung entstand die Idee zur Entwicklung einer Neugeborenenreihenuntersuchung zur Identifikation von Patienten mit Phenylketonurie bereits in den ersten Lebenstagen. Diese wurde in den 60er Jahren umgesetzt, als Dr. Robert Guthrie auf der Basis eines bakteriologischen Hemmtestes eine einfache, universell anwendbare Methode zum Nachweis erhöhter Phenylalaninkonzentrationen im Blut entwickelte. Seither gilt die Phenylketonurie als der Prototyp einer behandelbaren genetischen Erkrankung (Muntau, AC *et al.* 2010).

Zwei Formen der Phenylketonurie werden unterschieden. 98 % der Patienten mit Hyperphenylalaninämie tragen eine Mutation im *Phenylalaninhydroxylase (PAH)*-Gen. In 2 % der Fälle liegt der Hyperphenylalaninämie ein Defekt der Biosynthese oder der Regeneration des natürlichen Kofaktors der PAH, 6*R*-L-erythro-5,6,7,8-tetrahydrobiopterin (BH<sub>4</sub>), zu Grunde (atypische Phenylketonurie) (Thöny, B *et al.* 2000; Scriver, CR *et al.* 2001).

Heute sind 627 verschiedene krankheitsverursachende Mutationen im *PAH*-Gen bekannt ([www.pahdb.mcgill.ca](http://www.pahdb.mcgill.ca), [www.hgmd.org](http://www.hgmd.org)) (Scriver, CR *et al.* 2000). Bei 80 % dieser Mutationen handelt es sich um *missense* Mutationen, darüber hinaus wurden Deletionen, Insertionen, Stop-Mutationen, Splicing Varianten und Intron-Mutationen identifiziert. Die daraus resultierenden klinischen Phänotypen der Erkrankung werden auf der Grundlage der prätherapeutischen Phenylalaninkonzentrationen im Blut klassifiziert (Empfehlungen der Arbeitsgemeinschaft für Pädiatrische Stoffwechselerkrankungen (APS)): i) Klassische Phenylketonurie (> 1200 µmol/l), ii) Milde Phenylketonurie (600-1200 µmol/l) und iii) Milde Hyperphenylalaninämie (120-600 µmol/l). Aus dieser Einteilung resultieren therapeutische Empfehlungen. Während Patienten mit einer Phenylalaninkonzentration im Blut > 600 µmol/l, also einer milden oder klassischen Form der Phenylketonurie, lebensbegleitend eine streng phenylalaninarme Diät einhalten müssen, um Intelligenzeinbußen und das Auftreten neurologischer Symptome zu verhindern, können Patienten mit Milder Hyperphenylalaninämie auf eine eiweißarme Diät verzichten (Weglage, J *et al.* 2001). Etwa 69 % aller Patienten in Deutschland sind Träger von Mutationen, die zu einer der beiden mildereren Formen der Erkrankung führen.

Im Jahr 1999 machte die Arbeitsgruppe um Kure *et al.* eine interessante Entdeckung. Pharmakologische Konzentrationen des natürlichen Kofaktors der Phenylalaninhydroxylase,

BH<sub>4</sub>, führten bei vier Patienten mit Mutationen im *PAH*-Gen ohne Mangel des Kofaktors BH<sub>4</sub> zu einer Reduktion der Phenylalaninkonzentration im Blut (Kure, S *et al.* 1999). Weitere Studien haben gezeigt, dass BH<sub>4</sub> bei Patienten mit milderer Formen der PAH-Defizienz die Phenylalaninkonzentration im Blut senkt, die Enzymaktivität *in vivo* steigert und die diätetische Eiweißtoleranz deutlich erhöht (Muntau, AC *et al.* 2002). Damit wurde ein neuer klinischer Phänotyp der Phenylketonurie, der BH<sub>4</sub>-responsive Defekt der PAH, definiert. Im Rahmen weiterer klinischer Studien konnten Wirksamkeit und Sicherheit des Kofaktors nachgewiesen werden (Levy, HL *et al.* 2007; Lee, P *et al.* 2008; Trefz, FK *et al.* 2009) und 2007 (FDA) und 2008 (EMA) wurde Sapropterindihydrochlorid, die synthetisch hergestellte Form des Kofaktors, als *orphan drug* zur Therapie der Phenylketonurie durch BH<sub>4</sub>-responsiven Defekt der PAH zugelassen (Muntau, AC *et al.* 2002; Levy, HL *et al.* 2007; Trefz, FK *et al.* 2009).

## 1.2. Die Biochemie des Phenylalanin-Stoffwechsels

Phenylalanin ist eine essentielle Aminosäure im menschlichen Stoffwechsel. Die aromatische Aminosäure wird über eiweißhaltige Nahrungsmittel aufgenommen. Im weiteren Stoffwechsel wird Phenylalanin zur aromatische Aminosäure Tyrosin hydroxyliert, die zur Bildung des biogenen Amins Dopamin und der Katecholamine Noradrenalin und Adrenalin benötigt wird. Außerdem wird Tyrosin zur weiteren Synthese des Hautpigments Melanin benötigt (Abb. 1).

Abb. 1.

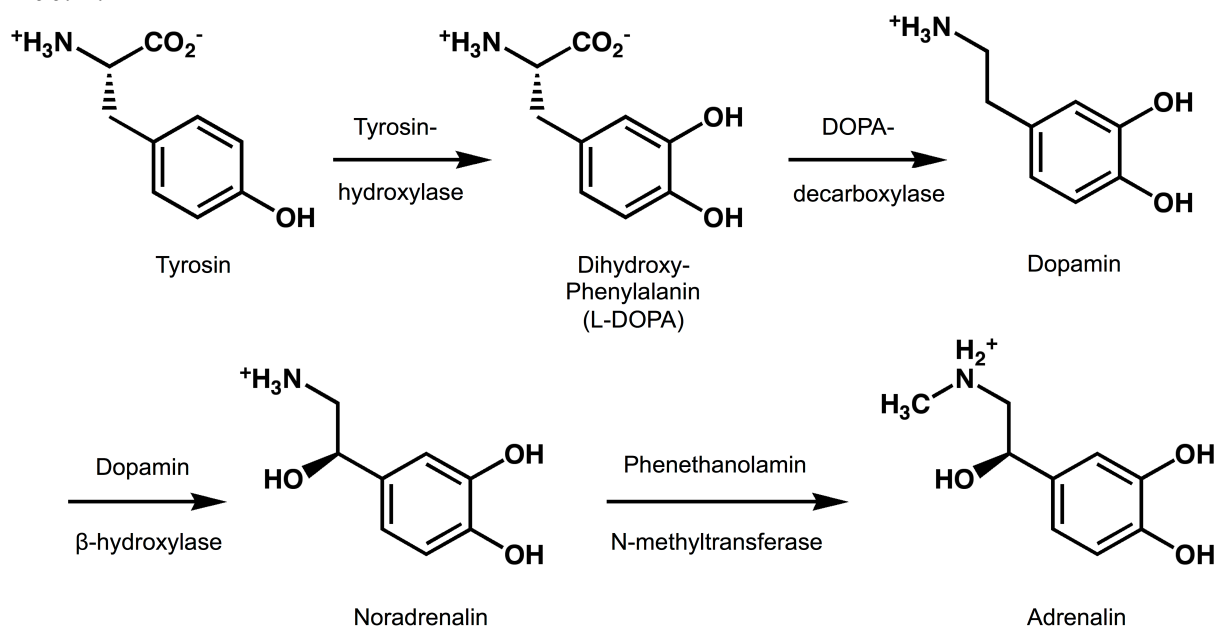


Abb. 1. Tyrosin wird in weiteren enzymatisch katalysierten Reaktionen zu Melanin und dem biogenen Amin Dopamin und der Katecholamine Noradrenalin und Adrenalin verstoffwechselt.

Die Hydroxylierungsreaktion von Phenylalanin zu Tyrosin wird durch die Phenylalaninhydroxylase katalysiert und ist der geschwindigkeitsbestimmende Schritt im Phenylalanin-Metabolismus. Dabei werden ca. 75 % des durch die Nahrung und des Protein-Katabolismus zur Verfügung gestellten Phenylalanins umgesetzt. Für diese Reaktion werden der natürliche Kofaktor BH<sub>4</sub> sowie molekularer Sauerstoff benötigt (Abb. 2).

Abb. 2.

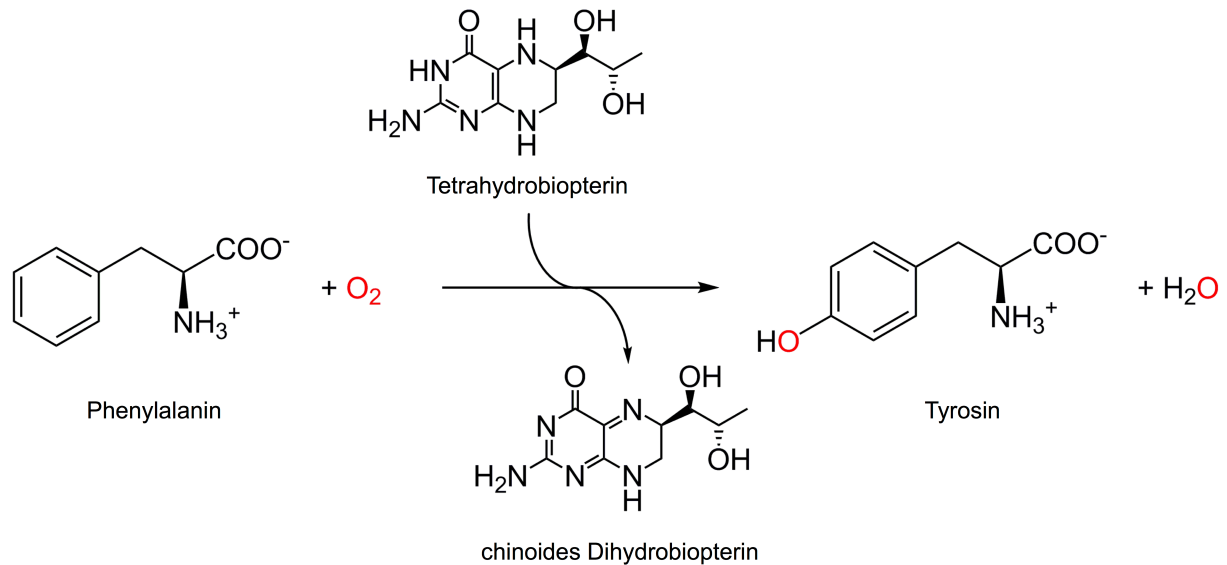


Abb. 2. Die Phenylalaninhydroxylase katalysiert die Hydroxylierung von Phenylalanin zu Tyrosin. Für diese Reaktion wird der natürliche Kofaktor Tetrahydrobiopterin ( $\text{BH}_4$ ) sowie molekularer Sauerstoff benötigt.

Eine Aktivitätsminderung des Enzyms PAH führt einerseits zum Anstieg der Phenylalaninkonzentration im Blut, andererseits zu Symptomen des Tyrosin- und Melaninmangels. Daraus ergeben sich die mit der Erkrankung assoziierten Symptome mit heller Hautfarbe, mentaler und motorischer Entwicklungsretardierung, sowie Autoaggressionen. Im Rahmen der Phenylketonurie wird Tyrosin zur essentiellen Aminosäure.

### 1.3 Enzymatische Funktion und Struktur der Phenylalaninhydroxylase

Die Phenylalaninhydroxylase ist im Zytosol der Zelle lokalisiert und wird vorwiegend in der Leber sowie, in weit geringerem Ausmaß, auch in der Niere exprimiert. Sie gehört mit der Tyrosin- und Tryptophanhydroxylase zur Familie der aromatischen Aminosäurehydroxylasen (Udenfriend, S *et al.* 1952; Fitzpatrick, PF 2000). Hierbei handelt es sich um so genannte Monooxygenasen, die molekularen Sauerstoff zur Durchführung der katalytischen Reaktion benötigen (Kaufman, S *et al.* 1962). Die PAH ist ein eisenabhängiges Enzym. Wie bei allen aromatischen Aminosäurehydroxylasen ist das Eisen-Atom nicht an einen heterozyklischen Porphyrinring gebunden. Während der Hydroxylierungsreaktion wird  $\text{Fe}^{3+}$  zu  $\text{Fe}^{2+}$  reduziert. Die für diese Reaktion benötigten Elektronen werden von  $\text{BH}_4$  zur Verfügung gestellt, wobei ein Elektron zur Reduktion von Eisen und ein weiteres zur Bildung von Wasser aus Sauerstoff benötigt wird.

Im Rahmen der Hydroxylierungsreaktion wird der Kofaktor der PAH  $\text{BH}_4$  zu Dihydrobiopterin ( $\text{BH}_2$ ) oxidiert. An der Regeneration des Kofaktors sind die Enzyme Pterin-Carbinolamin-Dehydratase (PCD) und Dihydropteridin-Reduktase (DHPR) beteiligt (Thöny, B *et al.* 2000; Werner, ER *et al.* 2011)(Abb. 3). Bei mangelnder DHPR-Aktivität wird chinoides Dihydrobiopterin nicht-enzymatisch zu 7,8-Dihydrobiopterin umgewandelt, ein Substrat der Dihydrofolat-Reduktase (DHFR).

Abb. 3.

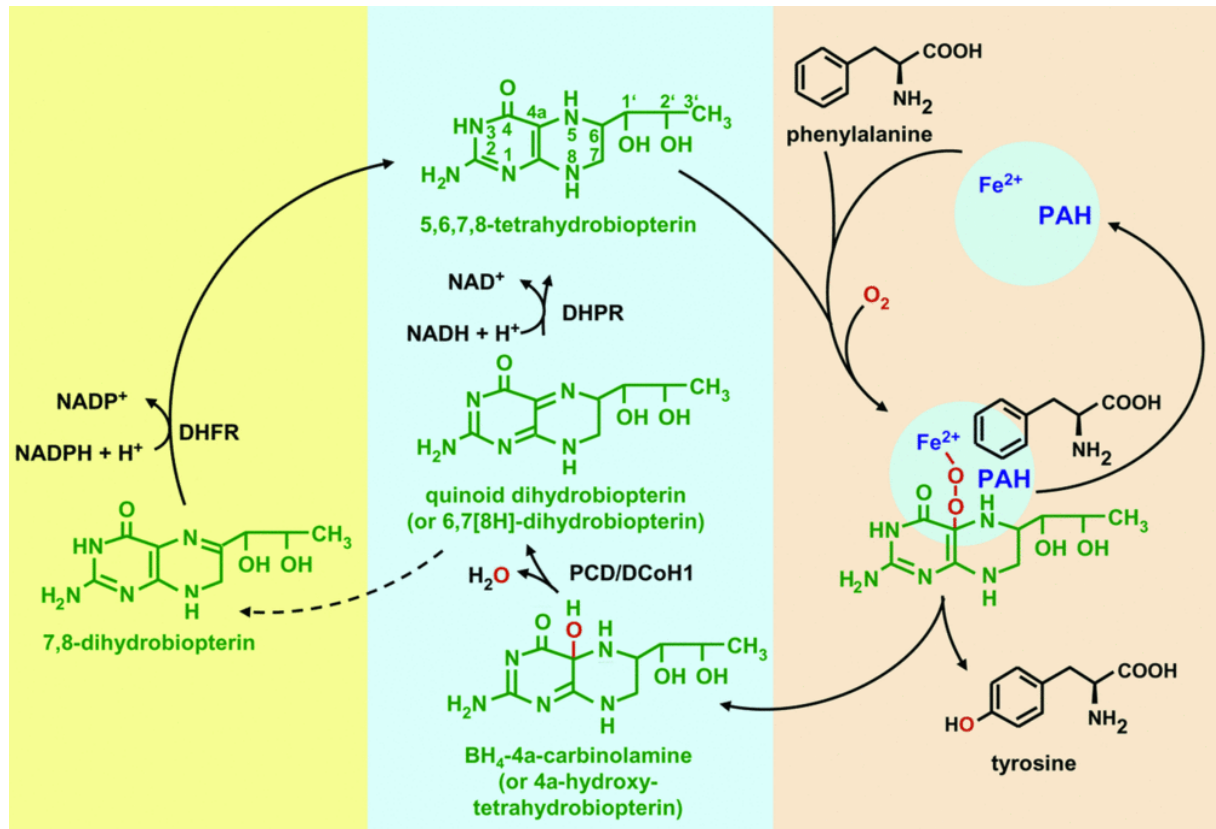
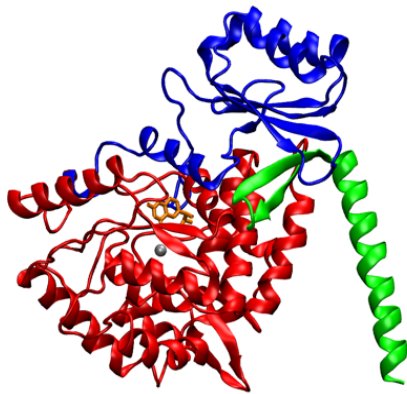


Abb. 3. 5,6,7,8-Tetrahydrobiopterin (BH<sub>4</sub>), der natürliche Kofaktor der PAH, wird im Rahmen der Hydroxylierungsreaktion über 4a-Hydroxy-Tetrahydrobiopterin durch die Pterin-Carbinolamin-Dehydratase (PCD) zu 6,7[8H]-Dihydrobiopterin umgewandelt. Die Dihydropteridin-Reduktase (DHPR) katalysiert die Reduktion von BH<sub>2</sub> in Anwesenheit von NADH/H<sup>+</sup> zu BH<sub>4</sub> (Werner, ER *et al.* 2011). Bei mangelnder DHPR-Aktivität wird chinoides Dihydrobiopterin nicht-enzymatisch zu 7,8-Dihydrobiopterin umgewandelt, ein Substrat der Dihydrofolat-Reduktase (DHFR).

Strukturell handelt es sich bei der PAH um ein Homotetramer, das als Dimer aus Dimeren aufgebaut ist (Kaufman, S 1993) (Abb. 4). Es besteht ein Fließgleichgewicht zwischen Homodimer und Homotetramer in einem Verhältnis von etwa 2/8 (Kappock, TJ *et al.* 1995). Das einzelne Monomer hat eine Größe von 52 kDa und besitzt drei funktionelle Domänen: eine N-terminal lokalisierte regulatorische Domäne (Aminosäuren 1-142), eine katalytische Domäne (Aminosäuren 143-410) mit den Bindungsstellen für Phenylalanin und BH<sub>4</sub> sowie eine Oligomerisierungsdomäne (Aminosäuren 411-452). Strukturelle Untersuchungen haben gezeigt, dass zwischen den einzelnen Untereinheiten und Domänen ein hohes Maß an strukturellen Interaktionen besteht (Erlandsen, H *et al.* 1997; Fusetti, F *et al.* 1998; Kobe, B *et al.* 1999).

Abb. 4A



4B

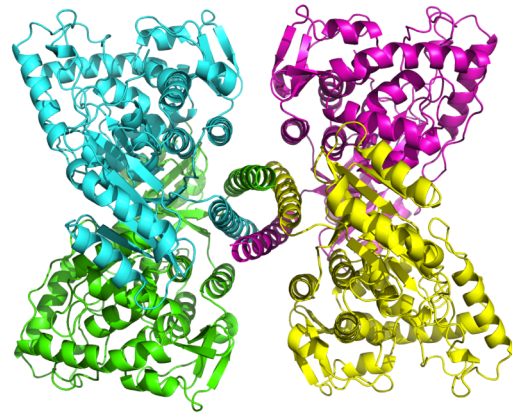


Abb. 4. Die PAH als Monomer und Tetramer. A, Das Monomer hat eine Größe von 52 kDa und besitzt drei funktionelle Domänen: eine N-terminal lokalisierte regulatorische Domäne (Aminosäuren 1-142, blau), eine katalytische Domäne (Aminosäuren 143-410, rot) mit den Bindungsstellen für Phenylalanin und  $\text{BH}_4$  (gelb) sowie eine Oligomerisierungsdomäne (Aminosäuren 411-452, grün) (Erlandsen, H *et al.* 1997). B, Die funktionelle PAH ist ein Tetramer zusammengesetzt aus vier einzelnen Monomeren, ein sogenanntes Dimer aus Dimeren (hellblau und grün sowie magenta und gelb).

Die PAH wird komplex reguliert. Dabei ist die katalytische Aktivität des Enzyms einerseits von Phosphorylierungsreaktionen, andererseits von der Bindung des Substrats und des natürlichen Kofaktors abhängig (Shiman, R *et al.* 1994; Shiman, R *et al.* 1994; Xia, T *et al.* 1994). Die Phosphorylierung des Enzyms an der Position Ser16 der regulatorischen Domäne wird u.a. über cAMP-abhängige Proteinkinasen gesteuert, wodurch die Aktivität auf das Dreifache gesteigert werden kann (Abita, JP *et al.* 1976). Während die Bindung des Substrats Phenylalanin an das Enzym zu einer Aktivierung führt, bewirkt die Bindung des natürlichen Kofaktors  $\text{BH}_4$  die Bildung eines inaktiven PAH- $\text{BH}_4$ -Komplexes (Shiman, R *et al.* 1980; Shiman, R *et al.* 1982; Shiman, R *et al.* 1990; Mitnaul, LJ *et al.* 1995). Es ist bekannt, dass die Bindung des Substrats zu konformationellen Veränderungen über das gesamte Enzym führt, die Orientierung und Position von gebundenem  $\text{BH}_4$  (Andersen, OA *et al.* 2002, Andersen, OA *et al.* 2003) und der regulatorischen Domäne verändern (Stokka, AJ *et al.* 2004).  $\text{BH}_4$  dagegen interagiert mit der N-terminalen autoregulatorischen Sequenz und der so genannten *pterin binding loop*, um einen binären Enzym- $\text{BH}_4$ -Komplex zu bilden (Solstad, T *et al.* 2003). All diese regulatorischen Mechanismen benötigen ein sehr flexibles Enzym und reversible konformationelle Veränderungen, die über das gesamte Enzym kommuniziert werden (Gersting, SW *et al.* 2010).

#### 1.4 Molekulare Mechanismen des Funktionsverlustes der PAH

Die Entdeckung des neuen klinischen Phänotyps des  $\text{BH}_4$ -responsiven PAH Defektes, bei dem pharmakologische Konzentrationen des natürlichen Kofaktors des defekten Enzyms die Phenylalaninkonzentration im Blut reduzieren und die Enzymaktivität normalisieren (Muntau, AC *et al.* 2002), führte zu einem Paradigmenwechsel in Bezug auf die klassische Sichtweise behandelbarer vererbbarer Stoffwechselerkrankungen und den damit verbundenen Funktionsverlust von Proteinen. Zum Zeitpunkt der Zulassung von Sapropterindihydrochlorid als orphan drug war die Wirksamkeit im Menschen zwar gut belegt, der Wirkmechanismus des neuen Medikamentes jedoch noch nicht verstanden.

Frühe Untersuchungen haben gezeigt, dass Mutationen im *PAH*-Gen zu Störungen der Oligomerisierung und zu einem beschleunigten Abbau varianter *PAH*-Proteine führen können (Knappskog, PM *et al.* 1996; Bjørge, E *et al.* 1998; Waters, PJ *et al.* 1998; Waters, PJ *et al.* 2000; Erlandsen, H *et al.* 2004; Pey, AL *et al.* 2004). Diese Beobachtungen führten zu der Hypothese, dass die Wirkungsweise des Kofaktors in einer Korrektur der Proteinehlfaltung liegt und der Kofaktor somit als Pharmakologisches Chaperon die *PAH* stabilisiert. (Muntau, AC *et al.* 2002; Waters, PJ 2003; Erlandsen, H *et al.* 2004; Pey, AL *et al.* 2004). Eines der Ziele unserer Arbeitsgruppe bestand daher darin, den molekularen Mechanismus des Funktionsverlusts der *PAH* und die strukturellen Konsequenzen von *missense* Mutationen im *PAH*-Gen zu untersuchen, um so die Grundlagen für die Erforschung des Wirkmechanismus von  $BH_4$  als Pharmakologisches Chaperon zu legen.

### **1.5. Bestimmung der Phenylalaninhydroxylase-Aktivität – Stand der Forschung**

Zur Bestimmung der *PAH*-Enzymaktivität stehen verschiedene Methoden zur Verfügung, die zumeist eine flüssigchromatographische Trennung des Substrats Phenylalanin vom Produkt Tyrosin erforderlich machen. Anschließend wird das Produkt über Radioaktivität oder Fluoreszenz detektiert. Ein anderer Ansatz detektiert die Oxidation von NADH bei der Regeneration des oxidierten Kofaktors durch Dihydropteridinreduktase und ist somit eine indirekte Methode (Andersen, OA *et al.* 2003). In der Annahme, dass hier sowohl Substrat und Kofaktor bei der Katalyse als auch Kofaktor und NAD bei der Kofaktorregeneration in stöchiometrischen Verhältnissen umgesetzt werden, kann aus dem NADH-Verbrauch auf die Tyrosinproduktion geschlossen werden. Insgesamt sind die bisher verfügbaren Messmethoden zeitraubend und ineffizient. Darüber hinaus verfolgen die meisten Methoden einen diskontinuierlichen Messansatz, d.h. Endpunktmessungen. Voraussetzung dafür ist, dass eine Reaktion über einen bestimmten Zeitraum stets linear verläuft. Üblicherweise ist dies bis zu einem Verbrauch von 10 % des eingesetzten Substrats gewährleistet. Durch Veränderungen der experimentellen Bedingungen, z.B. der Substratkonzentration, der Temperatur oder des pH-Wertes, kann die Dauer des linearen Reaktionsmechanismus jedoch variieren (Copeland, RA 2000).

Die Standardmethode zur Bestimmung der Aktivität rekombinanter *PAH* ist ein diskontinuierliches Messverfahren, bei der die Enzymaktivität der *PAH* über eine Minute bei verschiedenen Phenylalaninkonzentrationen und einer  $BH_4$ -Konzentration sowie einer Phenylalanin- und verschiedenen  $BH_4$ -Konzentrationen bestimmt wird. Bei der Analyse von Proben aus kultivierten Zellen oder Organen wird die Reaktionszeit des Versuchs auf 30-60 Minuten ausgeweitet. Nach Ablauf der Reaktionszeit werden Substrat und Produkt über Flüssigchromatographie (High Performance Liquid Chromatography, HPLC) getrennt, anschließend wird das Produkt mittels Fluoreszenz bei einer Exzitationswellenlänge von 275 nm und einer Emissionswellenlänge von 305 nm detektiert (Martinez, A *et al.* 1995; Miranda, FF *et al.* 2002). Diese Methode setzt jedoch voraus, dass die Reaktion auch unter veränderten Versuchsbedingungen mit Variation der Substrat- und Kofaktorkonzentrationen stets linear verläuft.

## 2. Ziele der Arbeit

Eingehende Kenntnisse zur enzymatischen Funktion der PAH bei unterschiedlichen Substrat- und Kofaktorkonzentrationen sind eine wichtige Voraussetzung für das Verständnis des fehlfaltungsbedingten Funktionsverlustes der PAH einerseits und der pharmakologischen Korrektur der Enzymfunktion andererseits. Im Rahmen der durchgeführten Arbeiten sollte zunächst ein Standard-Aktivitätstest in unserer Arbeitsgruppe etabliert werden, um die enzymkinetischen Parameter der PAH bestimmen zu können. Diese umfassen die Aktivität ( $V_{max}$ ), die Affinität von Substrat und Kofaktor ( $S_{0.5}$  bzw.  $K_m$ ), die Kooperativität ( $h$ ), die Substrataktivierung und die Substratinhibition. Mit diesem Verfahren sollte die Enzymaktivität rekombinant exprimierter und gereinigter Wildtyp-PAH und varianter PAH Proteine bestimmt werden, um den Einfluss von *missense* Mutationen auf die Parameter der spezifischen Aktivität zu untersuchen. In einem nächsten Schritt sollte eine neue fluoreszenzbaasierte Methode etabliert werden, die eine direkte kontinuierliche Messung der Enzymaktivität erlaubt. So sollte die PAH-Aktivität bei einem erheblich größeren Bereich an Substrat- und Kofaktorkonzentrationen als bisher bestimmt werden, um den optimalen Arbeitsbereich des rekombinanten Proteins zu vermessen und den wechselseitigen Einfluss von Substrat (aktivierend) und Kofaktor (inhibierend) zu analysieren. Darüber hinaus sollten das Bindungsverhalten des Enzyms gegenüber dem Kofaktor bei verschiedenen Substratkonzentrationen und somit der Einfluss des metabolischen Status auf die Wirkung des pharmakologischen Chaperons  $BH_4$  untersucht werden. Die an rekombinanten PAH-Proteinen erhobenen Ergebnisse sollten in einem weiteren Schritt mit Ergebnissen der Enzymaktivität nach stabiler Expression des Wildtyps und varianter PAH-Proteine in einem eukaryoten Zellkultursystem unter dem Einfluss verschiedener Substrat- und Kofaktorkonzentrationen verglichen und so der Einfluss auf die Menge funktionell aktiver PAH bestimmt werden. Schließlich sollten die gewonnenen Erkenntnisse durch Vergleich mit Daten aus  $BH_4$ -Belastungstest am Patienten in das humane System übersetzt werden, um so den Einfluss von Genotyp und physiologischem bzw. pathologischem metabolischen Status auf die therapeutische Kofaktorwirkung *in vivo* untersuchen zu können.

## 3. Ergebnisse eigener wissenschaftlicher Arbeiten

### 3.1 Arbeiten zur kumulativen Promotionsleistung

Gersting, S. W., Kemter, K. F., **Staudigl, M.**, Messing, D. D., Danecka, M. K., Lagler, F. B., Sommerhoff, C. P., Roscher, A. A. and Muntau, A. C. (2008) Loss of function in phenylketonuria is caused by impaired molecular motions and conformational instability. *American Journal of Human Genetics* 83(1): 5-17

In dieser ersten Arbeit wurden die molekularen Auswirkungen von Mutationen im *PAH*-Gen auf Struktur und Funktion des rekombinanten PAH-Proteins eingehend untersucht. Das experimentelle Vorgehen umfasste die rekombinante Expression und Reinigung der PAH sowie die anschließende Analyse von Struktur, Stabilität und Funktion mittels biophysikalischer und biochemischer Methoden. Die PAH ist ein Homotetramer, das durch Bindung von Substrat und Kofaktor komplex reguliert wird (Mitnau, LJ *et al.* 1995). Die Untereinheiten können in drei funktionelle Domänen eingeteilt werden: regulatorische Domäne (Aminosäuren 1-142), katalytische Domäne (143-410) und Oligomerisierungsdomäne (411-452). Es wurden 10 *missense* Mutationen im *PAH*-Gen ausgewählt, die bei Patienten mit einem Ansprechen auf pharmakologische Dosen des  $BH_4$ -Kofaktors identifiziert wurden. Diese Mutationen führen zum Austausch von Aminosäuren in allen drei Domänen.

Die spezifische Restaktivität varianter PAH war im Vergleich zum Wildtyp-Protein in 6 von 10 Fällen hoch, eine umfassende Charakterisierung der enzymkinetischen Parameter zeigte jedoch Veränderungen der Substrataktivierung und der Kooperativität. Dies deutete bereits auf eine veränderte Konformation mit gestörten molekularen Bewegungen hin. Durch Größenausschlusschromatographie wurden Veränderungen der Quartärstruktur erfasst, wobei sowohl vermehrte Aggregation als auch Störungen im Aufbau des Tetramers beobachtet wurden. Bemerkenswert war, dass auch eine Mutation, welche die N-terminale regulatorische Domäne betrifft, zu einer gestörten Oligomerisierung führte, obwohl eine deutliche räumliche Trennung zu Strukturen vorliegt, die dieser Funktion zugeordnet werden. Bei 4 der varianten Enzyme zeigte sich eine reduzierte proteolytische Stabilität gegen Proteinase K, die als nicht sequenzspezifische Protease bevorzugt entfaltete strukturelle Bereiche angreift. Bei der Untersuchung der thermalen Stabilität mittels *differential scanning fluorimetry* zeigten 5 Varianten eine beschleunigte Entfaltung der regulatorischen Domäne. Der Einfluss von thermalem Stress auf die Enzymfunktion wurde im Rahmen thermaler Inaktivierungsexperimente untersucht. Hier zeigten sich weniger stark ausgeprägte Effekte. Auffällig war jedoch, dass 2 der 3 Varianten, die eine reduzierte Stabilität aufwiesen, nicht der katalytischen Domäne zugeordnet waren.

Die mit biophysikalischen und biochemischen Methoden erhobenen Daten deuteten auf eine enge strukturelle Vernetzung der drei funktionellen Domänen der PAH hin. Um die beobachteten Fernwirkungen zwischen verschiedenen Domänen strukturell weiter aufzuklären, wurden die Aminosäureseitenketten an den von den Mutationen betroffenen Positionen im 3D-Modell analysiert. Hierbei konnten Netzwerke von Aminosäureseitenketten identifiziert werden, über die eine Fehlfaltung innerhalb des Proteins, teilweise über alle drei Domänen hinweg, kommuniziert werden könnte.

Zusammenfassend konnten wir mit dieser Arbeit Proteinefehlfaltung als Ursache des molekularen Phänotyps bei PKU nachweisen. Dies führte zu der inzwischen international akzeptierten Sichtweise, dass es sich bei der durch *missense* Mutation induzierten Phenylketonurie um eine Proteinfaltungserkrankung mit *loss of function* handelt. Von besonderer Bedeutung war die Erkenntnis, dass lokale Austausch von Aminosäureseitenketten zu globalen Konformationsänderungen führen, die molekulare Bewegungen behindern, die für die enzymologische Funktion des Enzyms essentiell sind.

#### *Eigener Beitrag zum Artikel*

Im Rahmen dieser Publikation wurde zunächst der weltweit eingeführte *state of the art assay* zur Bestimmung der PAH-Aktivität mittels Flüssigkeitschromatographie und Fluoreszenzmessung im eigenen Labor etabliert. In einem weiteren Schritt wurden die Enzymaktivitäten des rekombinant in *E. coli* exprimierten Wildtyp-Proteins und der zehn varianten Proteine bestimmt. Aus den erhobenen Daten erfolgte anschließend eine umfassende enzymkinetische Charakterisierung der PAH Proteine. Schließlich wurden die Ergebnisse in Hinblick auf den Einfluss von *missense* Mutationen auf Aktivität, Konformation und Allosterie des Proteins interpretiert und publiziert.

Gersting, S. W.\*, **Staudigl, M.\***, Truger, M. S., Messing, D. D., Danecka, M. K., Sommerhoff, C. P., Kemter, K. F. and Muntau, A. C. (2010) Activation of phenylalanine hydroxylase induces positive cooperativity toward the natural cofactor. *Journal of Biological Chemistry* 285(40): 30686-30697

\* contributed equally

Die PAH unterliegt einer komplexen Regulierung, bei der das Verhältnis des Substrates L-Phenylalanin zum Kofaktor BH<sub>4</sub> über Aktivierung bzw. Inhibierung die Enzymaktivität steuert (Mitnaul, LJ *et al.* 1995). Bei PKU-Patienten mit PAH-Defekt kommt es zu erhöhten Phenylalaninkonzentrationen im Blut und *iatrogen* durch die Gabe pharmakologischer Dosen des Kofaktors zu Veränderungen der BH<sub>4</sub>-Konzentration. Mit dem Ziel, den wechselseitigen Einfluss von Substrat und Kofaktor auf die Enzymfunktion untersuchen zu können, haben wir einen fluoreszenzbasierten Echtzeit-Enzymaktivitätstest entwickelt und validiert, der einen hohen Durchsatz und damit die gleichzeitige Analyse verschiedener Einflussfaktoren erlaubt. Interessanterweise stellten wir für die kofaktorabhängige Kinetik des über das Substrat aktivierten Enzyms ein kooperatives Verhalten fest, das dem Stand der Wissenschaft widersprach. Durch Analyse von mutationsbedingt präaktivierten natürlichen PAH-Varianten haben wir die konformationelle Umlagerung bei Aktivierung durch das Substrat als strukturelle Voraussetzung der kooperativen Bindung des Kofaktors ermittelt. Damit konnten wir einen Einfluss der Substrataktivierung des PAH-Proteins auf die Affinität zum Kofaktor nachweisen. Diese Ergebnisse sind vor dem Hintergrund, dass PKU-Patienten auch unter einer diätetischen Therapie hochnormale bis erhöhte Phenylalaninkonzentrationen im Blut aufweisen, von Bedeutung. Die Bindung und damit die Wirkung von BH<sub>4</sub> als Pharmakologisches Chaperon ist also vom metabolischen Status abhängig und dieser sollte bei der Findung der optimalen Dosis für den Patienten individuell berücksichtigt werden.

#### *Eigener Beitrag zum Artikel*

Zur Bestimmung des wechselseitigen Einflusses von Substrat und Kofaktor auf die Enzymaktivität der PAH wurde im Rahmen dieser Arbeit eine neue fluoreszenzbasierte Methode zur direkten kontinuierlichen Bestimmung der Enzymaktivität des Wildtyp-Proteins und präaktivierter varianter PAH Proteine entwickelt, etabliert und validiert. Nach Anwendung der Methode erfolgte für das Wildtyp-Protein und präaktivierte variante Proteine eine enzymkinetische Charakterisierung. Dies ermöglichte die Analyse des Bindungsverhaltens des Kofaktors an das Protein und erlaubte zusätzliche Aussagen über strukturelle Unterschiede der Konformationen der PAH unter dem Einfluss von Substrat und Kofaktor. Dabei konnte der Effekt der Substrataktivierung der PAH auf die Affinität zum Kofaktor nachgewiesen werden.

Somit wurde ein wichtiger Beitrag zum Verständnis der Auswirkungen der Bindung von BH<sub>4</sub> unter dem Einfluss von Phenylalanin bzw. dem metabolischen Status auf das PAH-Protein erbracht.

**Staudigl, M.\***, Gersting, S. W.\*, Danecka, M. K., Messing, D. D., Woidy, M., Pinkas, D., Kemter, K. F., Blau, N., and Muntau, A. C. (2011) The interplay between genotype, metabolic state, and cofactor treatment governs phenylalanine hydroxylase function and drug response. *Human Molecular Genetics* 20(13): 2628-2641

*\*contributed equally*

In einer weiteren Arbeit haben wir den wechselseitigen Einfluss von Phenylalanin und BH<sub>4</sub> auf die Funktion der PAH nicht nur am Wildtyp-Protein, sondern auch an PAH-Varianten und im Patienten untersucht. Der neu etablierte Enzymaktivitätstest wurde angewendet, um Substrat- und Kofaktorkonzentrationen simultan innerhalb der Matrix einer 96-well Platte zu variieren. Dabei wurden rekombinant exprimierte Wildtyp- und variante PAH jeweils mit Substrat präaktiviert, anschließend wurden Substrat und Kofaktor in unterschiedlichen Verhältnissen zugegeben. Die bioinformatikgestützte Darstellung der Enzymaktivität als dreidimensionale Funktion von L-Phenylalanin und BH<sub>4</sub> in Form von *activity landscapes* erlaubte eine Bestimmung des optimalen Arbeitsbereichs der PAH. Hierbei zeigte sich, dass variante PAH nicht nur eine Reduktion der Restaktivität aufweist, sondern es auch zu Verschiebungen der für die maximale Aktivität notwendigen Substrat- und Kofaktorkonzentrationen kommen kann. Aus diesen Daten lässt sich die Hypothese ableiten, dass eine individuelle Anpassung des metabolischen Status, d.h. der therapeutisch angestrebten Phenylalaninkonzentration im Blut, die Enzymrestfunktion verbessern kann. Dies konnte für zwei der häufigsten Mutationen, die mit BH<sub>4</sub>-Sensitivität assoziiert sind (R261Q und Y414C), durch die retrospektive Auswertung von BH<sub>4</sub>-Belastungstests am Patienten bestätigt werden. Diese *in vitro* und *in vivo* erhobenen Ergebnisse bilden die Basis für ein Modell, bei dem die Funktion der PAH sowohl vom Genotyp als auch vom metabolischen Status in Bezug auf die Phenylalaninkonzentration im Blut und von der therapeutischen Einstellung der BH<sub>4</sub>-Konzentration abhängt.

Diese Daten sind für den Patienten von Bedeutung, da sie belegen, dass bei unterschiedlichen zugrunde liegenden Mutationen unterschiedliche therapeutisch angestrebte Phenylalaninkonzentrationen und Dosierungen des pharmakologischen Chaperons BH<sub>4</sub> mit einer optimierten Enzymfunktion und damit Stoffwechseleinstellung einhergehen.

#### *Eigener Beitrag zum Artikel*

In dieser Arbeit wurde der neu etablierte Enzymaktivitätstest angewendet und in einem weiteren Schritt automatisiert, um Substrat- und Kofaktorkonzentrationen simultan innerhalb der Matrix einer 96-well Platte zu variieren. Die dabei gemessene Enzymaktivität wurde in Form von *activity landscapes* dargestellt, um die Funktion der PAH im physiologischen und pathologischen Substratbereich sowie im therapeutischen Kontext der Kofaktortherapie zu visualisieren. Dies ermöglichte Aussagen darüber, bei welcher Phenylalaninkonzentration, also bei welchem metabolischen Status und bei welcher BH<sub>4</sub>-Konzentration bzw. bei welcher Dosierung des Pharmakons die optimale Enzymaktivität erreicht werden kann.

Die dabei erhobenen Ergebnisse wurden in zwei unterschiedliche *in vivo* Systeme, ein eukaryotes Zellkultursystem mit stabiler Expression des PAH-Wildtyps und varianter PAH-Proteine und die Situation beim Patienten, übersetzt. Dazu wurden zunächst stabil transfierte Zellen zur Proteinexpression des Wildtyp-Proteins und varianter PAH Proteine hergestellt. Anschließend wurde die Enzymaktivität unter dem Einfluss verschiedener Phenylalanin- und BH<sub>4</sub>-Konzentrationen bestimmt. In einem nächsten Schritt wurde eine eingehende Literaturrecherche mit retrospektiver Auswertung von BH<sub>4</sub>-Belastungstests zur Bestim-

mung des Einflusses verschiedener Phenylalanin- und BH<sub>4</sub>-Konzentrationen auf die BH<sub>4</sub>-Responsivität in Abhängigkeit des Patienten-Genotyps durchgeführt. Diese erhobenen Daten und die Translation der Ergebnisse auf *in vivo* Systeme führten zu klinisch relevanten neuen Erkenntnissen.

### **3.2 Zusätzliche Arbeiten, die im Rahmen der Promotionsarbeit entstanden sind**

Gersting, S. W., Lagler, F. B., Eichinger, A., Kemter, K. F., Danecka, M. K., Messing, D. D., **Staudigl, M.**, Domdey, K. A., Zsifkovits, C., Fingerhut, R., Glossmann, H., Roscher, A. A. and Muntau, A. C. (2010) *Pah<sup>enu1</sup>* is a mouse model for tetrahydrobiopterin-responsive phenylalanine hydroxylase deficiency and promotes analysis of the pharmacological chaperone mechanism *in vivo*. *Human Molecular Genetics* 19(10): 2039-2049.

Lagler, F. B., Gersting, S. W., Zsifkovits, C., Steinbacher, A., Eichinger, A., Danecka, M. K., **Staudigl, M.**, Fingerhut, R., Glossmann, H. and Muntau, A. C. (2010) New insights into tetrahydrobiopterin pharmacodynamics from *Pah<sup>enu1/2</sup>*, a mouse model for compound heterozygous tetrahydrobiopterin-responsive phenylalanine hydroxylase deficiency. *Biochemical Pharmacology* 80(10): 1563-1571.

#### 4. Schlussbetrachtungen und Ausblick

Im Rahmen der hier vorgelegten kumulativen Promotionsarbeit haben wir uns eingehend mit der Enzymologie der PAH, einem Enzym mit hoher Krankheitsrelevanz beim Menschen, beschäftigt.

Zunächst wurde der weltweit eingeführte *state of the art assay* zur Bestimmung der PAH-Aktivität im eigenen Labor etabliert. Er wurde verwendet, um die enzymkinetischen Parameter der rekombinant in *E. coli* exprimierten PAH zu bestimmen. Hierbei wurden das Wildtyp-Protein und zehn variante Proteine, die sich von *missense* Mutationen ableiten, die mit dem neuen klinischen Phänotyp der BH<sub>4</sub>-responsiven PAH assoziiert sind, detailliert charakterisiert. Unsere Hypothese, dass es sich bei der PKU um eine Proteinfaltungserkrankung handeln könnte, wurde durch die Beobachtung gestärkt, dass die o.g. Mutationen nahezu ausnahmslos allosterische Parameter verändern, also zu globalen Konformationsänderungen des PAH-Proteins führen.

Obwohl sich das bisherige Testverfahren jahrzehntelang bewährt hat, ist es bezüglich des methodischen und zeitlichen Aufwandes und im Hinblick auf den limitierten Bereich an Substrat- und Kofaktorkonzentrationen, bei denen die Messung erfolgen kann, mit signifikanten Nachteilen behaftet. Eingehende Kenntnisse zur enzymatischen Funktion der PAH bei unterschiedlichen Substrat- und Kofaktorkonzentrationen sind eine wichtige Voraussetzung für das Verständnis des fehlfaltungsbedingten Funktionsverlustes der PAH einerseits und der pharmakologischen Korrektur der Enzymfunktion andererseits. Um uns diesen Zielen zu nähern, haben wir eine neue fluoreszenzbasierte Methode entwickelt und etabliert, die eine direkte kontinuierliche Messung der Enzymaktivität erlaubt. So konnte die PAH-Aktivität in einem 4-fach erweiterten Konzentrationsbereich an Substrat- und Kofaktorkonzentrationen als bisher bestimmt werden, um den optimalen Arbeitsbereich des rekombinanten Proteins zu vermessen und den wechselseitigen Einfluss von Substrat (aktivierend) und Kofaktor (inhibierend) auf das Enzym zu analysieren. Die Methode wurde automatisiert, wodurch der Durchsatz (96 Messungen pro Stunde) im Vergleich zum früheren Testverfahren (30 Messungen pro 48 Stunden) erheblich erhöht werden konnte.

Die Anwendung dieser neuen Technologie hat zu drei wesentlichen Ergebnissen geführt. i) Wir konnten erstmalig den tatsächlichen optimalen Arbeitsbereich der PAH in Bezug auf Substrat- und Kofaktorkonzentration bestimmen; dieser lag in einem deutlich anderen Bereich als durch die weniger gut auflösenden bisher verfügbaren Testverfahren vermutet. Hierbei konnte die Ratio aus Phenylalanin und BH<sub>4</sub>, die einerseits Reaktanten sind, andererseits aber gegenläufig regulierende Effekte auf das Enzym ausüben, als Schlüsselfaktor der Funktion identifiziert werden. ii) Die kontinuierliche Messung hat die Analyse des Bindungsverhaltens des Kofaktors an das Protein ermöglicht. Hierdurch konnte erstmalig gezeigt werden, dass zwei unterschiedliche strukturelle Konformationen der PAH mit unterschiedlicher Funktion existieren, die den Kofaktor BH<sub>4</sub> einmal kooperativ und einmal nicht-kooperativ binden. iii) Mit Hilfe bioinformatischer Methoden wurden zur dreidimensionalen Kartierung der PAH-Aktivität (Wildtyp und variante Proteine) bei unterschiedlichen Substrat- und Kofaktorkonzentrationen *activity landscapes* erstellt und somit die Funktion der PAH im physiologischen und pathologischen Substratbereich sowie im therapeutischen Kontext der Kofaktortherapie visualisiert. Hieran lässt sich ablesen, bei welcher Phenylalaninkonzentration, also bei welchem metabolischen Status und bei welcher BH<sub>4</sub>-Konzentration bzw. bei welcher Dosierung des Pharmakons, bei Vorliegen einer spezifischen Mutation die optimale Enzymaktivität erreicht werden kann.

In einem weiteren Schritt wurden die an rekombinanten PAH-Proteinen erhobenen Ergebnisse auf zwei unterschiedliche *in vivo* Systeme, ein eukaryotes Zellkultursystem mit stabi-

ler Expression des PAH-Wildtyps und varianter PAH-Proteine und die Situation beim Patienten, übertragen. Wesentliche, klinisch relevante neue Erkenntnisse hieraus waren, dass einerseits der Genotyp, andererseits die Phenylalaninkonzentration, also der metabolische Status des Patienten, in erheblichem Maße die PAH-Enzymaktivität und das Ansprechen auf pharmakologische Dosen des Chaperons BH<sub>4</sub> beeinflussen. So kann beispielsweise ein BH<sub>4</sub>-Belastungstest beim gleichen Patienten bei unterschiedlichen initialen Phenylalaninkonzentrationen zu völlig verschiedenen Ergebnissen (Reduktion der Phenylalaninkonzentration 0% bzw. 80%) und damit Interpretationen im Hinblick auf die BH<sub>4</sub>-Responsivität führen, woraus sich die folgenschwere Festlegung eines lebenslangen Therapieregimes (Diät oder pharmakologische Therapie) für den Patienten ergibt. Die hier gewonnenen Ergebnisse haben daher sehr dazu beigetragen, dass die Notwendigkeit individualisierter diagnostischer und therapeutischer Konzepte bei der Betreuung von Patienten mit Defekt der PAH nun international anerkannt wird.

Zusammenfassend konnten im Rahmen der hier vorliegenden Promotionsarbeit erhebliche technologische Fortschritte auf dem Gebiet der PAH-Enzymologie erreicht werden. In Anbetracht von mehr als 600 Mutationen im *PAH*-Gen ist es hierdurch möglich geworden, in Zukunft die Funktion einer Vielzahl von varianten Proteinen vollständig zu erfassen. Die Übertragung der neuen Erkenntnisse auf *in vivo*-Systeme und der translationale Ansatz mit Rückübertragung neuer Sichtweisen auf die Situation bei unseren Patienten hat zu konkreten, weltweit akzeptierten Änderungen in Bezug auf die diagnostischen und therapeutischen Vorgehensweisen geführt. Die Anwendung der hier entwickelten Technologie zur Generierung neuer Erkenntnisse bzgl. einer Vielzahl weiterer Mutationen und die systembiologische Analyse und Aufbereitung dieser Daten wird in Zukunft in erheblichem Maße zur Realisierung individualisierter Diagnostik- und Therapiekonzepte beitragen.

## 5. Zusammenfassung

Die Phenylketonurie ist seit vielen Jahrzehnten der Prototyp der behandelbaren angeborenen Stoffwechselerkrankung. Der Funktionsverlust des Enzyms Phenylalaninhydroxylase (PAH) durch Mutationen im *PAH*-Gen führt zu einem der schwersten neurologischen Phänotypen mit nahezu vollständigem Intelligenzverlust. Diese gravierenden Symptome können durch eine lebenslange phenylalaninarme Diät fast vollkommen verhindert werden. In den letzten Jahren haben neue klinische und wissenschaftliche Erkenntnisse zu einem Paradigmenwechsel bei der Behandlung dieser Erkrankung geführt. Eine Therapie mit Tetrahydrobiopterin (BH<sub>4</sub>), dem natürlichen Kofaktor der PAH, führt in pharmakologischen Dosen bei einer signifikanten Subpopulation der Patienten zu einer Normalisierung des biochemischen Phänotyps und der PAH-Enzymaktivität *in vivo* und wurde 2008 als *orphan drug* zugelassen. Der Wirkungsmechanismus war jedoch zum Zeitpunkt der Zulassung noch unklar. Wir und andere stellten die Hypothese auf, dass es sich bei der BH<sub>4</sub>-responsiven Phenylketonurie um eine Proteinfaltungserkrankung mit *loss of function*, also Verlust des funktionellen Proteins, handelt. Hierdurch entstand erheblicher neuer Forschungsbedarf auf dem Gebiet einer Erkrankung, die Ende der 1990er Jahre als vollständig erforscht und umfassend verstanden galt.

Die hier vorliegende Promotionsarbeit befasst sich mit den enzymologischen Aspekten zur Phenylketonurie. Wir etablierten zunächst den weltweit anerkannten Standardtest zur Aktivitätsbestimmung der PAH und nutzten diesen zur eingehenden Charakterisierung der enzymkinetischen Parameter der rekombinanten Wildtyp-PAH und zehn varianter BH<sub>4</sub>-responsiver PAH. Die Beobachtung, dass sämtliche Mutationen zu einer Veränderung der allosterischen Parameter der PAH, also zu globalen Konformationsänderungen im Enzym führen, war ein erster Beleg für die Richtigkeit der Proteinfehlaltungshypothese, die im Rahmen anderer Projekte der Arbeitsgruppe weiter verfolgt wurde.

In einem zweiten Teil der Arbeit wurde ein neues fluoreszenzbasiertes Verfahren zur direkten kontinuierlichen Messung der Enzymaktivität entwickelt, etabliert und automatisiert. Hierdurch konnte die Funktionsweise des Enzyms, insbesondere in Abhängigkeit von Substrat und Kofaktor, erschöpfend untersucht und ihr Funktionsoptimum bestimmt werden. Die Ergebnisse wurden mit Hilfe bioinformatischer Methoden als dreidimensionale *activity landscapes* visualisiert.

Der abschließende Projektanteil beschäftigt sich mit der Übertragung der experimentellen Ergebnisse auf ein stabil transfiziertes eukaryotes Zellkultursystem und die Anwendung der gewonnenen Sichtweisen beim Patienten. Wesentliche neue Erkenntnisse hieraus waren, dass der Genotyp, der metabolische Status des Patienten, also die Phenylalaninkonzentration im Blut, und die Dosis des verabreichten Medikaments BH<sub>4</sub> einen wechselseitigen Einfluss auf die enzymologische Funktion des PAH-Proteins ausüben.

Heute gilt die Phenylketonurie als Prototyp der genetisch bedingten Proteinfaltungserkrankung mit *loss of function* und BH<sub>4</sub> ist das erste pharmakologische Chaperon auf dem Markt. Unsere grundlagenorientierten Untersuchungen am rekombinanten PAH-Protein und die translationale Sichtweise mit Übertragung der Ergebnisse auf geeignete *in vivo*-Systeme und auf den Patienten haben zu international sichtbaren Veränderungen in Bezug auf individualisierte diagnostische und therapeutische Konzepte beim Patienten mit BH<sub>4</sub>-responsiver Phenylketonurie geführt.

## 6. Summary

For many years, phenylketonuria has been the prototype of a treatable inborn error of metabolism. Mutations in the *phenylalanine hydroxylase (PAH)* gene with a loss-of-function molecular phenotype result in severe neurological symptoms with near to complete loss of intelligence. A lifelong diet can prevent this severe phenotype almost completely. Recent clinical and experimental findings have led to a paradigm shift in the treatment of this disease. In a significant number of patients, pharmacological doses of tetrahydrobiopterin (BH<sub>4</sub>), which is the natural cofactor of the enzyme, lead to a normalization of the biochemical phenotype and PAH enzyme activity *in vivo*. In 2008, BH<sub>4</sub> was approved as an orphan drug in the treatment of phenylketonuria. Yet at the time of approval, the molecular mode of action had not been elucidated. We and others hypothesized that BH<sub>4</sub>-responsive phenylketonuria is a protein misfolding disorder leading to a loss of the functionally active enzyme. Consequently, new research projects were needed and had to evolve on a disease that was thought to be completely understood already by the end of the 90's.

The doctoral thesis presented here covers aspects of basic research on enzyme function in phenylketonuria. First, a standard PAH activity assay was established to determine enzyme kinetic parameters of recombinant wild-type PAH and ten variant PAH proteins associated with BH<sub>4</sub>-responsiveness. Initial observations, that most mutations lead to changes in enzyme allostery and thus to global conformational changes in the enzyme, corroborated the hypothesis that phenylketonuria is a protein misfolding disorder with loss-of-function. Second, a new fluorescence-based method for the direct continuous measurement of enzyme activity was developed, established and automated. It was thus possible to analyze substrate- and cofactor-dependent enzyme function as well as the range of substrate and cofactor concentrations leading to optimal enzyme function. The results were visualized as three-dimensional *activity landscapes* by means of bioinformatics.

Finally, these experimental results were translated into a stably transfected eukaryotic cell line and compared with data from patients with BH<sub>4</sub>-responsiveness. The finding of an impact of genotype, metabolic state with respect to blood phenylalanine, and BH<sub>4</sub>-dosage provided substantial new insight into diagnostics and therapy of PAH deficiency.

Today, phenylketonuria is the prototype of a genetic disease leading to protein misfolding with loss-of-function. Furthermore, BH<sub>4</sub> is the first pharmacological chaperone available on the market. Our basic research on the recombinant PAH protein and its translation into *in vivo*-systems as well as to the patient has paved the way for a personalized medicine approach for this monogenic trait.

## 7. Literaturverzeichnis

- Abita, J. P., et al. (1976). "In vitro activation of rat liver phenylalanine hydroxylase by phosphorylation." *J Biol Chem* 251(17): 5310-5314.
- Andersen, O. A., et al. (2002). "Crystal structure of the ternary complex of the catalytic domain of human phenylalanine hydroxylase with tetrahydrobiopterin and 3-(2-thienyl)-L-alanine, and its implications for the mechanism of catalysis and substrate activation." *J Mol Biol* 320(5): 1095-1108.
- Andersen, O. A., et al. (2003). "2.0Å resolution crystal structures of the ternary complexes of human phenylalanine hydroxylase catalytic domain with tetrahydrobiopterin and 3-(2-thienyl)-L-alanine or L-norleucine: substrate specificity and molecular motions related to substrate binding." *J Mol Biol* 333(4): 747-757.
- Bickel, H., et al. (1953). "Influence of phenylalanine intake on phenylketonuria." *Lancet* 265(6790): 812-813.
- Bickel, H., et al. (1954). "The influence of phenylalanine intake on the chemistry and behaviour of a phenyl-ketonuric child." *Acta Paediatr* 43(1): 64-77.
- Bjørge, E., et al. (1998). "Partial characterization and three-dimensional-structural localization of eight mutations in exon 7 of the human phenylalanine hydroxylase gene associated with phenylketonuria." *Eur J Biochem* 257(1): 1-10.
- Copeland, R. A. (2000). *Enzymes: a practical introduction to structure, mechanism, and data analysis*. New York, NY, Wiley-VCH.
- Erlandsen, H., et al. (1997). "Crystal structure of the catalytic domain of human phenylalanine hydroxylase reveals the structural basis for phenylketonuria." *Nat Struct Biol* 4(12): 995-1000.
- Erlandsen, H., et al. (2004). "Correction of kinetic and stability defects by tetrahydrobiopterin in phenylketonuria patients with certain phenylalanine hydroxylase mutations." *Proc Natl Acad Sci U S A* 101(48): 16903-16908.
- Fitzpatrick, P. F. (2000). "The aromatic amino acid hydroxylases." *Adv Enzymol Relat Areas Mol Biol* 74: 235-294.
- Følling, A. (1934). "Über Ausscheidung von Phenylbrenztraubensäure in den Harn als Stoffwechselanomalie in Verbindung mit Imbezillität." *Hoppe-Seyler's Z Physiol Chem* 227: 169-176.
- Fusetti, F., et al. (1998). "Structure of tetrameric human phenylalanine hydroxylase and its implications for phenylketonuria." *J Biol Chem* 273(27): 16962-16967.
- Gersting, S. W., et al. (2010). "Activation of phenylalanine hydroxylase induces positive cooperativity toward the natural cofactor." *J Biol Chem* 285(40): 30686-30697.
- Jervis, G. A. (1953). "Phenylpyruvic oligophrenia deficiency of phenylalanine-oxidizing system." *Proc Soc Exp Biol Med* 82(3): 514-515.
- Kappock, T. J., et al. (1995). "Spectroscopic and kinetic properties of unphosphorylated rat hepatic phenylalanine hydroxylase expressed in *Escherichia coli*. Comparison of resting and activated states." *J Biol Chem* 270(51): 30532-30544.
- Kaufman, S. (1993). "The phenylalanine hydroxylating system." *Adv Enzymol Relat Areas Mol Biol* 67: 77-264.
- Kaufman, S., et al. (1962). "The source of oxygen in the phenylalanine hydroxylase and the copamine-beta-hydroxylase catalyzed reactions." *Biochem Biophys Res Commun* 9: 497-502.
- Knappskog, P. M., et al. (1996). "Structure/function relationships in human phenylalanine hydroxylase. Effect of terminal deletions on the oligomerization, activation and cooperativity of substrate binding to the enzyme." *Eur J Biochem* 242(3): 813-821.
- Kobe, B., et al. (1999). "Structural basis of autoregulation of phenylalanine hydroxylase." *Nat Struct Biol* 6(5): 442-448.
- Kure, S., et al. (1999). "Tetrahydrobiopterin-responsive phenylalanine hydroxylase deficiency." *J Pediatr* 135(3): 375-378.
- Lee, P., et al. (2008). "Safety and efficacy of 22 weeks of treatment with sapropterin dihydrochloride in patients with phenylketonuria." *Am J Med Genet A* 146A(22): 2851-2859.

- Levy, H. L., et al. (2007). "Efficacy of sapropterin dihydrochloride (tetrahydrobiopterin, 6R-BH4) for reduction of phenylalanine concentration in patients with phenylketonuria: a phase III randomised placebo-controlled study." *Lancet* 370(9586): 504-510.
- Martinez, A., et al. (1995). "Expression of recombinant human phenylalanine hydroxylase as fusion protein in *Escherichia coli* circumvents proteolytic degradation by host cell proteases. Isolation and characterization of the wild-type enzyme." *Biochem J* 306 ( Pt 2): 589-597.
- Miranda, F. F., et al. (2002). "Phosphorylation and mutations of Ser(16) in human phenylalanine hydroxylase. Kinetic and structural effects." *J Biol Chem* 277(43): 40937-40943.
- Mitnaul, L. J. and R. Shiman (1995). "Coordinate regulation of tetrahydrobiopterin turnover and phenylalanine hydroxylase activity in rat liver cells." *Proc Natl Acad Sci U S A* 92(3): 885-889.
- Muntau, A. C. and S. W. Gersting (2010). "Phenylketonuria as a model for protein misfolding diseases and for the development of next generation orphan drugs for patients with inborn errors of metabolism." *J Inherit Metab Dis* 33(6): 649-658.
- Muntau, A. C., et al. (2002). "Tetrahydrobiopterin as an alternative treatment for mild phenylketonuria." *N Engl J Med* 347(26): 2122-2132.
- Nennstiel-Ratzel, U. and B. Liebl (2010). "Neugeborenen-Screening in Bayern, Newsletter Nr. 14: Ergebnisse und Empfehlungen." 1.
- Pey, A. L., et al. (2004). "Mechanisms underlying responsiveness to tetrahydrobiopterin in mild phenylketonuria mutations." *Hum Mutat* 24(5): 388-399.
- Scriver, C. R. and S. Kaufman (2001). *Hyperphenylalaninemia: phenylalanine hydroxylase deficiency*. New York, McGraw-Hill.
- Scriver, C. R., et al. (2000). "PAHdb: a locus-specific knowledgebase." *Hum Mutat* 15(1): 99-104.
- Shiman, R. and D. W. Gray (1980). "Substrate activation of phenylalanine hydroxylase. A kinetic characterization." *J Biol Chem* 255(10): 4793-4800.
- Shiman, R., et al. (1994). "Regulation of rat liver phenylalanine hydroxylase. I. Kinetic properties of the enzyme's iron and enzyme reduction site." *J Biol Chem* 269(40): 24637-24646.
- Shiman, R., et al. (1990). "Mechanism of phenylalanine regulation of phenylalanine hydroxylase." *J Biol Chem* 265(20): 11633-11642.
- Shiman, R., et al. (1982). "Regulation of phenylalanine hydroxylase activity by phenylalanine in vivo, in vitro, and in perfused rat liver." *J Biol Chem* 257(19): 11213-11216.
- Shiman, R., et al. (1994). "Regulation of rat liver phenylalanine hydroxylase. II. Substrate binding and the role of activation in the control of enzymatic activity." *J Biol Chem* 269(40): 24647-24656.
- Solstad, T., et al. (2003). "Studies on the regulatory properties of the pterin cofactor and dopamine bound at the active site of human phenylalanine hydroxylase." *Eur J Biochem* 270(5): 981-990.
- Stokka, A. J., et al. (2004). "Probing the role of crystallographically defined/predicted hinge-bending regions in the substrate-induced global conformational transition and catalytic activation of human phenylalanine hydroxylase by single-site mutagenesis." *J Biol Chem* 279(25): 26571-26580.
- Thöny, B., et al. (2000). "Tetrahydrobiopterin biosynthesis, regeneration and functions." *Biochem J* 347 Pt 1: 1-16.
- Trefz, F. K., et al. (2009). "Efficacy of sapropterin dihydrochloride in increasing phenylalanine tolerance in children with phenylketonuria: a phase III, randomized, double-blind, placebo-controlled study." *J Pediatr* 154(5): 700-707.
- Udenfriend, S. and J. R. Cooper (1952). "The enzymatic conversion of phenylalanine to tyrosine." *J Biol Chem* 194(2): 503-511.
- Waters, P. J. (2003). "How PAH gene mutations cause hyper-phenylalaninemia and why mechanism matters: insights from in vitro expression." *Hum Mutat* 21(4): 357-369.
- Waters, P. J., et al. (2000). "Characterization of phenylketonuria missense substitutions, distant from the phenylalanine hydroxylase active site, illustrates a paradigm for

- mechanism and potential modulation of phenotype." *Mol Genet Metab* 69(2): 101-110.
- Waters, P. J., et al. (1998). "Alterations in protein aggregation and degradation due to mild and severe missense mutations (A104D, R157N) in the human phenylalanine hydroxylase gene (PAH)." *Hum Mutat* 12(5): 344-354.
- Weglage, J., et al. (2001). "Normal clinical outcome in untreated subjects with mild hyperphenylalaninemia." *Pediatr Res* 49(4): 532-536.
- Werner, E. R., et al. (2011). "Tetrahydrobiopterin: biochemistry and pathophysiology." *Biochem J* 438(3): 397-414.
- Xia, T., et al. (1994). "Regulation of rat liver phenylalanine hydroxylase. III. Control of catalysis by (6R)-tetrahydrobiopterin and phenylalanine." *J Biol Chem* 269(40): 24657-24665.
- Zschocke, J. (2003). "Phenylketonuria mutations in Europe." *Hum Mutat* 21(4): 345-356.

## 8. Sonderdrucke der Publikationen im Rahmen der Promotionsarbeit

1. Gersting, S. W., Kemter, K. F., **Staudigl, M.**, Messing, D. D., Danecka, M. K., Lagler, F. B., Sommerhoff, C. P., Roscher, A. A. and Muntau, A. C. (2008) Loss of function in phenylketonuria is caused by impaired molecular motions and conformational instability. *American Journal of Human Genetics* 83(1): 5-17
2. Gersting, S. W.\*, Staudigl, M.\*, Truger, M. S., Messing, D. D., Danecka, M. K., Sommerhoff, C. P., Kemter, K. F. and Muntau, A. C. (2010) Activation of phenylalanine hydroxylase induces positive cooperativity toward the natural cofactor. *Journal of Biological Chemistry* 285(40): 30686-30697  
\* contributed equally
3. Staudigl, M.\*, Gersting, S. W.\*, Danecka, M. K., Messing, D. D., Woidy, M., Pinkas, D., Kemter, K. F., Blau, N., and Muntau, A. C. (2011) The interplay between genotype, metabolic state, and cofactor treatment governs phenylalanine hydroxylase function and drug response. *Human Molecular Genetics* 20(13): 2628-2641  
\*contributed equally

# Loss of Function in Phenylketonuria Is Caused by Impaired Molecular Motions and Conformational Instability

Søren W. Gersting,<sup>1</sup> Kristina F. Kemter,<sup>1</sup> Michael Staudigl,<sup>1</sup> Dunja D. Messing,<sup>1</sup> Marta K. Danecka,<sup>1</sup> Florian B. Lagler,<sup>2</sup> Christian P. Sommerhoff,<sup>3</sup> Adelbert A. Roscher,<sup>1</sup> and Ania C. Muntau<sup>1,\*</sup>

A significant share of patients with phenylalanine hydroxylase (PAH) deficiency benefits from pharmacological doses of tetrahydrobiopterin (BH<sub>4</sub>), the natural PAH cofactor. Phenylketonuria (PKU) is hypothesized to be a conformational disease, with loss of function due to protein destabilization, and the restoration of enzyme function that is observed in BH<sub>4</sub> treatment might be transmitted by correction of protein misfolding. To elucidate the molecular basis of functional impairment in PAH deficiency, we investigated the impact of ten *PAH* gene mutations identified in patients with BH<sub>4</sub>-responsiveness on enzyme kinetics, stability, and conformation of the protein (F55L, I65S, H170Q, P275L, A300S, S310Y, P314S, R408W, Y414C, Y417H). Residual enzyme activity was generally high, but allostery was disturbed in almost all cases and pointed to altered protein conformation. This was confirmed by reduced proteolytic stability, impaired tetramer assembly or aggregation, increased hydrophobicity, and accelerated thermal unfolding—with particular impact on the regulatory domain—observed in most variants. Three-dimensional modeling revealed the involvement of functionally relevant amino acid networks that may communicate misfolding throughout the protein. Our results substantiate the view that PAH deficiency is a protein-misfolding disease in which global conformational changes hinder molecular motions essential for physiological enzyme function. Thus, PKU has evolved from a model of a genetic disease that leads to severe neurological impairment to a model of a treatable protein-folding disease with loss of function.

## Introduction

Deficiency of phenylalanine hydroxylase (PAH; EC 1.14.16.1) causes phenylketonuria (PKU [MIM 261600]) and is the most common inborn error of amino acid metabolism in European-descended populations. Since the introduction of a dietary treatment fifty years ago, PKU has been the prototype for a treatable genetic disease and, later, for genetic screening in human populations.<sup>1</sup> The recent recognition of a new pharmacologically treatable phenotype of PAH deficiency challenged the classical view of hereditary diseases that result in loss of enzyme function. We previously showed that a significant share of PKU patients responds to oral administration of the natural PAH cofactor (tetrahydrobiopterin, BH<sub>4</sub>) although these individuals do not display biochemical evidence of BH<sub>4</sub> deficiency. The treatment reduces blood phenylalanine concentrations, restores enzyme activity in vivo, and significantly increases dietary-protein tolerance.<sup>2</sup> Some authors proposed that restoration of enzyme function observed under treatment with pharmacological doses of BH<sub>4</sub> is transmitted by correction of PAH misfolding.<sup>2–5</sup>

About 80% of all mutations in the *PAH* gene are missense, and experimental data on the conformational impact of single amino acid replacements on allostery, stability, and folding of the PAH protein is scarce. Because the crystal structure of full-length PAH has not yet been completely solved,<sup>6–8</sup> a composite model is commonly used

for 3D structural analysis.<sup>9</sup> PAH is a homotetrameric enzyme, with each subunit composed of three functional domains: the N-terminal regulatory domain (residues 1–142); the catalytic domain (residues 143–410), which includes binding sites for substrate and cofactor; and the oligomerization domain at the C terminus (residues 411–452). There is a high degree of structural interplay between the single domains and the subunits, respectively.<sup>6–8,10–13</sup> Substrate (L-phenylalanine) and cofactor binding induce conformational changes, which are transmitted through networks of side-chain interactions.<sup>14,15</sup> This is the basis for homotropic allostery that allows for fine-tuned regulation of PAH enzyme activity comprising substrate activation, modulation of oligomerization, and the affinity to substrate and cofactor.<sup>3,4,12,15</sup> We hypothesized that the structural flexibility of PAH permits gross conformational changes required for enzyme function and thus renders the enzyme susceptible to protein misfolding. This view was supported by previous studies demonstrating disturbed oligomerization and accelerated degradation of some variant PAH proteins.<sup>3,4,16–19</sup> However, only little is known about the structural mechanisms leading to loss of function in phenylketonuria and in other inherited diseases that exhibit loss-of-function pathogenesis.

The aim of this study, therefore, was to elucidate the molecular basis of loss of function in PKU. The impact of single side-chain replacements associated with BH<sub>4</sub>-responsiveness on function and conformational stability of

<sup>1</sup>Department of Molecular Pediatrics, Children's Research Center, Dr. von Hauner Children's Hospital, Ludwig Maximilians University, 80337 Munich, Germany; <sup>2</sup>Department of Medical Genetics, Molecular and Clinical Pharmacology, Innsbruck Medical University, 6020 Innsbruck, Austria; <sup>3</sup>Department of Clinical Chemistry and Clinical Biochemistry, Surgical Clinic, Ludwig Maximilians University, 80337 Munich, Germany

\*Correspondence: [ania.muntau@med.uni-muenchen.de](mailto:ania.muntau@med.uni-muenchen.de)

DOI 10.1016/j.ajhg.2008.05.013. ©2008 by The American Society of Human Genetics. All rights reserved.

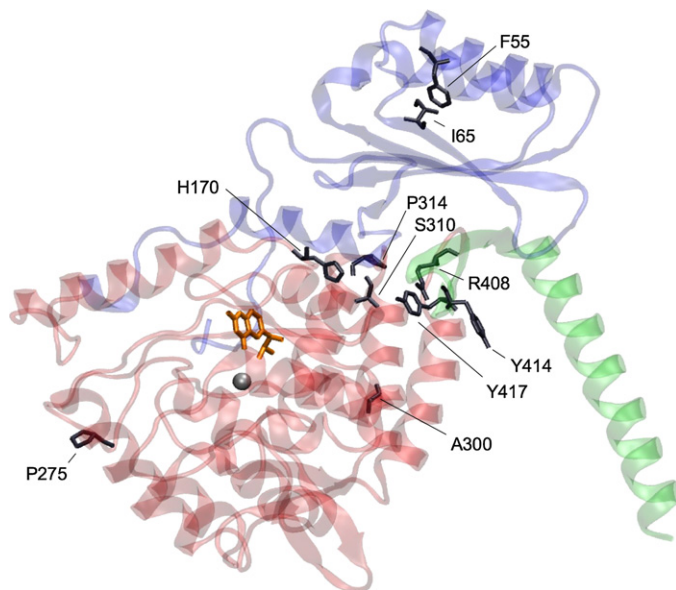


**Figure 1. Structural Localization of PAH Missense Mutations Analyzed**

The PAH monomer, shown as a ribbon representation, is composed of three functional domains: the N-terminal regulatory domain (residues 19–142, blue), the central catalytic domain (residues 143–410, red), and the C-terminal oligomerization domain (residues 411–452, green). The active-site iron (silver sphere) and the cofactor (orange stick model) are shown. Amino acid residues affected by mutations are shown as stick models.

the PAH protein was analyzed on the basis of enzyme kinetics, oligomerization, limited proteolysis, thermal inactivation, thermal unfolding, and 3D structural modeling. The mutations analyzed in this study caused pleiotropic effects. Residual enzyme activity was generally high, but allostery was disturbed in almost all cases and pointed to altered protein conformation. Reduced proteolytic stability of most variants, impaired tetramer assembly or aggregation, increased hydrophobicity, and accelerated thermal unfolding with particular impact on the regulatory domain corroborated the hypothesis of protein misfolding. To explain the remote effects on structure and function that were observed, we propose a model of protein misfolding as communicated throughout the protein by disruption of functional networks due to single amino acid replacements.

In the past twenty years, scientists have made significant efforts to identify a consistent relationship between the PAH genotype, in vitro residual enzyme activities, and the clinical phenotype.<sup>20–22</sup> A recent report from Pey and colleagues in this journal marked a breakthrough by opening the view on global conformation of PAH.<sup>23</sup> Using computational analyses, they predicted conclusive correlations between the mutational energetic impact on the protein and the clinical phenotype. Our results now provide experimental evidence and new insights into how PAH missense mutations induce conformational protein destabilization and loss of PAH function.

## Material and Methods

### Subjects and Mutations

In a previous study, we identified five unrelated patients bearing six mutations in the PAH gene that have not yet been characterized in vitro.<sup>2</sup> Three individuals were classified as having mild PKU (plasma phenylalanine concentrations in the absence of treatment exceeded 600  $\mu\text{mol/l}$  but do not reach values higher than 1200

$\mu\text{mol/l}$ ): patient 1, a Turkish girl born to consanguineous parents; patient 2, a German girl born to nonconsanguineous parents; and patient 5, a Turkish boy born to consanguineous parents. Patient 3, a German girl, and patient 4, a female German newborn, were classified as having mild hyperphenylalaninemia, with plasma phenylalanine concentrations consistently below 600  $\mu\text{mol/l}$  on an unrestricted diet. In all patients, hyperphenylalaninemia had been detected by newborn-screening programs, and BH<sub>4</sub>-responsiveness was subsequently demonstrated in an extended BH<sub>4</sub>-loading test.<sup>2</sup> BH<sub>4</sub> deficiency due to genetic disorders of biosynthesis or regeneration of the cofactor had been ruled out in all cases by the determination of urinary pterins and the activity of dihydropteridin reductase in erythrocytes. We obtained written informed consent for genotyping from the families. Mutations and clinical phenotypes of the individual patients are summarized in Table S1. The structural localization of mutations characterized in this study was mapped to the composite model of a PAH monomer (Figure 1). The mutations were located in the regulatory domain (F55L, I65S), in the catalytic domain (H170Q, P275L, A300S, S310Y, P314S, R408W), or in the dimerization motif of the oligomerization domain (Y414C, Y417H).

### Plasmid Constructs and Site-Directed Mutagenesis

The cDNA of human phenylalanine hydroxylase (EST clone obtained from imaGenes, formerly RZPD, Germany) was cloned into the pMAL-c2E expression vector (New England Biolabs) encoding an N-terminal MBP (maltose-binding protein) tag and an enterokinase cleavage site. PAH mutants were constructed with the use of the QuikChange site-directed mutagenesis kit (Stratagene). Authenticity of the mutagenesis was verified by DNA sequencing.

### Expression and Purification

Expression plasmids were transformed into *E. coli* DH5 $\alpha$ . Bacteria were grown to midexponential phase at 37°C, and overexpression of wild-type and variant MBP-PAH fusion proteins was induced with 0.3 mM isopropylthio- $\beta$ -D-galactoside (IPTG). MBP-PAH fusion proteins were more prone to form high-molecular-weight aggregates at two hours of induction than they were at longer induction periods, but the relative recovery of the tetrameric and the dimeric form was similar (own and previous observations<sup>24</sup>). To avoid artificial formation of aggregated PAH, we chose an induction time of 20 hr. Proteins were purified on ÄKTAexpress (GE Healthcare) at 4°C by affinity chromatography (amylose resin, New England Biolabs) as described previously,<sup>25</sup> followed by size-exclusion chromatography with a HiLoad 16/60 Superdex 200 column (GE Healthcare). The isolated tetrameric fusion proteins were collected, and protein concentrations were determined spectrophotometrically with the use of the absorption coefficient A<sub>280</sub>,<sup>25</sup> or the dye-binding Bradford assay.

It was previously shown that the MBP tag does not significantly affect PAH enzyme activity, kinetic parameters, or the oligomeric state of the protein.<sup>16,17,25–27</sup> Moreover, a comparative analysis of limited proteolysis, thermal inactivation, and thermal denaturation with the fusion protein and the cleaved PAH protein revealed no significant difference (data not shown).

### Analysis of Oligomerization

Oligomerization profiles were obtained by size-exclusion chromatography, and peaks corresponding to aggregated forms, tetramers, dimers, and monomers were determined with the use of LMW and HMW gel-filtration calibration kits (GE-Healthcare). Relative amounts of the different oligomeric states were calculated by deconvolution of the chromatograms with the use of the ACD/ChromManager software (Advanced Chemistry Development). Blue dextran was used for determination of the void volume ( $V_0$ , 45.3 ml).

### PAH-Activity Assay

PAH activity was determined as previously described.<sup>25,28</sup> Tetrameric wild-type or variant MBP-PAH (0.01 mg/ml) was preincubated with the L-phenylalanine (L-Phe) substrate for 5 min at 25°C in a standard reaction buffer containing 15 mM Na HEPES, pH 7.3 and 1 mg/ml catalase. After the addition of 10 μM ferrous ammonium sulfate and an additional incubation of 1 min, the reaction was initiated with BH<sub>4</sub> (6[R]-L-erythro-5,6,7,8-tetrahydrobiopterin, Cayman Chemicals) stabilized in 2 mM dithiothreitol (DTT). Kinetic parameters were determined at standard L-Phe concentration (1 mM) with variable cofactor concentrations (0–704.1 μM BH<sub>4</sub>) or at standard BH<sub>4</sub> concentration (75 μM) and variable L-Phe concentrations (0–1 mM), respectively. Because of early substrate inhibition, L-Phe concentrations were restricted to 0–250 μM for P314S and to 0–500 μM for Y414C and Y417H, respectively. To determine the level of substrate activation, a preincubation with the substrate was omitted and the reaction was triggered by simultaneous addition of 1 mM L-Phe and 75 μM BH<sub>4</sub>. All concentrations mentioned refer to the final concentration in a 100 μl reaction mixture. The amount of the L-tyrosin (L-Tyr) product formed after 1 min was measured by HPLC and assayed as triplicates. Steady-state kinetic parameters of three independent experiments were calculated by nonlinear regression analysis with the use of GraphPad Prism 4.0c (GraphPad Software). Enzyme kinetic parameters at variable substrate concentrations displayed cooperativity and were calculated with the Hill equation. Enzyme kinetic parameters at variable cofactor concentrations were calculated with the Michaelis-Menten equation or with the modified Michaelis-Menten equation<sup>29</sup> in the case of cofactor inhibition (WT, F55L, I65S, P314S, Y417H). All experimental data were confirmed by repeated analyses of different protein purifications.

### Limited Proteolysis by Proteinase K

The purified tetrameric MBP-PAH fusion proteins of wild-type PAH and its variant forms were digested with proteinase K at 37°C in a buffer containing 20 mM Na HEPES, 200 mM NaCl, and 38.4 mM DTT at pH 7.0. Stocks of proteinase K and MBP-PAH were prepared in 20 mM Na HEPES, 200 mM NaCl, pH 7.0 at final concentrations of 1 μg/ml and 1 mg/ml, respectively, and mixed at protease to substrate ratio of 1:5000 by weight. Proteolysis was terminated at 5, 10, 15, 20, 30, 60, 90, and 120 min time points by addition of the inhibitor phenylmethylsulphonyl fluoride (PMSF) at a final concentration of 4 mM. The reaction mixtures

were subjected to SDS-PAGE under reducing conditions with 4%–12% gradient polyacrylamide gels (Invitrogen). The pattern of proteolysis was monitored by immunoblotting. MBP-PAH fusion proteins and their proteolytic fragments were detected by mouse monoclonal anti-phenylalanine hydroxylase IgG<sub>1</sub> (PH8, Calbiochem, 1:2000 dilution) and alkaline phosphatase conjugated anti-mouse IgG (Promega, 1:7500 dilution). Bound antibodies were visualized by chemiluminescence with the CDP-Star substrate (Roche) for alkaline phosphatase. Chemiluminescence was monitored with the DIANA III imaging system, and the resulting protein bands were quantified by AIDA-software (Raytest). The densitometry data of quadruplicate assays of one protein purification were normalized to the band corresponding to intact MBP-PAH fusion protein and analyzed by nonlinear curve fitting of single exponential function in the case of the fusion protein. The formation of the PAH fragment upon cleavage of the fusion protein and subsequent degradation of the PAH fragment was determined by nonlinear curve fitting of a double exponential “Bateman function”:

$$Y = C \times \frac{K_i}{K_i - K_e} \times (e^{-K_e \times t} - e^{-K_i \times t})$$

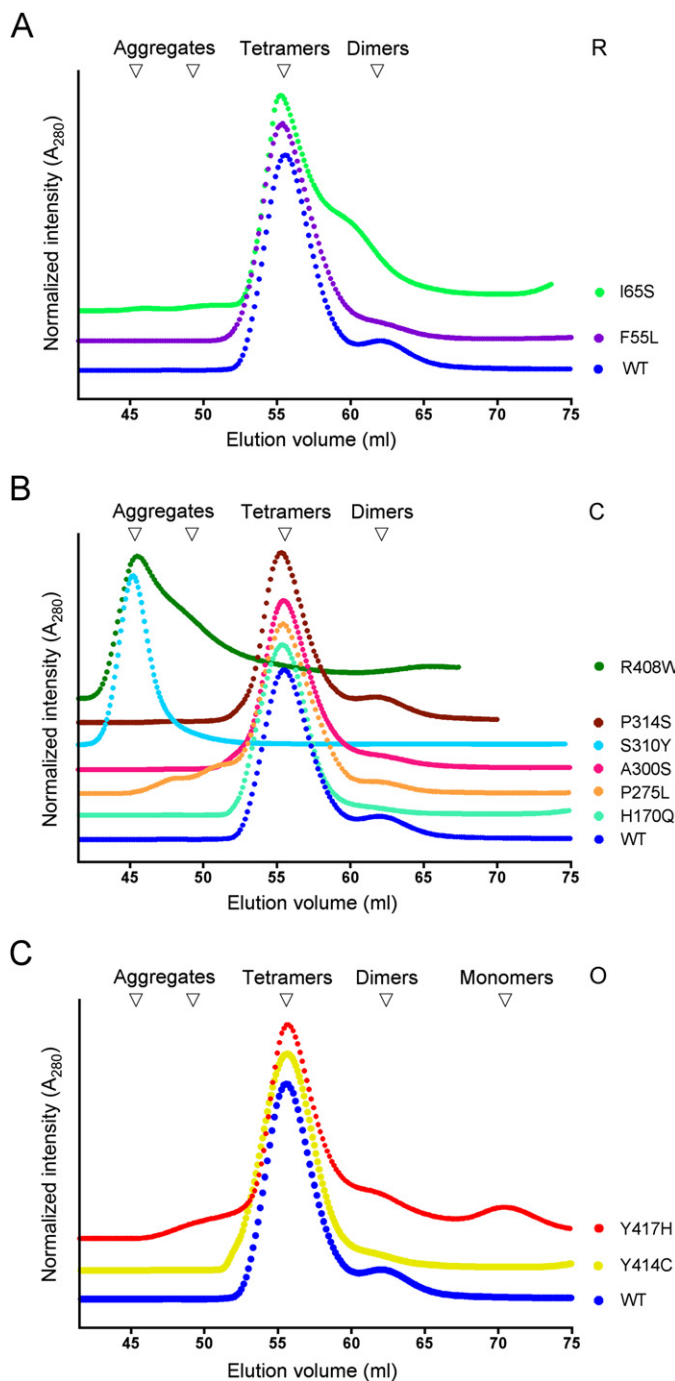
in which  $Y$  is the amount of the PAH protein;  $C$  is the theoretical amount of the MBP-PAH fusion protein;  $K_i$  and  $K_e$  are the rate constants for invasion and elimination of the PAH fragment, respectively; and  $t$  is the incubation time.

### Thermal Inactivation

Thermal inactivation of wild-type and variant MBP-PAH was determined by analysis of the decay of enzyme activity as a function of temperature. Aliquots of protein (1 μg/μl) were incubated in 20 mM Na HEPES, 200 mM NaCl, pH 7.0 for 10 min at 22 different temperatures ranging from 20°C to 75°C and then chilled on ice. PAH enzyme activity was subsequently measured as described above. Residual activities were normalized to initial enzyme activity without incubation. Data points were subjected to nonlinear regression analysis, and midpoints of thermal inactivation ( $T_m$ ) at 50% residual activity observed in three independent experiments were calculated with the use of GraphPad Prism 4.0c with the Boltzmann sigmoidal fit (GraphPad Software).

### Thermal Denaturation

Fluorescence measurements were performed on a Cary Eclipse fluorescence spectrophotometer equipped with a temperature-controlled Peltier multicell holder (Varian). Samples contained MBP-PAH fusion proteins (6 μM PAH subunit) in 20 mM Na HEPES, 200 mM NaCl, pH 7.0, 10 μM ferrous ammonium sulfate, and 1 mM DTT. Thermal denaturation was monitored by the following of changes in 8-anilino-1-naphthalenesulfonic acid (ANS; Sigma Aldrich)-fluorescence emission (excitation at 395 nm and emission at 500 nm, 5.0/10.0 nm slit widths). Thermal denaturation was performed at a rate of 1.2°C/min in a 25°–85°C range. Thermal denaturation curves were obtained by the plotting of fluorescence intensities against temperature. The phase transitions observed in three independent experiments were determined, and the respective transition midpoints were calculated by differentiation of the increasing part of the curves. Significances for the differences between the wild-type and the variants were calculated by two-tailed Student's  $t$  test. Thermal denaturation of the MBP protein occurs at temperatures above 62°C, as previously shown<sup>30</sup> and confirmed for this experimental setup. Therefore, MBP



denaturation did not interfere with the unfolding curves of the PAH protein for ANS fluorescence.

### Structural Analyses and Figure Preparation

A composite model of the 3D structure (PDB codes 1PAH, 1PHZ, 2PHM, 2PAH, 3PAH, 1J8T, and 1J8U) of tetrameric PAH was constructed with the use of the DeepView/Swiss-PdbViewer.<sup>31</sup> In the presence of hydrogen atoms, H bonds were computed with the following constraints: 1.2–2.76 Å distance, 120° angles. When hydrogen atoms were absent, H bonds were computed with the following constraints: 2.35–3.2 Å distance, 90° angles. Figures were prepared with the use of Visual Molecular Dynamics software.<sup>32</sup>

### Figure 2. PAH Mutations in All Three Domains Can Lead to Aggregation or Impaired Tetramer Assembly

Oligomerization profiles of wild-type and variant PAH were determined by size-exclusion chromatography. Chromatograms of variant PAH were normalized to the tetramer peak of the wild-type. Arrows mark the elution volumes of soluble aggregates (45 to 47 ml), tetramers (56 ml), dimers (63 ml), and monomers (71 ml).

(A) Profiles of variants arising from mutations located in the regulatory domain (R). I65S showed increased amounts of dimers, whereas F55L was almost exclusively eluted as tetramers.

(B) Profiles of variants arising from mutations located in the catalytic domain (C). S310Y and R408W eluted as high-molecular-weight aggregates without any detectable tetramers. The variants H170Q, P275L, A300S, and P314S eluted mainly in the tetrameric form. For P275L, two additional peaks of higher molecular weight were detected.

(C) Profiles of variants arising from mutations mapping to the dimerization motif of the oligomerization domain (O). Y417H showed significant amounts of monomers and increased amounts of dimers, whereas Y414C showed only tetramers.

## Results

### Disturbed Oligomerization Manifests as Aggregation or Impaired Tetramer Assembly

Wild-type PAH and ten variant forms of PAH were purified by affinity chromatography with subsequent size-exclusion chromatography, and oligomeric states were quantified by deconvolution analysis (Figure 2 and Table 1). Wild-type PAH was eluted mainly in the tetrameric form (86.2%), with a small amount of dimers (13.8%). Five variant PAH proteins (F55L, H170Q, A300S, P314S, Y414C) that mapped to all three domains showed elution profiles similar to that of wild-type with minor changes of the dimer-tetramer equilibrium. The remaining variants displayed disturbed oligomerization, with only one mutant residue (Y417H) mapping to the oligomerization domain. Impaired tetramer assembly was observed for the I65S mutation located in the regulatory domain and the Y417H mutation located in the dimerization motif of the oligomerization domain. The I65S mutation showed increased amounts of dimers (28.5%). This is in line with previously reported observations for the I65T substitution showing a shifted equilibrium of tetramers and dimers and proneness to aggregation.<sup>18,33,34</sup> For the Y417H variant we observed an oligomerization profile previously not described for recombinant variant PAH. We detected a significant amount of monomers (11.1%), with an increased amount of dimers (17.7%) in relation to tetramers (63.7%), and some aggregates (7.5%). Although the residue Y414 is in close proximity to Y417, the variant Y414C showed an oligomerization pattern resembling that of the wild-type protein. This is in contrast to previous studies that reported aggregate formation for Y414C.<sup>35</sup> Two mutations located in the catalytic domain (S310Y,

**Table 1. Quantitative Analysis of Wild-Type and Variant PAH Oligomerization Profiles**

Missense Mutation	Aggregates	Tetramers	Dimers	Monomers
WT		86.2	13.8	
F55L		94.1	5.9	
I65S		71.5	28.5	
H170Q		94.8	5.2	
P275L	13.2	82.2	4.6	
A300S	2.4	87.0	10.6	
S310Y	100			
P314S		83.2	16.8	
R408W	100			
Y414C		92.5	7.5	
Y417H	7.5	63.7	17.7	11.1

Relative amounts of the eluted fractions corresponding to different oligomeric states of wild-type (WT) and variant PAH proteins are given as percentages. The relative amounts were calculated by deconvolution analysis of the size-exclusion chromatograms.

R408W) resulted in formation of high-molecular-weight aggregates (100%) without the occurrence of any tetrameric PAH, suggesting a severe folding defect. In addition, the variant P275L also formed some aggregates (13.2%), of which the largest fraction (82.2%) was the tetrameric form.

In summary, we observed disturbed oligomerization not only for mutations located in the oligomerization domain but also for mutations located in the two other domains. Our results confirm that PAH mutations can lead to misfolding, with aggregation and/or disturbed tetramer assembly.

### Residual Enzyme Activity of Variant PAH is High, but Allostery is Disturbed

Detailed analyses of steady-state kinetic parameters were performed for all purified tetrameric PAH proteins (Table 2). Enzyme activity of variant PAH was reduced in comparison to wild-type with respect to  $V_{\max}$  determined at variable L-Phe concentrations. However, the reduction in activity was generally moderate ( $\geq 50\%$  residual activity), with the exception of P314S (22% residual activity). For most of the variant proteins analyzed, the affinity of variant PAH to its cofactor BH<sub>4</sub> or to its substrate L-Phe was not reduced. Only P275L showed decreased cofactor affinity, with a threefold increase in  $K_m$  (65  $\mu\text{M}$ ). By contrast, the  $K_m$  values for A300S (17  $\mu\text{M}$ ) and Y414C (16  $\mu\text{M}$ ) were slightly decreased. The affinity to the substrate was not reduced but was even increased for P275L and P314S, as shown by decreased values for  $S_{0.5}$  (76 and 49  $\mu\text{M}$ , respectively).

Tetrameric wild-type PAH displayed positive cooperativity for L-Phe binding (Hill coefficient [ $h$ ], 3.0) and substrate activation (activation fold, 3.0). Notably, all but one of the PAH variants showed alterations in allostery. Positive cooperativity was reduced for all variant proteins except H170Q. Most variants showed reduced substrate activation, ranging from a mild decrease (P275L and Y414C; activation fold 2.3 and 2.0, respectively) to a near-complete loss (F55L, I65S, P314S, and Y417H; activation fold 1.5, 1.0, 1.3, and 1.5, respectively).

Taken together, the results show that reduction in enzyme activity was moderate for most variant PAH proteins, and only one variant showed reduced affinity to the cofactor. However, allostery was severely affected by mutations in all three domains. This indicates that side-chain replacements can induce global conformational changes, with remote effects on PAH enzyme function.

### Susceptibility to Proteinase K is Increased

Misfolded subunits and incorrectly assembled oligomeric forms of proteins are more susceptible to degradation by proteases in mammalian cells.<sup>5</sup> Previous studies using a transcription and translation system or the protease trypsin showed that mutations in the PAH gene can lead to decreased protein stability.<sup>3-5,18</sup>

In this study, we probed protein conformation of PAH by limited proteolysis with proteinase K. Here, the proteolytic event is predominantly governed by the stereochemistry and flexibility of the protein substrate and not by the specificity of the protease.<sup>36</sup> Because MBP was fused to the N-terminal regulatory domain of PAH, we hypothesized that altered folding of this domain could lead to increased susceptibility of the linker region to proteolytic cleavage. This was confirmed by the finding that the half-life of the fusion protein was decreased by  $\geq 50\%$  for six out of eight MBP-PAH variants. Stability of the PAH fragment was also decreased in most cases (Table 3). Mutations in the regulatory domain and the oligomerization domain led to minor reductions of PAH half-life, whereas severe destabilization was detected for three mutations of the catalytic domain (H170Q, P275L, A300S; 60%, 55%, and 50% of the wild-type, respectively). Interestingly, one catalytic mutation (P314S) did not lead to destabilization but even induced marked stabilization of both the fusion protein (167%) and the PAH fragment (143%) in comparison to that of the wild-type.

The increased susceptibility to proteinase K observed here is in line with the hypothesis that PAH destabilization is due to partial protein unfolding.

### Protein Unfolding Predominantly Affects the Regulatory Domain of the Protein

To directly investigate whether variant PAH is prone to aberrant folding, we analyzed conformational alterations in the ground state and upon thermal denaturation. Two distinct transitions were previously described for the denaturation of wild-type PAH. These form the basis for a three-stage model of thermal PAH denaturation: (i) a low-temperature transition representing unfolding of the four regulatory domains, (ii) a high-temperature transition representing unfolding of two catalytic domains, and (iii) irreversible protein denaturation.<sup>37</sup>

Thermal protein denaturation was analyzed by ANS fluorescence (Figures 3A, 3B, and 3C). Transition midpoints are summarized in Table 4. The usage of the hydrophobic fluorophore ANS allowed us to monitor overall unfolding events because it binds to hydrophobic groups of the denaturing

**Table 2. Enzyme Kinetic Parameters**

Missense Mutation	L-Phe <sup>a</sup>				BH <sub>4</sub> <sup>b</sup>	
	V <sub>max</sub> <sup>e</sup> (nmol L-Tyr/min × mg protein)	[S] <sub>0.5</sub> <sup>e</sup> (μM)	<i>h</i>	Activation Fold	V <sub>max</sub> <sup>e</sup> (nmol L-Tyr/min × mg protein)	K <sub>m</sub> <sup>e</sup> (μM)
WT	3470 ± 75	155 ± 6	3.0	3.0	3425 ± 139	24 ± 3
F55L	2088 ± 66	128 ± 9	1.5	1.5	2408 ± 112	22 ± 3
I65S	2214 ± 130	168 ± 20	1.4	1.0	3762 ± 152	29 ± 3
H170Q	2174 ± 37	125 ± 4	3.1	3.6	2197 ± 43	25 ± 2
P275L	1706 ± 25	76 ± 3	1.6	2.3	3216 ± 67	65 ± 4
A300S	2990 ± 64	148 ± 6	2.4	3.7	3320 ± 58	17 ± 2
P314S <sup>c</sup>	780 ± 22	49 ± 2	1.9	1.3	760 ± 39	25 ± 4
Y414C <sup>d</sup>	1877 ± 51	104 ± 40	2.2	2.0	1870 ± 50	16 ± 2
Y417H <sup>d</sup>	2258 ± 54	135 ± 40	2.5	1.5	2866 ± 188	31 ± 4

Steady-state kinetic parameters of wild-type (WT) and variant tetrameric MBP-PAH fusion proteins. Activation fold represents the substrate activation as the ratio of specific activity with and without prior incubation with L-Phe. Apparent affinities for L-Phe ([S]<sub>0.5</sub>) and BH<sub>4</sub> (K<sub>m</sub>) and the Hill-coefficient (*h*) as a measure of cooperativity are shown.

<sup>a</sup> Enzyme kinetic parameters determined at variable L-Phe concentrations and standard BH<sub>4</sub> concentration in three independent experiments.

<sup>b</sup> Enzyme kinetic parameters determined at variable BH<sub>4</sub> concentrations and standard L-Phe concentration in three independent experiments.

<sup>c</sup> L-Phe concentrations restricted to 0–250 μM.

<sup>d</sup> L-Phe concentrations restricted to 0–500 μM.

<sup>e</sup> Values are given as means ± SEM.

protein and shows a high quantum yield in its bound state but not when solved in aqueous buffers.<sup>38</sup> ANS-fluorescence analysis of tetrameric wild-type PAH fusion proteins revealed a low-temperature transition and a high-temperature transition, with their respective midpoints at 47.3°C and 55.0°C. This is in agreement with previous results obtained by differential scanning calorimetry.<sup>37</sup>

The two mutations located in the regulatory domain (F55L, I65S) induced alterations in unfolding patterns. An elevated fluorescence signal for I65S in comparison to wild-type was detected in the ground state at 25°C. This indicates an increased hydrophobicity due to partial protein unfolding. The same was true to a minor extent for F55L.

**Table 3. Proteolytic Stability of Wild-Type and Variant PAH**

Missense Mutation	t <sub>1/2</sub> FP (% of WT)			t <sub>1/2</sub> PAH (% of WT)		
	SEM	p Value		SEM	p Value	
WT	100			100		
F55L	71	7	0.039	75	15	ns
I65S	34	7	0.001	85	17	ns
H170Q	26	5	0.001	60	12	0.003
P275L	40	4	0.001	55	16	0.002
A300S	31	9	0.001	50	16	0.001
P314S	167	10	0.013	143	16	0.019
Y414C	47	13	0.004	70	16	0.017
Y417H	52	4	0.003	86	18	ns

Stability of wild-type (WT) and variant PAH against limited proteolysis by proteinase K. Degradation of the MBP-PAH fusion protein and formation with subsequent degradation of the PAH fragment were probed by western-blotting analyses. Densitometry data were normalized to intact MBP-PAH fusion protein and the resulting data points were fitted by single exponential function (MBP-PAH fusion proteins) and by double exponential Bateman function (PAH fragment). The calculated half-lives of fusion proteins (t<sub>1/2</sub> FP) and of PAH fragments (t<sub>1/2</sub> PAH) are given in percent ± SEM of *n* = 4 independent experiments. Significances for the differences between wild-type and the variants were calculated by two-tailed Student's *t* test.

During thermal unfolding, F55L showed a left-shift of the low-temperature transition in comparison with the wild-type protein (t<sub>m1/2</sub> 43.7°C), whereas a complete loss of the low-temperature transition was observed for I65S. By contrast, neither F55L nor I65S significantly affected the high-temperature transition. These findings indicate that the two mutations located in the regulatory domain induced misfolding and facilitated unfolding of the respective domain but did not influence the conformational stability of the catalytic domain.

Thermal unfolding of variant PAH was also affected by the four mutations located in the catalytic domain. All variants but P275L showed elevated ground-state levels of ANS fluorescence. All residue substitutions in the catalytic domain induced a left-shift of the low-temperature transition that reached statistical significance for A300S (t<sub>m1/2</sub> 44.6°C) and P275L (t<sub>m1/2</sub> 44.1°C). Interestingly, none of the mutations located in the catalytic domain significantly altered the high-temperature transition, indicating that these mutations did not affect unfolding of the catalytic domain itself but induced a loss of structural integrity of the regulatory domain.

Distinct alterations of thermal-unfolding parameters were observed for the two mutations located in the oligomerization domain (Y414C, Y417H). In contrast to other variants exhibiting accelerated thermal unfolding, the ground-state ANS fluorescence of Y414C and Y417H remained unchanged. However, the low-temperature transition was considerably left-shifted for Y414C (t<sub>m1/2</sub> 43.1°C) and for Y417H (t<sub>m1/2</sub> 41.9°C), whereas no effect on the high-temperature transition was detected. The residues Y414 and Y417 are located close to the site of interaction between the oligomerization domain and the regulatory domain within one PAH subunit. This might explain the effect of these side-chain replacements on the stability of the regulatory domain.

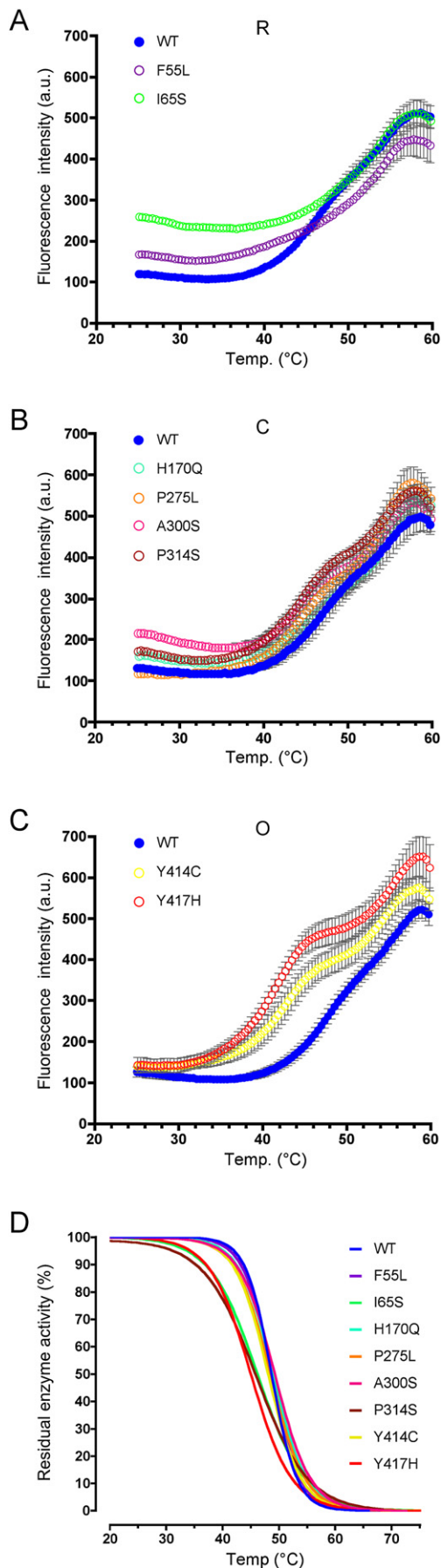


### Figure 3. PAH Mutations Lead to Accelerated Thermal Unfolding and Early Thermal Inactivation for Some Variants

(A–C) Thermal-unfolding profiles of wild-type and variant PAH monitored by ANS fluorescence. Intensities of the fluorescent dye ANS, which binds to hydrophobic groups of the protein presented upon unfolding, are plotted as a function of increasing temperatures. Error bars represent the mean  $\pm$  SEM of three independent experiments. The resulting denaturation curves consist of three segments: a native baseline and two partially overlapping phase transitions corresponding to unfolding of the regulatory domain (first transition) and of the catalytic domain (second transition), respectively. Ground-state ANS fluorescence was markedly elevated for I65S and A300S, indicating increased protein areas available for dye binding. I65S lacked the first transition; all other variants showed a left-shift of the first transition, indicating a destabilization of the regulatory domain in comparison to the wild-type. The second transition was not affected. R denotes regulatory domain; C denotes catalytic domain; O denotes oligomerization domain.

(D) Time course of thermal inactivation of wild-type and variant PAH. Proteins were incubated at increasing temperatures, and the residual enzyme activities were determined. Data points of residual activities were normalized to the initial enzyme activity and subjected to nonlinear regression analysis. For three variants that mapped to all domains (I65S, P314S, and Y417H), curves were left-shifted in comparison to the wild-type. The remaining five variants showed inactivation profiles comparable to that of wild-type PAH.

To assess the impact of thermal stress on PAH enzyme activity, we performed thermal-inactivation assays (Figure 3D). A reduction of the thermal-inactivation midpoints at 50% residual activity ( $T_m$ ) in comparison to the wild-type protein (48.8°C) was observed for three variants (I65S, P314S, Y417H,  $T_m$ ; 46.2, 44.5, and 45.0°C, respectively), whereas thermal inactivation of the other variants was not altered (Table 4). The affected residues mapped to all protein domains, demonstrating that mutations located outside the catalytic domain can also disturb enzyme function.

In summary, the results of thermal denaturation show that mutations in the PAH gene lead to substantial distortion of the protein's conformation, with particular impact on the regulatory domain.

### Local Amino Acid Replacements Can Affect Networks of Amino Acid Interactions

We constructed a composite 3D model of the full-length PAH tetramer and performed 3D structural modeling. Side-chain interactions in the local environment of amino acid residues affected by mutations in our patients were analyzed in order to investigate whether these amino acid residues are directly or indirectly involved in networks of side-chain interactions with functional and conformational impact. Our observations indicate that local amino acid replacements can induce global conformational changes, with remote effects on enzyme function and stability of the PAH.

**Table 4. Transition Midpoints and Midpoints of Thermal Inactivation for Thermal Denaturation of Wild-Type and Variant PAH**

Protein Domain Affected	ANS Fluorescence				Thermal Inactivation						
	Missense Mutation	$t_{m1/2}$	SEM	p Value	$t_{m2/3}$	SEM	p Value	Missense Mutation	$T_m$	SEM	p Value
-	WT	47.0	0.03		54.8	0.30		WT	48.85	0.52	
R	F55L	43.7	0.57	0.004	54.5	0.03	ns	F55L	47.96	0.72	ns
R	I65S	-	-	-	53.9	0.30	ns	I65S	46.17	0.56	0.042
-	WT	47.0	0.52		55.1	0.30					
C	H170Q	46.1	0.00	ns	55.4	0.52	ns	H170Q	48.92	0.20	ns
C	P275L	44.1	0.52	0.029	54.6	0.05	ns	P275L	48.40	0.76	ns
C	A300S	44.6	0.30	0.016	54.5	0.03	ns	A300S	49.46	0.61	ns
C	P314S	44.9	0.60	ns	54.5	0.03	ns	P314S	44.50	1.05	0.021
-	WT	47.9	0.52		55.1	0.30					
O	Y414C	43.1	0.30	0.001	54.5	0.03	ns	Y414C	48.42	0.43	ns
O	Y417H	41.9	0.30	0.001	55.4	0.03	ns	Y417H	44.99	0.21	0.011
-	WT (mean)	47.3	0.26		55.0	0.16					

Transition midpoints and midpoints of thermal inactivation obtained by thermal denaturation of wild-type PAH were compared to variants arising from mutations in the regulatory (R), catalytic (C), and the oligomerization (O) domain. For ANS-fluorescence three sets of experiments covering the mutations of different domains were carried out separately. The transition midpoints of the first ( $t_{m1/2}$ ) and the second transitions ( $t_{m2/3}$ ) were calculated by differentiation of the increasing part of the curves and are given in °C as means  $\pm$  SEM of  $n = 3$  independent experiments. For thermal inactivation residual activities were subjected to nonlinear regression analysis and the midpoints of thermal inactivation ( $T_m$ ) were calculated.  $T_m$ -values representing the temperature at 50% residual activity are given in °C as means  $\pm$  SEM of quadruplicate assays in  $n = 2$  independent experiments. Significances for the differences between wild-type and the variants were calculated by two-tailed Student's *t* test.

F55 and I65 are part of the hydrophobic core of the regulatory domain. Whereas F55L showed no impact on tetramer assembly, I65S displayed disturbed oligomerization, with increased amounts of dimeric protein in comparison to the wild-type (Figure 2). The assembly of dimers to tetrameric PAH is promoted by coiled-coil interactions of the C-terminal  $\alpha$  helices,<sup>7</sup> which are preceded by two antiparallel strands forming a  $\beta$  ribbon that comprises the dimerization motif (residues 411–427).<sup>15,17</sup> This  $\beta$  ribbon interacts with the regulatory domain in the same subunit and with the catalytic domain in the adjacent subunit within the dimer (Figures 4A–4D). The electrostatic interactions of D415 and E422 with R71 located in the prominent loop 68–75 play a pivotal role for the proper position of the dimerization motif, resulting in the right orientation of the  $\alpha$ -helical tetramerization motif for correct tetramer assembly. A distortion of the hydrophobic packing in the regulatory domain due to a substitution of the hydrophobic isoleucine by the polar serine at position 65 is supposed to lead to a displacement of the loop 68–75.<sup>10</sup> Hence, an alteration of the interaction of this loop with the dimerization motif might lead to dislocation of the  $\alpha$ -helical tetramerization motif and result in altered oligomerization with increased amounts of dimers.

Two of the PAH variants located in the catalytic domain (S310Y and R408W) were exclusively purified as high-molecular-weight aggregates lacking all residual enzyme activity (Table 1 and Figure 2). Formation of aggregates was previously described for R408W and structurally explained by potential disruption of hydrogen bonding to L308 and L311.<sup>7,8</sup> The S310 residue builds a hydrogen bond to G307, which interacts with L311. We thus inferred that both S310 and R408 are part of a hydrogen-bonding network formed by G307, L308, S310, L311, and R408 (Figures 4B

and 4C). The R408 residue is located between two proline residues, which define a sharp turn preceding the dimerization motif. This hinge region anchors the oligomerization domain to the catalytic domain and thereby ensures its proper orientation. A disruption of the network by the nonconservative substitutions S310Y and R408W could therefore well induce severe distortion of the protein's oligomeric state.

P314 adopts a central position in a network that comprises residues of the regulatory and the catalytic domain (Figure 4C). There is only one direct interaction between the backbone carbonyl of P314 and the backbone amide of Y317. However, the P314 residue is located in a loop (residues 311–314) connecting  $\alpha$  helices C $\alpha$ 8 and C $\alpha$ 9 that define the active site. The neighboring residues D315 and A313 form a network of interactions with R252 near the pterin-binding loop (residues 248–251), with K113 in the regulatory domain, and with D27 in the autoregulatory sequence. Thus, local changes of the protein conformation in the neighborhood of P314 could induce structural changes at the active site, at the pterin-binding site, and in the regulatory domain. This is in line with the observation that the variant P314S affected various enzyme kinetic parameters with low residual activity, loss of activation, and reduced cooperativity.

Y414C and Y417H, the variants arising from mutations mapping to the oligomerization domain, surprisingly exhibited clearly different oligomerization patterns although they are located in close proximity to each other. Both residues are part of the dimerization motif (Figure 4D). Y414 interacts with the catalytic domain of the same subunit, whereas Y417 is located at the interface of monomer-monomer interactions in the dimer, where it builds a network with T238, R261, and Q304 of the adjacent subunit.

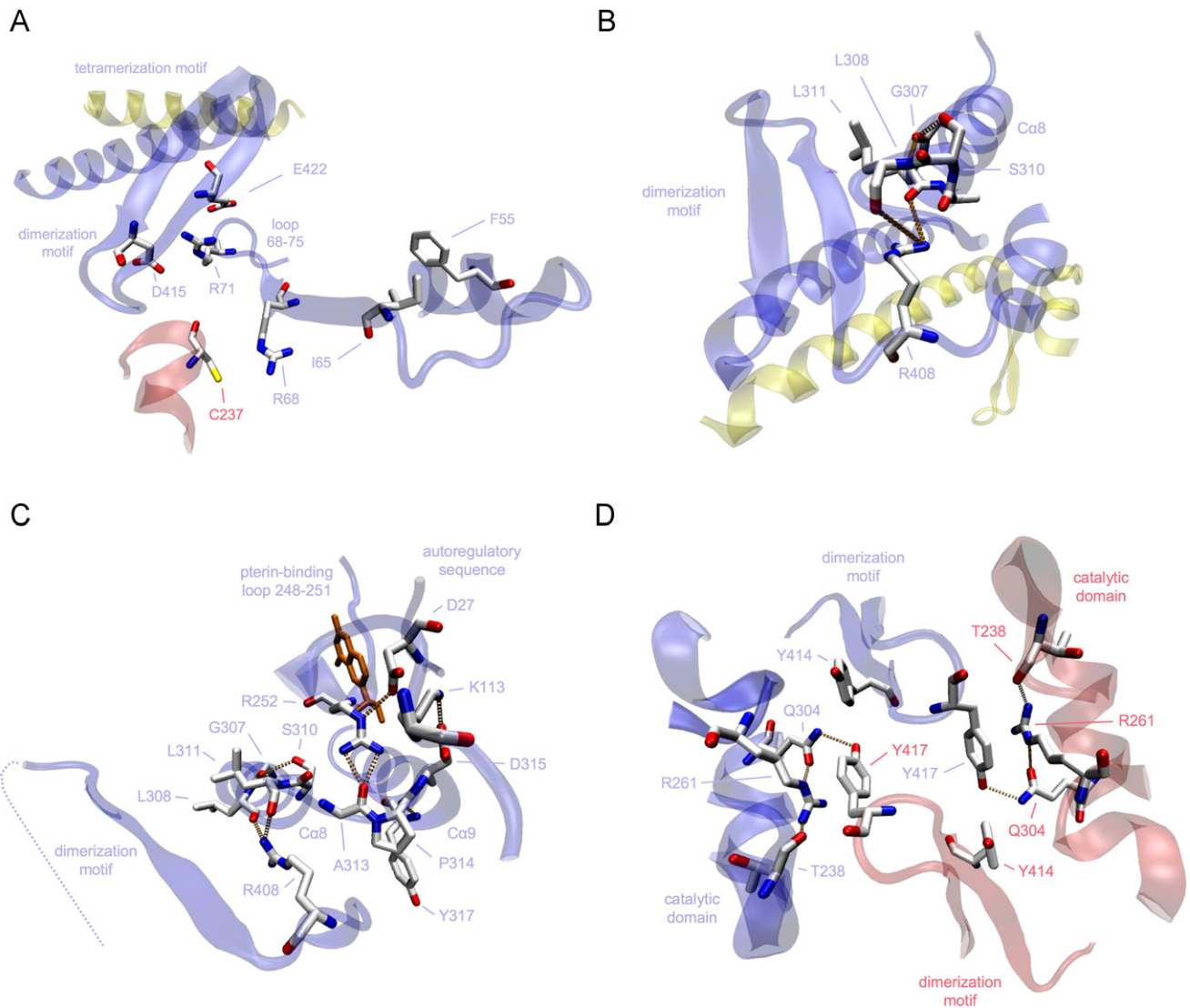


**Figure 4. Amino Acid Residues Affected by PAH Mutations Are Involved in Functional Networks of Side-Chain Interactions**

Selected parts of subunit backbones are shown as ribbon representations, and selected residues are depicted as stick models with carbon atoms in white, oxygen atoms in red, and nitrogen atoms in blue. Hydrogen bonds are shown as golden dotted lines.

(A) Residues F55 and I65 are located in the hydrophobic core of the regulatory domain (subunit A, blue) followed by the prominent loop 68–75. Upon substrate activation, R68 builds a hydrogen bond to C237 in the catalytic domain of the adjacent monomer (subunit D, red). R71 establishes electrostatic interactions with D415 and E422 in the dimerization motif, followed by coiled-coil interaction of the tetramerization motif with the adjacent dimer (subunit B, yellow). The electrostatic interactions are supposed to hold the  $\beta$ -ribbon in its proper spatial position resulting in the right orientation of the  $\alpha$ -helical tetramerization motif.

(B) Residues S310 and R408 are both part of a hydrogen-bonding network that anchors the entire oligomerization domain to the catalytic domain within one subunit. The coiled-coil interaction of subunits A (blue) and B (yellow) of both dimers contributes to tetramer assembly. R408 builds hydrogen bonds to the main-chain carbonyl oxygens of L308 and L311 located in the active-site helix  $C\alpha 8$ . S310 contributes to this network through interaction with G307 that builds a hydrogen bond to the main-chain amide of L311.

(C) P314 is part of the loop 311–314 connecting  $\alpha$  helices  $C\alpha 8$  and  $C\alpha 9$  that define the bottom of the active site. The network of R252, A313, P314, D315, and Y317 contributes to the correct spatial orientation of the active site and the pterin-binding loop 248–251. It is expanded via interaction with residues D27, located in the intrinsic autoregulatory sequence (1–33), and K113, located in a hinge-bending region (111–117) connecting the catalytic to the regulatory domain. This area is in close proximity to the network comprising residues S310 and R408 (B), which constitutes the connection of the whole region with the dimerization motif of the oligomerization domain.  $BH_4$  at the active site is shown as an orange stick model.

(D) Y414 and Y417 are located in a loop connecting two antiparallel  $\beta$  strands forming the dimerization motif. Y417 joins a network comprising residues Q304, R261, and T238, which tightly links the dimerization motif to the catalytic domain of the adjacent subunit (subunit A, blue; subunit D, red). The hydroxyl group of Y417 builds a hydrogen bond to Q304, and the aromatic ring of Y417 stacks with the positively charged guanidinium group of R261. Q304 and T238 are connected to R261 via hydrogen bonds. Y414 is localized in close proximity to residue Y417 but does not contribute to the monomer-monomer interaction.

Y417H is supposed to disrupt the hydrogen bond to Q304 and to damage the polar  $\pi$  stacking due to repulsions between the histidine and the positively charged guanidinium group of R261. This would result in hindrance of dimer formation with the appearance of monomers, and, as a consequence, disturbed tetramerization.

Taken together, the results of the *in silico* structural analysis of this subset of variants support the notion that local replacement of an amino acid at one site can disturb amino acid networks and, as a consequence, induce global changes in conformation that also affect remote parts of the protein at the functional level.

## Discussion

Despite the severe clinical phenotype of PKU, many missense mutations in the *PAH* gene have previously been shown to be associated with surprisingly high residual enzyme activities *in vitro*. It therefore has to be anticipated that mutations lead to loss of function through mechanisms other than impaired catalysis. Previous studies reported on *PAH* protein aggregation and rapid degradation,<sup>3,4,18,39</sup> raising the hypothesis that aberrant folding is a consequence of *PAH* mutations. Recent work substantiated this hypothesis, providing predictions about the effect of *PAH* mutations on native-state-protein stability.<sup>23</sup> Here, we present several lines of experimental evidence that support the hypothesis that *PAH* missense mutations associated with the newly recognized clinical phenotype of BH<sub>4</sub>-responsive *PAH* deficiency lead to protein misfolding. Two mutations (S310Y and R408W) caused severe structural distortion, with protein aggregation and complete loss of enzyme function. The others showed milder alterations of conformation but were associated with impaired enzyme-kinetic parameters, oligomerization, and protein stability at different degrees. Moreover, we showed that *PAH* mutations not only have an impact on the local structural environment of the affected side chain but rather induce alterations consistent with distortion of the enzyme's global conformation.

Interestingly, all variant *PAH* proteins analyzed in our study showed disturbed regulation. Allostery in general and *PAH* allostery in particular are complex events in which numerous side-chain interactions transmit structural changes throughout the whole oligomer. Extensive previous work has defined specific sites that are involved in *PAH* allostery.<sup>12,15,34</sup> Allosteric conformational changes in substrate binding result not only in positive cooperativity but also in activation of the enzyme. We observed that all but one variant led to reduced cooperativity, and six mutations that mapped to all three domains induced a loss of substrate activation. This led us to assume that mutations affecting sites involved in allostery cause a cascade of structural consequences, with alteration of conformational flexibility. As a result, remote functional units of side-chain interactions could be disturbed. Indeed, we ob-

served a negative impact of the I65S mutation located in the regulatory domain on the tetramer-dimer equilibrium. On a structural level, this can be explained by the multiple interactions required for *PAH* oligomerization that are not limited to the oligomerization domains but also involve allosteric contacts of all domains.

Additional evidence for protein misfolding arose from results demonstrating destabilization of variant *PAH* against proteolytic attack by proteinase K. In general, misfolded or partly unfolded proteins show enhanced backbone flexibility and thus facilitate proteolytic attack.<sup>36</sup> Results from limited proteolysis pointed to altered folding of the N-terminal regulatory domain. Moreover, mutations located on the protein surface (H170Q, P275L) were shown to be particularly prone to proteolytic attack, whereas mutations buried in the core of the protein (F55L, I65S, Y417H) were not. Direct experimental evidence for alterations in global protein conformation arose from the analysis of *PAH* hydrophobicity in the ground state and during thermal denaturation. Presentation of hydrophobic groups at the variant protein's surface caused by protein misfolding facilitates binding of the ANS fluorophore. Indeed, an increase in ANS fluorescence in the ground state was observed for the two mutations in the regulatory domain and for most mutations in the catalytic domain. Interestingly, all variant *PAH* showed accelerated thermal unfolding. Furthermore, our investigations revealed that independent of the position of the affected residue, *PAH* mutations had the most impact on the unfolding of the regulatory domain. This was confirmed by analysis of the inactivation of enzyme function by thermal stress. Only three mutations led to accelerated thermal inactivation (I65S, P314S, Y417H); among these, just one mapped to the catalytic domain. Altogether, data from stability assays indicate that the structural conformation of the *PAH* regulatory domain is particularly unstable. This observation can be explained by the structural characteristics of this domain. Recently, Liberles et al. provided strong evidence that the regulatory domain of *PAH* comprises an evolutionary mobile regulatory module, the ACT domain.<sup>12</sup> It facilitates allosteric regulation via transmission of finely tuned conformational changes, a process that appears to be set by the regulatory domains' interactions with the partner domains. These interactions require a high degree of conformational flexibility. For *PAH* isolated from a cold-adapted organism, it was shown that an increase in conformational flexibility is accompanied by an increase in thermostability.<sup>40</sup> Thus, the mobility of the regulatory domain that allows for complex regulation of activity and the oligomeric state might on the other hand cause reduced stability against thermal stress and proteolytic attack. Moreover, the extensive networking of the regulatory domain with other parts of the protein could account for the adoption of misfolding from remote sites. By contrast, missense mutations, if not structurally disruptive, hardly affected the integrity of the catalytic domain. This was shown by unchanged patterns of thermal unfolding of the catalytic

domain and further supported by the variant's high residual enzyme activity and minor changes in thermal-inactivation experiments. The domain's dense tertiary structure with few flexible regions could be the reason for these observations.

Taken together, the results presented here indicate that *PAH* missense mutations can lead to protein misfolding and conformational destabilization at different degrees. Our findings are in agreement with recent results from computational analyses using the FoldX algorithm. This study showed that a significant share of a large set of *PAH* mutations is predicted to provoke protein misfolding. Moreover, the authors raised the hypothesis that residues buried in the 3D structure, unlike those in flexible regions, are particularly prone to severe misfolding.<sup>23</sup> Our findings confirm this at the experimental level for a subset of ten mutations identified in patients with BH<sub>4</sub>-responsive *PAH* deficiency. Mutations at the center of the protein structure (S310Y, R408W) were shown to lead to severe aggregation and complete disruption of structural integrity. Conversely, mutations in flexible regions of the protein (H170Q, P275L, P314S, Y417H) did not primarily show severe protein misfolding. However, they can indeed cause milder conformational changes, which still exert deleterious effects on enzyme function. Features like oligomerization, allostery, activation, and cooperativity need complex conformational rearrangements, which are communicated through flexible regions of the protein via networks of amino acid interactions. Our observations imply that mutations, even those in flexible protein regions, can severely affect enzyme function and stability if they directly or indirectly disrupt these networks. In addition to our results from naturally occurring mutations, this was previously shown by analysis of artificial mutations of amino acid residues in flexible hinge-bending regions. These are involved in substrate-triggered molecular motions, and the corresponding proteins showed a reduced conformational stability in comparison to that of wild-type *PAH*.<sup>13</sup> Finally, two observations exemplify that there also appears to be no general rule for missense mutations of buried residues leading to severe misfolding with protein destabilization and impaired enzyme function. Both A300 and P314 are located in the active center of the protein; A300 is part of helix C $\alpha$ 8, which together with helix C $\alpha$ 9 defines the catalytic core, whereas P314 lies in a flexible loop between helices C $\alpha$ 8 and C $\alpha$ 9. A300S led to conformational destabilization, with distinct proneness to proteinase K and elevated ground-state ANS fluorescence. Nonetheless, enzyme function remained virtually unaffected. Conversely, P314S showing a clear stabilization toward proteinase K led to a marked reduction in enzyme activity and to accelerated thermal inactivation.

The results from our experimental work revealed that *PAH* misfolding is probably communicated throughout the protein by disruption of functionally crucial networks of amino acid interactions. Thus, the classical domain-associated view of mutational effects on the protein might

be insufficient for understanding of the molecular phenotype, and it disregards the well-known complexity in structure and regulation of the *PAH* protein.<sup>15,37</sup> We therefore propose a view of *PAH* that not only considers three primary-structure domains but takes into account that the *PAH* enzyme is an entity of functional units that arise from the tertiary and quaternary protein structure. If this holds true, mutations in the *PAH* gene exert their effects by disturbance of these functional units.

PKU has evolved from a model of a genetic disease that leads to severe neurologic impairment to a model of a treatable protein-folding disease with loss of function. The new insights into molecular mechanisms of protein misfolding are a prerequisite for the unraveling of how the natural cofactor BH<sub>4</sub> corrects the biochemical consequences of *PAH* gene mutations and will help treatment of patients on an individually tailored basis.

### Supplemental Data

One supplemental table is available with this article online at <http://www.ajhg.org/>.

### Acknowledgments

This work was supported by the Bavarian Genome Research Network (BayGene). We are indebted to our patients and to their families; to Eduard Manzinger for generating the expression clones; to Susi Wullinger for excellent technical assistance; to Doris Bruer for genotyping; to Esther M Maier for important discussions; and to Dietrich Reinhardt for continuous support. This article is part of an M.D. thesis to be submitted by M.S. and of Ph.D. theses to be submitted by D.D.M. and by M.K.D.

Received: February 19, 2008

Revised: May 9, 2008

Accepted: May 17, 2008

Published online: June 5, 2008

### Web Resources

The URLs for data presented herein are as follows:

BIOPKU: International Database of Patients and Mutations causing BH<sub>4</sub>-responsive HPA/PKU, <http://www.bh4.org/biopku.html>

Online Mendelian Inheritance in Man (OMIM), <http://www.ncbi.nlm.nih.gov/Omim/>

PAHdb, <http://www.pahdb.mcgill.ca/>

PDB, <http://www.rcsb.org/pdb/>

### References

1. Scriver, C.R. (2007). The *PAH* gene, phenylketonuria, and a paradigm shift. *Hum. Mutat.* 28, 831–845.
2. Muntau, A.C., Röschinger, W., Habich, M., Demmelmair, H., Hoffmann, B., Sommerhoff, C.P., and Roscher, A.A. (2002). Tetrahydrobiopterin as an alternative treatment for mild phenylketonuria. *N. Engl. J. Med.* 347, 2122–2132.

3. Erlandsen, H., Pey, A.L., Gámez, A., Pérez, B., Desviat, L.R., Aguado, C., Koch, R., Surendran, S., Tyring, S., Matalon, R., et al. (2004). Correction of kinetic and stability defects by tetrahydrobiopterin in phenylketonuria patients with certain phenylalanine hydroxylase mutations. *Proc. Natl. Acad. Sci. USA* *101*, 16903–16908.
4. Pey, A.L., Pérez, B., Desviat, L.R., Martínez, M.A., Aguado, C., Erlandsen, H., Gámez, A., Stevens, R.C., Thóroflsson, M., Ugarte, M., et al. (2004). Mechanisms underlying responsiveness to tetrahydrobiopterin in mild phenylketonuria mutations. *Hum. Mutat.* *24*, 388–399.
5. Waters, P.J. (2003). How PAH gene mutations cause hyperphenylalaninemia and why mechanism matters: insights from in vitro expression. *Hum. Mutat.* *21*, 357–369.
6. Kobe, B., Jennings, I.G., House, C.M., Michell, B.J., Goodwill, K.E., Santarsiero, B.D., Stevens, R.C., Cotton, R.G., and Kemp, B.E. (1999). Structural basis of autoregulation of phenylalanine hydroxylase. *Nat. Struct. Biol.* *6*, 442–448.
7. Fusetti, F., Erlandsen, H., Flatmark, T., and Stevens, R.C. (1998). Structure of tetrameric human phenylalanine hydroxylase and its implications for phenylketonuria. *J. Biol. Chem.* *273*, 16962–16967.
8. Erlandsen, H., Fusetti, F., Martínez, A., Hough, E., Flatmark, T., and Stevens, R.C. (1997). Crystal structure of the catalytic domain of human phenylalanine hydroxylase reveals the structural basis for phenylketonuria. *Nat. Struct. Biol.* *4*, 995–1000.
9. Flatmark, T., and Stevens, R.C. (1999). Structural insight into the aromatic amino acid hydroxylases and their disease-related mutant forms. *Chem. Rev.* *99*, 2137–2160.
10. Erlandsen, H., and Stevens, R.C. (1999). The structural basis of phenylketonuria. *Mol. Genet. Metab.* *68*, 103–125.
11. Freimer, N., and Sabatti, C. (2003). The human genome project. *Nat. Genet.* *34*, 15–21.
12. Liberles, J.S., Thóroflsson, M., and Martínez, A. (2005). Allosteric mechanisms in ACT domain containing enzymes involved in amino acid metabolism. *Amino Acids* *28*, 1–12.
13. Stokka, A.J., Carvalho, R.N., Barroso, J.F., and Flatmark, T. (2004). Probing the role of crystallographically defined/predicted hinge-bending regions in the substrate-induced global conformational transition and catalytic activation of human phenylalanine hydroxylase by single-site mutagenesis. *J. Biol. Chem.* *279*, 26571–26580.
14. Andersen, O.A., Stokka, A.J., Flatmark, T., and Hough, E. (2003). 2.0 Å resolution crystal structures of the ternary complexes of human phenylalanine hydroxylase catalytic domain with tetrahydrobiopterin and 3-(2-thienyl)-L-alanine or L-norleucine: substrate specificity and molecular motions related to substrate binding. *J. Mol. Biol.* *333*, 747–757.
15. Thóroflsson, M., Teigen, K., and Martínez, A. (2003). Activation of phenylalanine hydroxylase: effect of substitutions at Arg68 and Cys237. *Biochemistry* *42*, 3419–3428.
16. Bjørge, E., Knappskog, P.M., Martínez, A., Stevens, R.C., and Flatmark, T. (1998). Partial characterization and three-dimensional-structural localization of eight mutations in exon 7 of the human phenylalanine hydroxylase gene associated with phenylketonuria. *Eur. J. Biochem.* *257*, 1–10.
17. Knappskog, P.M., Flatmark, T., Aarden, J.M., Haavik, J., and Martínez, A. (1996). Structure/function relationships in human phenylalanine hydroxylase. Effect of terminal deletions on the oligomerization, activation and cooperativity of substrate binding to the enzyme. *Eur. J. Biochem.* *242*, 813–821.
18. Waters, P.J., Parniak, M.A., Akerman, B.R., and Scriver, C.R. (2000). Characterization of phenylketonuria missense substitutions, distant from the phenylalanine hydroxylase active site, illustrates a paradigm for mechanism and potential modulation of phenotype. *Mol. Genet. Metab.* *69*, 101–110.
19. Waters, P.J., Parniak, M.A., Hewson, A.S., and Scriver, C.R. (1998). Alterations in protein aggregation and degradation due to mild and severe missense mutations (A104D, R157N) in the human phenylalanine hydroxylase gene (PAH). *Hum. Mutat.* *12*, 344–354.
20. Guldberg, P., Rey, F., Zschocke, J., Romano, V., Francois, B., Michiels, L., Ullrich, K., Hoffmann, G.F., Burgard, P., Schmidt, H., et al. (1998). A European multicenter study of phenylalanine hydroxylase deficiency: classification of 105 mutations and a general system for genotype-based prediction of metabolic phenotype. *Am. J. Hum. Genet.* *63*, 71–79.
21. Scriver, C.R. (2006). Preface. In *PKU and BH<sub>4</sub>-Advances in Phenylketonuria and Tetrahydrobiopterin*, N. Blau, ed. (Heilbronn: SPS Verlagsgesellschaft), pp. 23–31.
22. Scriver, C.R., and Waters, P.J. (1999). Monogenic traits are not simple: lessons from phenylketonuria. *Trends Genet.* *15*, 267–272.
23. Pey, A.L., Stricher, F., Serrano, L., and Martínez, A. (2007). Predicted effects of missense mutations on native-state stability account for phenotypic outcome in phenylketonuria, a paradigm of misfolding diseases. *Am. J. Hum. Genet.* *81*, 1006–1024.
24. Solstad, T., and Flatmark, T. (2000). Microheterogeneity of recombinant human phenylalanine hydroxylase as a result of nonenzymatic deamidations of labile amide containing amino acids. Effects on catalytic and stability properties. *Eur. J. Biochem.* *267*, 6302–6310.
25. Martínez, A., Knappskog, P.M., Olafsdottir, S., Døskeland, A.P., Eiken, H.G., Svebak, R.M., Bozzini, M., Apold, J., and Flatmark, T. (1995). Expression of recombinant human phenylalanine hydroxylase as fusion protein in *Escherichia coli* circumvents proteolytic degradation by host cell proteases. Isolation and characterization of the wild-type enzyme. *Biochem. J.* *306*, 589–597.
26. Gámez, A., Perez, B., Ugarte, M., and Desviat, L.R. (2000). Expression analysis of phenylketonuria mutations. Effect on folding and stability of the phenylalanine hydroxylase protein. *J. Biol. Chem.* *275*, 29737–29742.
27. Pey, A.L., and Martinez, A. (2005). The activity of wild-type and mutant phenylalanine hydroxylase and its regulation by phenylalanine and tetrahydrobiopterin at physiological and pathological concentrations: an isothermal titration calorimetry study. *Mol. Genet. Metab.* *86 (Suppl 1)*, S43–S53.
28. Miranda, F.F., Teigen, K., Thóroflsson, M., Svebak, R.M., Knappskog, P.M., Flatmark, T., and Martínez, A. (2002). Phosphorylation and mutations of Ser(16) in human phenylalanine hydroxylase. Kinetic and structural effects. *J. Biol. Chem.* *277*, 40937–40943.
29. Copeland, R.A. (2000). *Enzymes: a practical introduction to structure, mechanism, and data analysis* (New York, Chichester: J. Wiley).
30. Novokhatny, V., and Ingham, K. (1997). Thermodynamics of maltose binding protein unfolding. *Protein Sci.* *6*, 141–146.
31. Guex, N., and Peitsch, M.C. (1997). SWISS-MODEL and the Swiss-PdbViewer: an environment for comparative protein modeling. *Electrophoresis* *18*, 2714–2723.

32. Humphrey, W., Dalke, A., and Schulten, K. (1996). VMD: visual molecular dynamics. *J. Mol. Graph.* *14*, 33–38, 27–28.
33. Nascimento, C., Botelho, H.M., Tavares de Almeida, I., Gomes, C.M., and Leandro, P. (2007). Folding rescue of mild PKU mutations by chemical chaperones. *J. Inherit. Metab. Dis.* *30* (Suppl 1), 11.
34. Pey, A.L., Thórolfsson, M., Teigen, K., Ugarte, M., and Martínez, A. (2004). Thermodynamic characterization of the binding of tetrahydropterins to phenylalanine hydroxylase. *J. Am. Chem. Soc.* *126*, 13670–13678.
35. Pey, A.L., Desviat, L.R., Gámez, A., Ugarte, M., and Pérez, B. (2003). Phenylketonuria: genotype-phenotype correlations based on expression analysis of structural and functional mutations in PAH. *Hum. Mutat.* *21*, 370–378.
36. Fontana, A., de Laureto, P.P., Spolaore, B., Frare, E., Picotti, P., and Zambonin, M. (2004). Probing protein structure by limited proteolysis. *Acta Biochim. Pol.* *51*, 299–321.
37. Thórolfsson, M., Ibarra-Molero, B., Fojan, P., Petersen, S.B., Sanchez-Ruiz, J.M., and Martínez, A. (2002). L-phenylalanine binding and domain organization in human phenylalanine hydroxylase: a differential scanning calorimetry study. *Biochemistry* *41*, 7573–7585.
38. Royer, C.A. (1995). Fluorescence spectroscopy. *Methods Mol. Biol.* *40*, 65–89.
39. Pérez, B., Desviat, L.R., Gomez-Puertas, P., Martínez, A., Stevens, R.C., and Ugarte, M. (2005). Kinetic and stability analysis of PKU mutations identified in BH4-responsive patients. *Mol. Genet. Metab.* *86* (Suppl 1), S11–S16.
40. Leiros, H.K., Pey, A.L., Innselset, M., Moe, E., Leiros, I., Steen, I.H., and Martínez, A. (2007). Structure of phenylalanine hydroxylase from *Colwellia psychrerythraea* 34H, a monomeric cold active enzyme with local flexibility around the active site and high overall stability. *J. Biol. Chem.* *282*, 21973–21986.

# Activation of Phenylalanine Hydroxylase Induces Positive Cooperativity toward the Natural Cofactor<sup>\*[5]</sup>

Received for publication, March 16, 2010, and in revised form, June 29, 2010. Published, JBC Papers in Press, July 27, 2010, DOI 10.1074/jbc.M110.124016

Søren W. Gersting<sup>†1</sup>, Michael Staudigl<sup>†1,2</sup>, Marietta S. Truger<sup>‡</sup>, Dunja D. Messing<sup>‡</sup>, Marta K. Danecka<sup>‡</sup>, Christian P. Sommerhoff<sup>§</sup>, Kristina F. Kemter<sup>‡</sup>, and Ania C. Muntau<sup>†3</sup>

From the <sup>†</sup>Department of Molecular Pediatrics, Dr. von Hauner Children's Hospital, Munich 80337 and the <sup>§</sup>Department of Clinical Chemistry and Clinical Biochemistry, Surgical Clinic, Ludwig-Maximilians-University, Munich 80336, Germany

Protein misfolding with loss-of-function of the enzyme phenylalanine hydroxylase (PAH) is the molecular basis of phenylketonuria in many individuals carrying missense mutations in the *PAH* gene. PAH is complexly regulated by its substrate L-Phenylalanine and its natural cofactor 6*R*-L-erythro-5,6,7,8-tetrahydrobiopterin (BH<sub>4</sub>). Sapropterin dihydrochloride, the synthetic form of BH<sub>4</sub>, was recently approved as the first pharmacological chaperone to correct the loss-of-function phenotype. However, current knowledge about enzyme function and regulation in the therapeutic setting is scarce. This illustrates the need for comprehensive analyses of steady state kinetics and allostery beyond single residual enzyme activity determinations to retrace the structural impact of missense mutations on the phenylalanine hydroxylating system. Current standard PAH activity assays are either indirect (NADH) or discontinuous due to substrate and product separation before detection. We developed an automated fluorescence-based continuous real-time PAH activity assay that proved to be faster and more efficient but as precise and accurate as standard methods. Wild-type PAH kinetic analyses using the new assay revealed cooperativity of activated PAH toward BH<sub>4</sub>, a previously unknown finding. Analyses of structurally preactivated variants substantiated BH<sub>4</sub>-dependent cooperativity of the activated enzyme that does not rely on the presence of L-Phenylalanine but is determined by activating conformational rearrangements. These findings may have implications for an individualized therapy, as they support the hypothesis that the patient's metabolic state has a more significant effect on the interplay of the drug and the conformation and function of the target protein than currently appreciated.

Phenylalanine hydroxylase (PAH<sup>4</sup>; EC 1.14.16.1) is a non-heme iron monooxygenase that catalyzes the hydroxylation of the substrate L-Phe to L-Tyr in the presence of its natural cofac-

tor 6*R*-L-erythro-5,6,7,8-tetrahydrobiopterin (BH<sub>4</sub>) and molecular dioxygen. Mutations in the *PAH* gene can lead to protein misfolding with loss of function and subsequently to phenylketonuria ([MIM 261600]), the most common inborn error of amino acid metabolism in European-descended populations (1, 2). Pharmacological doses of BH<sub>4</sub> can correct protein misfolding in a significant number of patients with PAH deficiency, and sapropterin dihydrochloride, the synthetic form of the natural PAH cofactor, was recently approved as the first pharmacological chaperone to treat phenylketonuria patients (3–5).

The enzyme is a homotetramer built as a dimer of dimers with each subunit consisting of an N-terminal regulatory domain (residues 1–142), a catalytic domain (residues 143–410), and a C-terminal oligomerization domain (residues 411–452). Elaborate functional and kinetic studies have revealed complex enzyme regulation by its substrate and cofactor as well as by phosphorylation (6–8). Binding of the substrate induces a catalytically competent (activated) enzyme, whereas binding of BH<sub>4</sub> leads to formation of an inactive dead-end PAH-BH<sub>4</sub> complex (9–12). These regulatory mechanisms require reversible conformational changes that are transmitted throughout the enzyme upon binding of BH<sub>4</sub> and L-Phe (13). Structural analyses of BH<sub>4</sub> binding revealed that the cofactor interacts with the N-terminal autoregulatory sequence and the pterin binding loop, leading to stabilizing hydrogen bonds and to formation of a binary enzyme-BH<sub>4</sub> complex (14). The largest conformational changes were observed upon binding of L-Phe, where local changes at the active site are propagated globally through hinge-bending motions in the catalytic domain, also altering the position and orientation of bound BH<sub>4</sub> (13, 15) and of the regulatory domain (16).

Analyses of the effects of missense mutations in the *PAH* gene on PAH enzyme kinetic properties have shown that residual enzyme activity generally is high, yet allostery is often disturbed (17–19), with reduced cooperativity for substrate binding, decreased substrate activation, or altered affinity to the substrate and the cofactor. Thus, the evaluation of kinetics and allostery can help to assess to which extent local single amino acid replacements lead to global conformational alterations compromising enzyme function. In this context, comprehensive steady state kinetic analyses beyond single determination of residual enzyme activity are needed to retrace the structural impact of missense mutations on the phenylalanine hydroxylating system. Yet, the current standard activity assays requiring substrate and product separation before L-Tyr detection by radioactivity or fluorescence signals (20–22) are laborious and

\* This work was supported by the Bavarian Genome Research Network (BayGene).

[5] The on-line version of this article (available at <http://www.jbc.org>) contains supplemental Materials and Methods, Tables 1 and 2, and Figs. 1 and 2.

<sup>1</sup> These authors contributed equally to this work.

<sup>2</sup> Part of an M.D. thesis to be submitted at Ludwig-Maximilians-University, Munich, Germany.

<sup>3</sup> To whom correspondence should be addressed: Lindwurmstrasse 4, 80337 Munich, Germany. Tel.: 49-89-5160-7928; Fax: 49-89-5160-7792; E-mail: ania.muntau@med.lmu.de.

<sup>4</sup> The abbreviations used are: PAH, phenylalanine hydroxylase; IFE, inner filter effect; BH<sub>4</sub>, 6*R*-L-erythro-5,6,7,8-tetrahydrobiopterin; L-Phe, L-phenylalanine; L-Tyr, L-tyrosine.

time consuming. In addition, designed as end-point measurements, these discontinuous assays assume a linear range of activity for the time period chosen, although variations of temperature and pH as well as concentrations of enzyme, substrate, and cofactor can dramatically change the linearity of a reaction over the fixed time window (23). Therefore, we aimed to develop an automated continuous real-time assay of PAH activity. Our new fluorescence-based multi-well assay has given rise to the possibility of evaluating PAH kinetics and allostery faster and more efficiently but as precisely and accurately as the standard methods. Surprisingly, by application of this technique, the data obtained for BH<sub>4</sub>-dependent PAH kinetics did not fit to the well accepted model of a single hyperbolic function (Michaelis-Menten kinetic model). Instead, a good fit was found using a sigmoidal binding curve (Hill kinetic model). Although positive cooperativity for the binding of L-Phe has been extensively studied (24, 25), cooperativity toward BH<sub>4</sub> has not been described to date. However, cofactor-dependent kinetic studies were routinely performed using the non-activated PAH enzyme (19, 26), whereas an L-Phe preincubated (activated) enzyme was applied in our experiments.

Thus, we aimed to characterize BH<sub>4</sub>-dependent PAH kinetics in more detail and to investigate whether activation of PAH is a prerequisite for the positive cooperativity observed. Real-time fluorescence kinetic analyses using L-Phe-activated and non-activated PAH were performed. Furthermore, genetic variants of PAH, which are structurally preactivated by single amino acid replacements, were analyzed. To discriminate between non-cooperative and cooperative enzyme kinetics, in-depth model comparisons by nonlinear regression analysis were conducted with fitting of the data to the Michaelis-Menten or the Hill kinetic model.

## EXPERIMENTAL PROCEDURES

**Expression and Purification of Recombinant PAH Enzymes**—The cDNA of human phenylalanine hydroxylase (EST clone obtained from Imagines, formerly RZPD, Germany) was cloned into the pMAL-c2E and pMAL-c2X expression vectors (New England Biolabs) encoding an N-terminal maltose-binding protein (MBP) tag and enterokinase or Factor Xa cleavage sites, respectively. PAH mutants were constructed by site-directed mutagenesis as described (17). *Escherichia coli* DH5 $\alpha$  were transformed with the expression vector for wild-type and mutant MBP-PAH fusion proteins. Proteins were purified by affinity chromatography (MBP Trap, GE Healthcare) followed by size-exclusion chromatography using a HiLoad 26/60 Superdex 200 column (GE Healthcare) on an ÄKTExpress system as previously described (17). The isolated tetrameric fusion proteins were collected, and protein concentrations were determined spectrophotometrically using  $\epsilon_{280}$  (1 mg/ml) = 1.63. Tetrameric fusion protein was cleaved by factor Xa (10 units of factor Xa:1 mg of fusion protein) at 4 °C for 16 h and isolated by size-exclusion chromatography using a HiLoad 16/60 Superdex 200 prep grade column (GE Healthcare). Protein concentrations of the cleaved tetrameric PAH were determined spectrophotometrically using  $\epsilon_{280}$  (1 mg/ml) = 1.0.

**Verifying Direct Fluorescence Detection of Enzymatic L-Tyr Production**—To verify the spectral separation needed for the direct in-well fluorescence detection of enzymatic L-Tyr production, L-Tyr (0–150  $\mu$ M) (Sigma) in 17 mM NaHepes, pH 7.3, was added to all wells of a 96-well plate (NUNC F96) containing a reaction mixture with 1 mg/ml catalase (Sigma), 10  $\mu$ M ferrous ammonium sulfate (Fe<sup>2+</sup>) (Fluka), and L-Phe (0–1000  $\mu$ M) (Sigma) yet lacking the apoenzyme and BH<sub>4</sub>. L-Tyr fluorescence intensity was subsequently measured using a fluorescence photometer (FLUOstar OPTIMA, BMG Labtech) at an excitation wavelength of 274 nm and an emission wavelength of 304 nm. Individual experiments were assayed as triplicates. All concentrations mentioned refer to a final volume of 204  $\mu$ l.

**Quantification of L-Tyr Production**—For the quantification of L-Tyr production, standards consisting of L-Tyr (0–463  $\mu$ M) and L-Phe (547  $\mu$ M) in 17 mM NaHepes, pH 7.3, 1 mg/ml catalase, and 10  $\mu$ M ferrous ammonium sulfate were measured before each experiment using the fluorescence photometer (excitation 274 nm, emission 304 nm). Individual experiments were assayed as triplicates before enzyme kinetic measurements on each experimental day. All concentrations mentioned refer to a final volume of 204  $\mu$ l.

**Analysis of the Inner Filter Effect (IFE) of BH<sub>4</sub>**—A 96-well plate was prepared with L-Tyr (0–150  $\mu$ M) in 17 mM NaHepes, pH 7.3, and a standard reaction mixture containing the standard concentration of 1 mM L-Phe in 17 mM NaHepes, pH 7.3, 1 mg/ml catalase, 10  $\mu$ M ferrous ammonium sulfate, and 15 mM NaHepes, pH 7.0. Subsequent to injection of BH<sub>4</sub> (0–125  $\mu$ M) (6R-L-erythro-5,6,7,8-tetrahydrobiopterin, Schircks Laboratories) stabilized in 2 mM dithiothreitol (DTT) (Fluka), L-Tyr fluorescence intensity was measured using the fluorescence photometer (excitation 274 nm, emission 304 nm). The IFE of BH<sub>4</sub> was corrected by defining a correction factor for each BH<sub>4</sub> concentration added to the reaction mixture:  $q = f$  (at each [BH<sub>4</sub>])/f (fluorophore alone), where  $f$  is the fluorescence intensity, and  $q$  is the correction factor for the substrate concentration (27, 28). All measurements were assayed as triplicates before enzyme kinetic measurements on each experimental day. All concentrations mentioned refer to a final volume of 204  $\mu$ l.

**Time-dependent Enzyme Activity Measurement**—For time-dependent enzyme activity measurements, the assay was performed with and without preincubation of the enzyme with 1 mM L-Phe. A reaction buffer containing 1 mg/ml catalase, 10  $\mu$ M ferrous ammonium sulfate, and the tetrameric MBP-PAH fusion protein (0.01 mg/ml) was prepared. After preincubation with 1 mM L-Phe in 22.35 mM NaHepes, pH 7.3, for 5 min at 25 °C, the reaction was initiated by the addition of 75  $\mu$ M BH<sub>4</sub> stabilized in 2 mM DTT. For enzyme activity measurements without L-Phe preincubation, the reaction was initiated by simultaneous injection of 1 mM L-Phe and 75  $\mu$ M BH<sub>4</sub>.

Time-dependent substrate production was assessed by detection of the increase in L-Tyr fluorescence intensity at an excitation wavelength of 274 nm and an emission wavelength of 304 nm using a fluorescence spectrophotometer (Cary Eclipse, Varian). All concentrations mentioned refer to the final concentration in a 204- $\mu$ l reaction mixture.

## PAH Cooperativity for BH<sub>4</sub>

**Multiwell Enzyme Activity Assay with and without L-Phe Preactivation**—For PAH activity measurement, L-Phe in 22.35 mM NaHepes, pH 7.3, was added to 12 wells of a 96-well plate with varying L-Phe concentrations (0–1000 μM) or at a constant L-Phe concentration (1 mM) using the injection system of a fluorescence photometer. A reaction buffer containing 1 mg/ml catalase, 10 μM ferrous ammonium sulfate, and the tetrameric MBP-PAH fusion protein (0.01 mg/ml) was prepared and injected in all 12 wells. After preincubation with L-Phe for 5 min at 25 °C, the reaction was initiated by the addition of BH<sub>4</sub> stabilized in DTT for a final concentration of 75 μM BH<sub>4</sub> with varying L-Phe concentrations (0–1000 μM) or varying BH<sub>4</sub> concentrations (0–125 μM) at 1 L-Phe concentration (1 mM) and 2 mM DTT.

For enzyme activity measurements without L-Phe preincubation, the reaction buffer was prepared and injected to 12 wells. The reaction was initiated by simultaneous injection of varying L-Phe concentrations (0–1000 μM) and 1 BH<sub>4</sub> concentration (75 μM) or 1 L-Phe concentration (1 mM) and varying BH<sub>4</sub> concentrations (0–125 μM).

Steady state kinetics of PAH were determined at 25 °C and a 60-s measurement time per well. Substrate production was assessed by detection of the increase in L-Tyr fluorescence intensity at an excitation wavelength of 274 nm and an emission wavelength of 304 nm using a fluorescence photometer (FLUOstar OPTIMA, BMG Labtech) and assayed as duplicates on 3 consecutive days. Fluorescence intensity signals were corrected for the quenching effect of BH<sub>4</sub>. All concentrations mentioned refer to the final concentration in a 204 μl reaction mixture.

For all enzyme activity measurements, fluorescence intensity was recorded and, after subtraction of the blank reaction, converted to enzyme activity units (nmol Tyr/min × mg protein) using the standard curve obtained by L-Tyr concentration measurements. Data were analyzed by nonlinear regression analysis using the single hyperbolic model (Michaelis-Menten kinetic model),

$$v = \frac{V_{\max}[S]}{K_m + [S]} \quad (\text{Eq. 1})$$

where  $v$  is the observed rate of enzyme catalysis,  $V_{\max}$  is the maximum rate of enzyme catalysis,  $[S]$  is the substrate concentration, and  $K_m$  is the substrate concentration at which  $V_{\max}/2$  is reached and the sigmoidal kinetic model (Hill kinetic model),

$$v = \frac{V_{\max}}{\left(1 + \left[\frac{EC_{50}}{[S]}\right]^h\right)} \quad (\text{Eq. 2})$$

where  $v$  is the observed rate of enzyme catalysis,  $V_{\max}$  is the maximum rate of enzyme catalysis,  $[S]$  is the substrate concentration,  $EC_{50}$  is the substrate concentration at which  $V_{\max}/2$  is reached, and  $h$  is the Hill coefficient (GraphPad Prism 4.0c). Values are given as the mean ± S.E. of three independent experiments. The coefficient of variation was determined as the ratio of the S.D. to the mean value. Comparison of model fitting was performed using the F-test (GraphPad Prism QuickCal), residuals of values, the S.D. of the residuals ( $S_{y,x}$ ), the runs test, and

the square of residuals ( $R^2$ ) (see supplemental Tables S1 and S2 and Fig. S2) (29–34).

**Tryptophan Fluorescence Measurements**—For tryptophan fluorescence emission scans, wild-type PAH, dimeric PAH 103–427, and variant PAH R68S were diluted to 11 μM subunits PAH (0.6 μg/μl) in 20 mM NaHepes and 200 mM NaCl, pH 7.0, containing 10 μM ferrous ammonium sulfate and 2 mM DTT. Fluorescence measurements were performed using a fluorescence spectrophotometer (Cary Eclipse, Varian) at an excitation wavelength of 295 nm with excitation and emission slits set to 2.5 and 5 nm, respectively.

**Differential Scanning Fluorimetry**—Differential scanning fluorimetry analyses were performed on a Cary Eclipse fluorescence spectrophotometer equipped with a temperature-controlled Peltier multicell holder (Varian). Denaturation of 6 μM MBP-PAH subunits diluted in 20 mM NaHepes and 200 mM NaCl, pH 7.0, containing 2 mM DTT was performed by scanning a temperature range of 25 to 70 °C at a rate of 1.2 °C/min. In the cases indicated, L-Phe was added to a final concentration of 1 mM. Changes in 8-anilino-1-naphthalenesulfonic acid fluorescence emission (Sigma) were monitored at 500 nm (excitation 395 nm, slit widths 5.0/10.0 nm). The phase transitions of three to eight independent experiments were determined, and the respective transition midpoints were calculated using the Boltzmann sigmoidal equation. Transition midpoints for wild-type and variant PAH with and without L-Phe were plotted and compared using a paired  $t$  test.

## RESULTS

**Direct Fluorescence Detection of Enzymatic L-Tyr Production**—To date measurement of PAH activity is routinely performed using a standard reaction mixture containing the apoenzyme, Fe<sup>2+</sup>, L-Phe, and BH<sub>4</sub> followed by time-consuming chromatographic separation of substrate and product. Yet differences in the fluorescence properties of the aromatic amino acids L-Phe and L-Tyr, such as emission and excitation wavelengths as well as the quantum yield, would allow for spectral separation of these substances even in a mixed solution.

To determine spectral separation of the two substances, we assessed fluorescence signal intensities of varying L-Tyr concentrations at 304 nm (35), the L-Tyr emission wavelength, as a function of increasing L-Phe concentrations. We showed that direct in-well detection of L-Tyr was unaffected by the various L-Phe concentrations used in our assay (Fig. 1A and supplemental Fig. 1A). This was true for all L-Tyr concentrations expected in the following enzyme kinetic measurements. However, L-Tyr fluorescence signal intensities decreased with increasing BH<sub>4</sub> concentrations (supplemental Fig. 1B), suggesting an IFE of BH<sub>4</sub> on L-Tyr excitation and emission. Therefore, we determined specific correction factors on the basis of the factorial decrease of signal intensity for every BH<sub>4</sub> concentration added to account for the IFE (Fig. 1B) (27, 28). Evaluation of the IFE of BH<sub>4</sub> and calculation of the correction factor for each BH<sub>4</sub> concentration added to the reaction mixture was performed before each enzyme kinetic measurement (Fig. 1B).

The analysis of steady state enzyme kinetics using direct in-well detection of L-Tyr production revealed a time-dependent change of enzyme activity upon the addition of BH<sub>4</sub>, with an

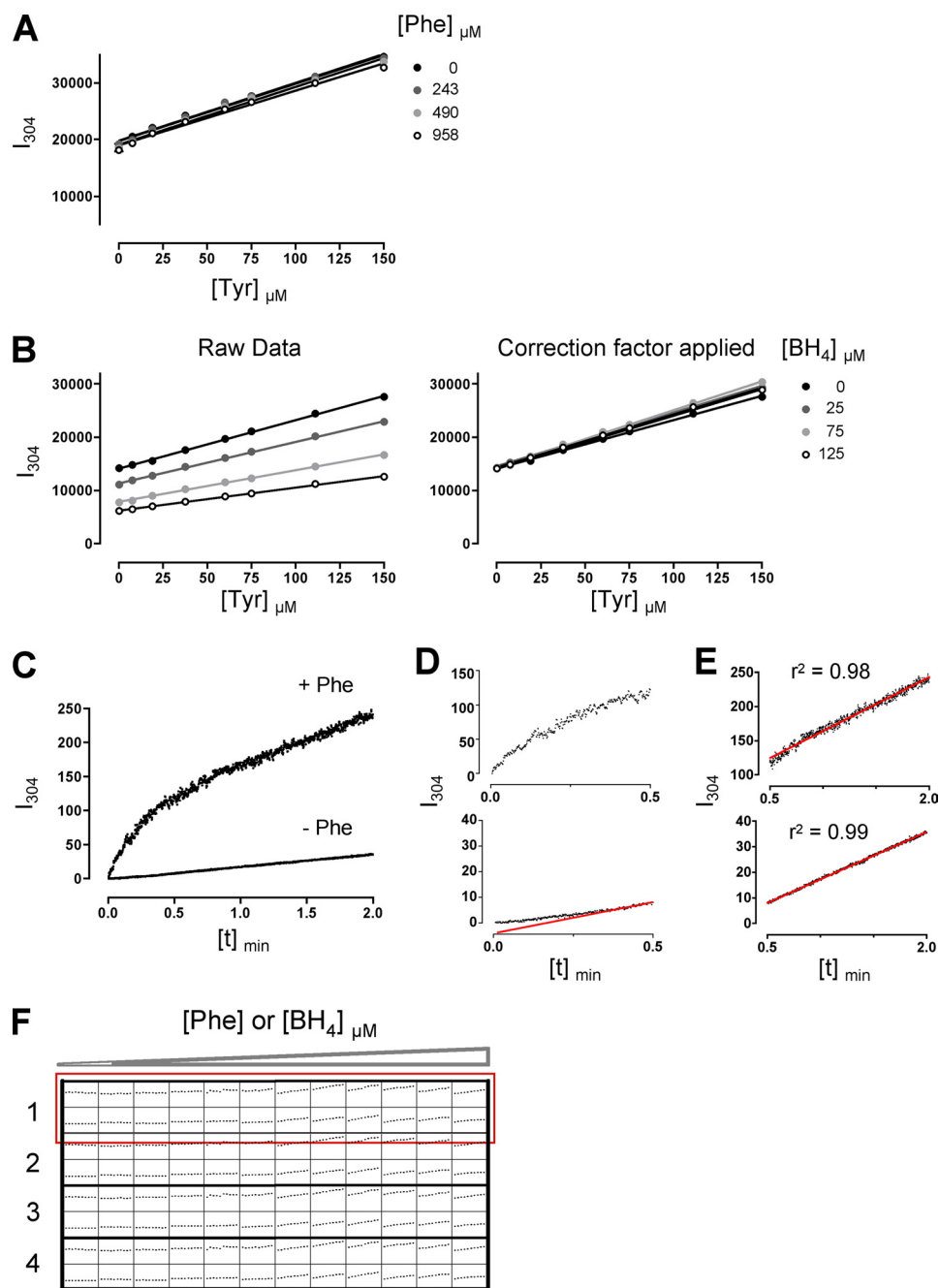


**FIGURE 1. A novel continuous assay for the measurement of PAH activity.** *A*, fluorescence intensity ( $I_{304}$ ) of L-Tyr concentrations (0–150  $\mu\text{M}$ ) with increasing L-Phe concentrations (0, 243, 490, and 958  $\mu\text{M}$ ) is shown. L-Tyr fluorescence intensity was not influenced by increasing L-Phe concentrations, confirming spectral separation of the two substances in one mixed solution. Values are given as the mean  $\pm$  S.E. of three independent measurements. *B*, quenching of L-Tyr fluorescence intensity by BH<sub>4</sub> is shown. Measurement of L-Tyr (0–150  $\mu\text{M}$ ) subsequent to the addition of increasing BH<sub>4</sub> concentrations (0, 25, 75, and 125  $\mu\text{M}$ ), revealed an inner filter effect of BH<sub>4</sub> on L-Tyr excitation and emission (*left panel*). For each BH<sub>4</sub> concentration used in the assay, a correction factor was calculated according to the factorial decrease in signal intensity to account for the inner filter effect (*right panel*). Values are given as the mean  $\pm$  S.E. of three independent measurements. *C*, continuous measurement of time-dependent wild-type PAH kinetics with and without preincubation of the enzyme with 1 mM L-Phe are shown. *D*, L-Phe preincubation (activation) led to burst-phase kinetics within the first 30 s of the reaction (*top*) followed by a linear phase of L-Tyr production. Without L-Phe preincubation, an initial lag-phase before steady state enzyme kinetics was found (*bottom*, a red line was used to guide the eye). *E*, the time frame chosen for the measurement of steady state enzyme kinetics between 30 and 120 s showed a linear rate of reaction (*top*, with L-Phe preincubation; *bottom*, without L-Phe preincubation). *F*, a 96-well plate for sequential measurement of PAH enzyme kinetics is shown. Direct in-well measurements of enzyme kinetics of up to four different PAH enzymes (*numbers 1–4*) were performed by the sequential analysis of 2 rows, consisting of 24 wells (*red box*). Each row contained the PAH enzyme varying substrate concentrations (0–1 mM) and one cofactor concentration (75  $\mu\text{M}$ ) or varying cofactor concentrations (0–125  $\mu\text{M}$ ) and one substrate concentration (1 mM). Repeated cycles allowed kinetic measurements of 24 wells over a time period of 60 s.

initial high activity burst phase (Fig. 1C and Fig. 1D, *top*) followed by a linear steady state rate of catalysis for the L-Phe preincubated (activated) enzyme (Fig. 1C and Fig. 1E, *top*). In contrast, the non-activated enzyme showed an initial lag-phase

(Fig. 1C and Fig. 1D, *bottom*) before a linear phase of L-Tyr production (Fig. 1C and Fig. 1E, *bottom*).

In addition, time-dependent initial velocity measurements require substrate turnover to remain less than 10% that of the

## PAH Cooperativity for BH<sub>4</sub>

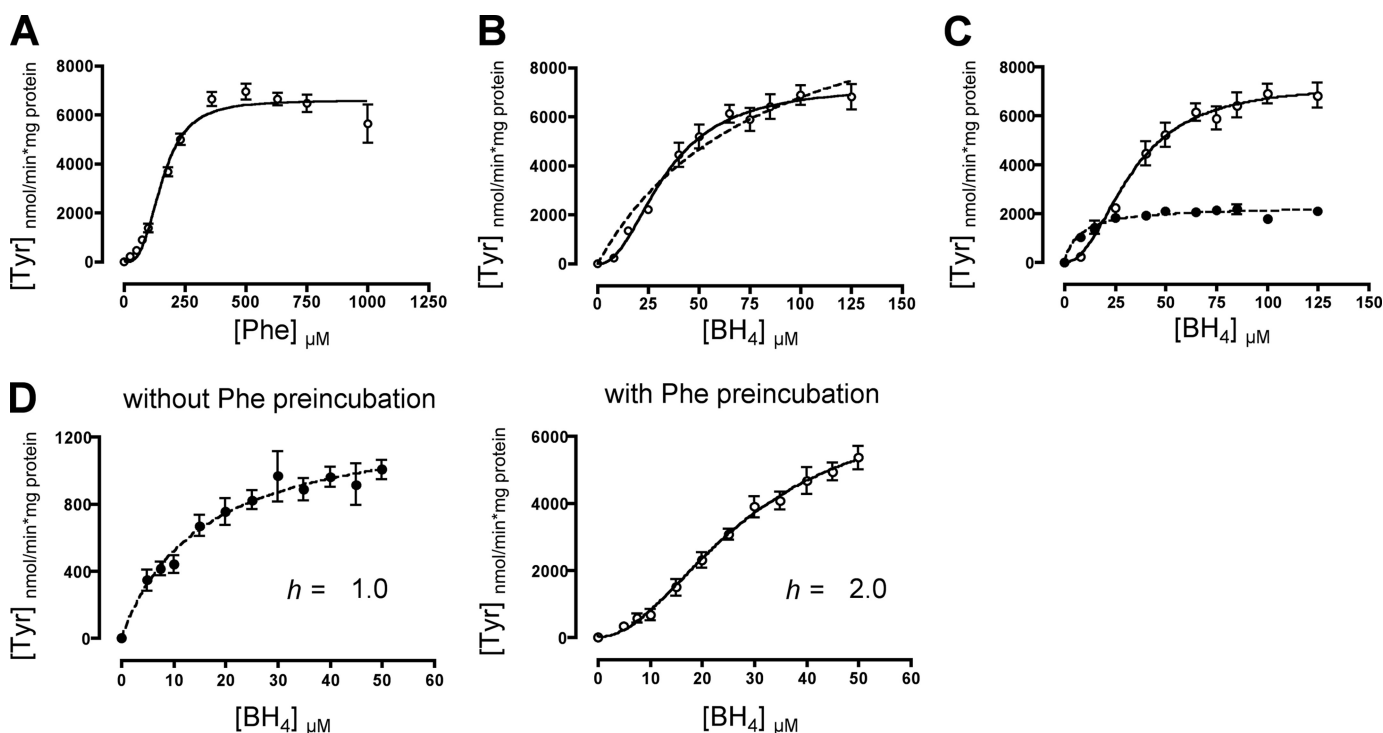


**FIGURE 2. Measurements of wild-type PAH kinetics.** *A*, reaction rates at variable L-Phe concentrations (0–1 mM) and one BH<sub>4</sub> concentration (75 μM) are shown. Before initiation of the reaction by BH<sub>4</sub>, the enzyme was preincubated for 5 min at 25 °C with L-Phe to activate the enzyme. Nonlinear regression analysis was performed using the Hill equation. *B* and *C*, reaction rates at variable BH<sub>4</sub> concentrations (0–125 μM) and one L-Phe concentration (1 mM) are shown. *B*, data obtained for the L-Phe preincubated (activated) enzyme were evaluated using the Michaelis-Menten equation (*dashed line*) and the Hill equation (*solid line*). *C*, a comparison of enzyme kinetics measured using the non-activated (●) and the activated (○) wild-type PAH is shown. The non-activated enzyme showed non-cooperative binding of BH<sub>4</sub>. The activated enzyme indicated positive cooperativity for the binding of BH<sub>4</sub>. *D*, enzyme kinetics of non-activated and activated PAH at variable BH<sub>4</sub> concentrations (0–50 μM) and one L-Phe concentration (1 mM) are shown. Data obtained for the non-activated enzyme were fit to the Michaelis-Menten equation (*left panel*). Data of the activated enzyme followed Hill kinetics (*right panel*). For all enzyme activity measurements, fluorescence intensity was recorded and after subtraction of the blank reaction converted to enzyme activity units (nmol L-Tyr/min × mg protein) using the standard curve obtained by L-Tyr concentration measurements. Values are given as the mean ± S.E. of three independent experiments.

substrate concentrations added to the reaction mixture (23). A time frame of 60 s for measurement of steady state enzyme kinetics starting 30 s after the addition of BH<sub>4</sub> proved to best fulfill the criteria of linearity and limited substrate turnover.

To allow for an accurate and efficient performance of the enzyme kinetic assay, liquid handling and signal detection were automated using a multi-well fluorescence detection device with an integrated injection system. Various substrate or cofactor concentrations were injected for L-Phe or BH<sub>4</sub>-dependent kinetics, respectively, and process automation enabled sequential duplicate measurements of up to four different PAH enzymes, resulting in reduced time for experimental preparation and procedure (Fig. 1*F*).

Thus, real-time measurement of PAH product formation revealed that direct in-well detection of L-Tyr during the catalytic reaction without prior separation of substrate and product is feasible when BH<sub>4</sub> quenching is taken into account. In addition, real-time kinetics give more insights into both pre-steady state and steady state kinetics of phenylalanine hydroxylation, allowing thorough analysis of PAH enzyme kinetics.

**A Continuous PAH Activity Assay Reveals BH<sub>4</sub>-dependent Cooperativity**—The newly developed continuous assay was used to determine enzyme kinetic parameters at varying substrate concentrations (L-Phe, 1–1000 μM) and a constant cofactor concentration (BH<sub>4</sub>, 75 μM) or at varying cofactor

concentrations (BH<sub>4</sub>, 0–125 μM) and a constant substrate concentration (L-Phe, 1 mM).

Measurement of L-Phe-dependent PAH kinetics showed sigmoidal behavior for the activated enzyme (Fig. 2*A*) as previously described (24, 36–38). Enzyme kinetic parameters were calculated by nonlinear regression analysis using the Hill equation, accounting for substrate cooperativity and compared with the results of a standard discontinuous PAH activity assay (Table 1) (17). Values for  $V_{\max}$  were substantially higher when determined by the continuous assay (6598 nmol Tyr/min × mg protein) as compared with the discontinuous assay (3470 nmol Tyr/min × mg protein). However, apparent affinity to the substrate ( $S_{0.5}$  156 μM), cooperativity (Hill coefficient,  $h_{\text{Phe}}$  3.0), and substrate activation (activation-fold 2.8) showed virtually identical results in both experiments (discontinuous assay;  $S_{0.5}$  155 μM,  $h_{\text{Phe}}$  3.0, activation-fold 3.0). As expected from previous studies using recombinant human PAH (26, 37) and the rat enzyme (36), enzyme kinetic parameters obtained without L-Phe preincubation gave different results (Table 1).  $V_{\max}$  was markedly lower (2533 nmol Tyr/min × mg protein), and the apparent affinity of the enzyme to L-Phe ( $K_m$  318 μM) was reduced. In addition, binding of L-Phe to the non-activated enzyme was found to be non-cooperative ( $h_{\text{Phe}}$  1.0). This is in concordance with studies using surface plasmon resonance (25). The enzyme kinetic parameters determined for both acti-

**TABLE 1**

**Comparison of L-Phe-dependent enzyme kinetic parameters obtained by standard PAH activity assay and direct in-well detection of L-Tyr production**

Steady state kinetic parameters of WT MBP-PAH fusion protein are shown. Apparent affinities for L-Phe ( $S_{0.5}$ ,  $K_m$ , and the Hill-coefficient ( $h_{Phe}$ ) as a measure of cooperativity are shown. Measurements were performed with (+) and without (–) L-Phe preincubation of the enzyme. Enzyme kinetic parameters were determined at variable L-Phe concentrations (0–1000  $\mu$ M) and standard BH<sub>4</sub> concentrations (75  $\mu$ M). CV, coefficient of variation, defined as the ratio of the S.D. to the mean value.

L-Phe preincubation		$V_{max}$	CV	$S_{0.5}$	CV	$K_m$	$h_{Phe}$	Activation fold <sup>a</sup>
		nmol L-Tyr/min $\times$ mg protein	%	$\mu$ M	%	$\mu$ M		
WT <sup>b</sup>	–	495 <sup>c</sup>		318 <sup>c</sup>			1.5 <sup>c</sup>	–
	+	1550 <sup>c</sup>		154 <sup>c</sup>			2.2 <sup>c</sup>	3.1 <sup>c</sup>
WT <sup>c</sup>	+	3470 $\pm$ 75 <sup>d</sup>	2	155 $\pm$ 6 <sup>d</sup>	4		3.0 <sup>d</sup>	3.0 <sup>d</sup>
	–	2533 $\pm$ 217		–		318 $\pm$ 68	1.0	–
	+	6598 $\pm$ 190	3	156 $\pm$ 9	6		3.0	2.8

<sup>a</sup> Fold increase in PAH activity by L-Phe preincubation calculated at the standard L-Phe (1 mM) and BH<sub>4</sub> (75  $\mu$ M) concentrations.

<sup>b</sup> Measurement by standard discontinuous PAH activity assay (HPLC and fluorimetric detection). Values are given as the mean  $\pm$  S.E. of three independent experiments.

<sup>c</sup> From Knappskog *et al.* (37); activation fold was calculated from  $V_{max}$ .

<sup>d</sup> From Gersting *et al.* (17).

<sup>e</sup> Measurement by continuous PAH activity assay (direct in-well fluorescence detection). Values are given as the mean  $\pm$  S.E. of four independent experiments.

**TABLE 2**

**Comparison of BH<sub>4</sub>-dependent enzyme kinetic parameters obtained by standard PAH activity assay and direct in-well detection of L-Tyr production**

Steady state kinetic parameters of WT MBP-PAH fusion protein are shown. Apparent affinities for BH<sub>4</sub> ( $C_{0.5}$ ) and the Hill-coefficient ( $h_{BH4}$ ) as a measure of cooperativity are shown. Measurements were performed with (+) and without (–) L-Phe preincubation of the enzyme. Enzyme kinetic parameters were determined at variable BH<sub>4</sub> concentrations (0–125  $\mu$ M) and standard L-Phe concentrations (1 mM). CV, coefficient of variation, defined as the ratio of the S.D. to the mean value.

L-Phe preincubation		$V_{max}$	CV	$K_m$	CV	$C_{0.5}$	CV	$h_{BH4}$
		nmol L-Tyr/min $\times$ mg protein	%	$\mu$ M	%	$\mu$ M	%	
WT <sup>a</sup>	+	3425 $\pm$ 139 <sup>b</sup>	4	24 $\pm$ 3 <sup>b</sup>	12.5	–	–	1.0
WT <sup>c</sup>	–	2277 $\pm$ 84		8 $\pm$ 1		–	–	1.0
	+	7288 $\pm$ 282	4	–		33 $\pm$ 2	6	2.2

<sup>a</sup> Measurement by standard discontinuous PAH activity assay (HPLC and fluorimetric detection). Values are given as the mean  $\pm$  S.E. of three independent experiments.

<sup>b</sup> From Gersting *et al.* (17).

<sup>c</sup> Measurement by continuous PAH activity assay (direct in-well fluorescence detection). Values are given as mean  $\pm$  S.E. of four independent experiments.

vated and non-activated PAH were well comparable with the data found in previous studies (Table 1) (17, 37).

Surprisingly, the data obtained for BH<sub>4</sub>-dependent PAH kinetics did not fit to the well accepted Michaelis-Menten kinetic model. Instead, the data showed a sigmoidal behavior, indicating BH<sub>4</sub>-dependent cooperativity (Fig. 2B). Although BH<sub>4</sub>-dependent kinetics was as yet mainly determined using the non-activated enzyme (19, 26), we conducted the assay utilizing the L-Phe-preincubated (activated) enzyme. To examine whether the Hill kinetic model describing BH<sub>4</sub>-dependent kinetic parameters depends on the activation state of the enzyme, the assay was run with and without prior incubation of the enzyme by L-Phe, and the results were compared with data from the literature (Table 2). Similar to L-Phe-dependent enzyme kinetics,  $V_{max}$  of the activated enzyme was markedly lower in the discontinuous assay (3425 nmol Tyr/min  $\times$  mg protein) when compared with the continuous assay (7288 nmol Tyr/min  $\times$  mg protein), but the values for the apparent affinity to the ligand were comparable for both methods used ( $K_m$  24  $\mu$ M;  $C_{0.5}$  33  $\mu$ M) (Table 2). Although the analysis of the non-activated enzyme showed a reduction in  $V_{max}$  (2277 nmol Tyr/min  $\times$  mg protein), an increased apparent affinity to BH<sub>4</sub> ( $K_m$  8  $\mu$ M) was observed. In addition, steady state kinetic analysis of activated PAH indicated BH<sub>4</sub>-dependent-positive cooperativity (Hill coefficient,  $h_{BH4}$  2.2), whereas Michaelis-Menten kinetics for the non-activated PAH was confirmed (Fig. 2C). To obtain a better resolution of the range that best discriminates between both kinetic models, the assay was repeated in the limits of 0–50  $\mu$ M BH<sub>4</sub> (Fig. 2D). The data obtained for the activated enzyme clearly followed Hill kinetics ( $h_{BH4}$  2.0). This was in contrast to the non-activated enzyme, where nonlinear

regression analysis showed hyperbolic kinetics following the Michaelis-Menten kinetic model ( $h_{BH4}$  1.0).

The enzyme kinetic parameters determined for L-Phe- and BH<sub>4</sub>-dependent enzyme kinetics were well comparable with previous studies using the standard discontinuous assay (17, 19), confirming the accuracy of our newly developed continuous assay. Furthermore, we aimed to determine the assay precision and calculated the coefficient of variation for all enzyme kinetic parameters of the activated enzyme, comparing the standard discontinuous with the continuous assay. The coefficients of variation for both L-Phe- and BH<sub>4</sub>-dependent kinetic parameters were similar for the two assays, revealing equal precision in enzyme kinetic measurements (Tables 1 and 2).

In conclusion, allosteric parameters obtained using the newly developed PAH activity assay were well comparable with results from standard discontinuous assays. The assay accuracy as well as precision confirmed the suitability of this method for the evaluation of enzyme kinetic parameters of PAH. In addition, PAH kinetic analysis using the continuous assay gave evidence for BH<sub>4</sub>-dependent cooperativity with PAH activation as a prerequisite.

*BH<sub>4</sub>-dependent Cooperativity Relies on an Activated Structural Conformation of PAH*—Three variant PAH enzymes, R68S, V106A, and the dimeric double-truncated form 103–427 (19, 37, 39, 40), were used to characterize the interrelation of enzyme activation and BH<sub>4</sub>-dependent cooperativity in more detail. In particular, we aimed to investigate whether the shift in enzyme kinetics from Michaelis-Menten to the Hill kinetic model depends on the presence of the L-Phe substrate itself or on structural attributes of the activated enzyme. It is known that substrate activation induces conformational changes (16,

PAH Cooperativity for BH<sub>4</sub>

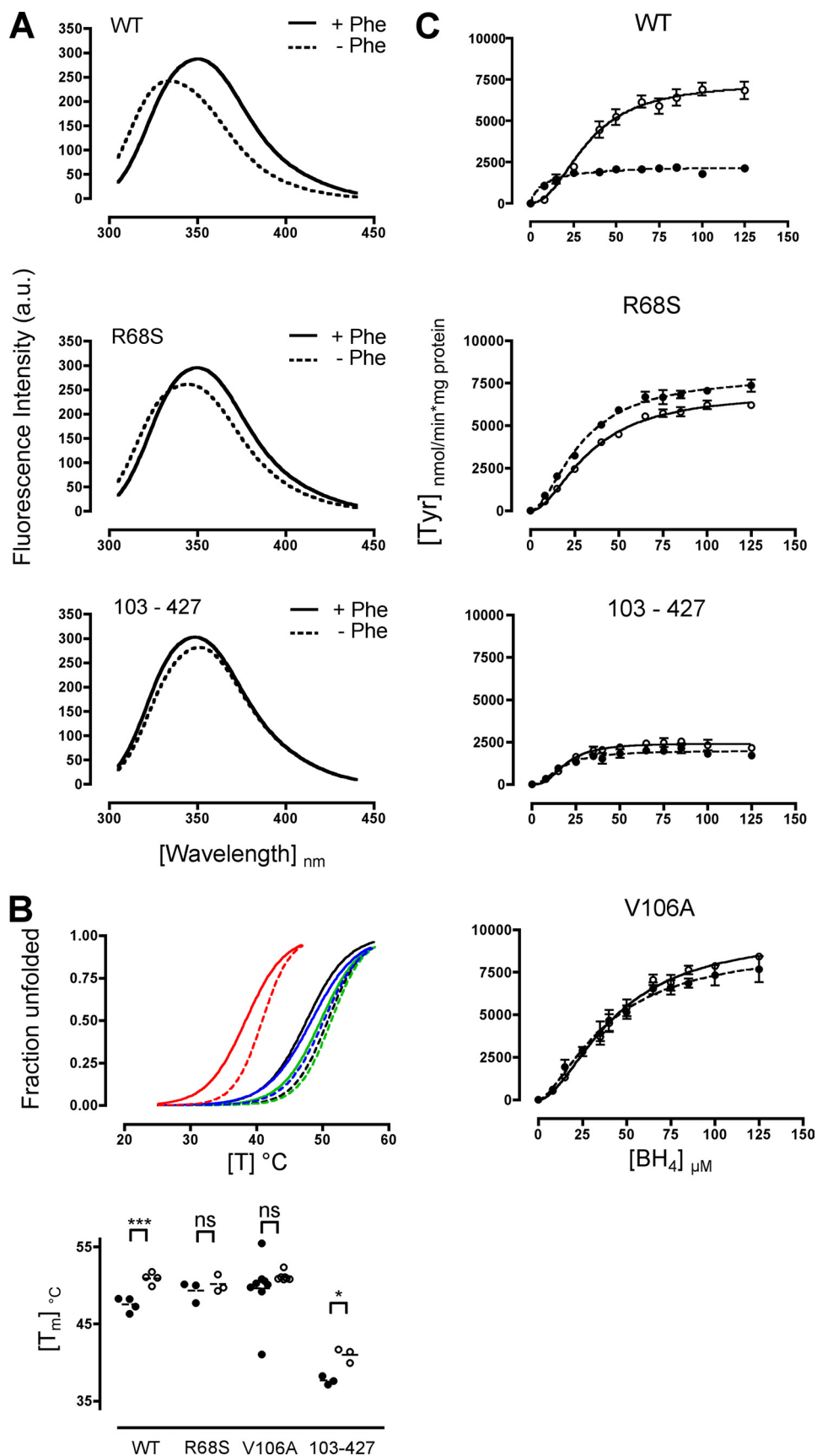


TABLE 3

## Trp emission scans of PAH cleaved by factor Xa

Tryptophan fluorescence emission spectra were obtained with and without L-Phe (1 mM) preincubation of the cleaved WT PAH and preactivated variants. Fluorescence measurements were performed using a fluorescence spectrophotometer at an excitation wavelength of 295 nm with excitation and emission slits set to 2.5 and 5 nm, respectively. a.u., arbitrary units.

	Without L-Phe preincubation		With L-Phe preincubation	
	Wavelength	Fluorescence intensity	Wavelength	Fluorescence intensity
	<i>nm</i>	<i>a.u.</i>	<i>nm</i>	<i>a.u.</i>
WT	340	247	351	296
R68S	345	266	351	304
103–427	350	288	350	310

37, 41–45) that convert the enzyme from a low activity T-state to a high activity R-state (Monod Wyman Changeux model) (46, 47). This is accompanied by an increase in quantum yield and a red-shifted emission maximum of the Trp-120 residue (48, 49). To determine the level of preactivation, structural attributes of the variants were compared with wild-type PAH. Spectral differences with and without preincubation by the substrate were utilized to assess the activation state.

Tryptophan emission scans of wild-type PAH and the variants R68S and 103–427 were performed. As expected, wild-type PAH revealed a red shift in the emission maximum (340 to 351 nm) and an increase in intrinsic tryptophan fluorescence (247–296 arbitrary units) upon the addition of L-Phe (Fig. 3A) (Table 3). Both variants showed a red-shifted emission maximum in the absence of L-Phe, which was more pronounced for the dimeric variant. Upon L-Phe preincubation, R68S yielded an emission maximum of the activated wild-type (351 nm), whereas the emission maximum of the dimeric PAH remained unchanged (350 nm). Both variants showed an increase in quantum yield but to a lesser extent than observed for wild-type PAH. Furthermore, we determined activation-induced structural rearrangements for all three variants by thermal unfolding using temperature-dependent differential scanning fluorimetry (Fig. 3B). Although the addition of L-Phe induced a highly significant increase in the transition midpoint for wild-type PAH ( $p = 0.0006$ ), no significant increase was found for the variants R68S and V106A (Fig. 3B) (Table 4). These variants already showed increased transition midpoints at the activated wild-type level even without L-Phe preincubation. The dimeric PAH 103–427, although showing markedly decreased transition midpoints in general, revealed a significant increase when L-Phe was added ( $p = 0.0345$ ). Taken together, all variants dis-

TABLE 4

## Mean transition midpoints of thermal denaturation assays

Calculation of transition midpoints from differential scanning fluorimetry of WT PAH and preactivated variants with and without 1 mM L-Phe. Transition midpoints were calculated using the Boltzmann sigmoidal equation. Transition midpoints are given as the mean  $\pm$  S.E. of three to four for V106A eight independent experiments. Mean transition midpoints with and without L-Phe were compared using a paired  $t$  test, two-tailed. NS, not significant.

	$T_m$		$p$ value
	Without L-Phe preincubation	With L-Phe preincubation	
	$^{\circ}\text{C}$		
WT	47.49 $\pm$ 0.46	50.90 $\pm$ 0.38	$p = 0.0006$
R68S	49.28 $\pm$ 0.78	50.15 $\pm$ 0.64	NS
V106A	49.63 $\pm$ 1.40	51.11 $\pm$ 0.21	NS
103–427	37.68 $\pm$ 0.32	40.99 $\pm$ 0.54	$p = 0.0345$

played structural characteristics that are indicative of mutation-induced conformational preactivation but to different extents.

According to the results on structural preactivation, evaluation of the activation-fold determined by the continuous assay (Fig. 3C) (Table 5) confirmed functional preactivation of the variants without L-Phe preincubation (R68S, 0.9; V106A, 1.0; 103–427, 1.3). Nonlinear regression analysis of BH<sub>4</sub>-dependent kinetics of all three preactivated variants followed the Hill model as shown for activated wild-type PAH. Although distinctly positive, the Hill-coefficients ranging from 1.6 to 2.1 were lower than that determined for activated wild-type PAH ( $h$ , 2.2). The dimeric variant 103–427 showed a  $V_{\max}$  (1980 nmol Tyr/min  $\times$  mg protein) comparable with that of the non-activated wild-type PAH, which did not change markedly upon L-Phe preincubation (2421 nmol Tyr/min  $\times$  mg protein). This is in contrast to an increase by 3.2-fold observed for wild-type PAH preincubated with L-Phe. However, for the variants R68S and V106A, a  $V_{\max}$  comparable with the activated wild-type PAH was found without L-Phe preincubation, and no further increase was measured when the substrate was present. R68S and V106A without L-Phe preincubation showed lower cofactor affinities than the non-activated wild-type PAH; however, the values were at the same level as determined for the L-Phe preincubated wild-type PAH.  $C_{0.5}$  of the dimeric PAH 103–427 was 2-fold higher as compared with the non-activated wild-type PAH. Notably, no marked changes in sigmoidal behavior and kinetic parameters were observed for all variants irrespective of whether they were preincubated by L-Phe (Fig. 3C) (Table 5). In summary, analyses of structurally preactivated variants substantiated BH<sub>4</sub>-dependent positive cooperativity of

FIGURE 3. **Determining the activated structural and functional conformation.** A, intrinsic tryptophan fluorescence emission spectra of the Factor Xa cleaved wild-type PAH, variant PAH R68S, and 103–427 are shown. Fluorescence emission spectra were acquired in the absence (dashed line) or presence (solid line) of 1 mM L-Phe. The excitation wavelength for Trp fluorescence measurements was 295 nm, with an excitation and emission slit of 2.5 and 5 nm, respectively. a.u., arbitrary units. B, differential scanning fluorimetry of the wild-type PAH and variant PAH R68S, V106A, and 103–427 fusion protein are shown. Denaturation of PAH was monitored by scanning a temperature range of 25 to 70  $^{\circ}\text{C}$  at a rate of 1.2  $^{\circ}\text{C}/\text{min}$ . Changes in 8-anilino-1-naphthalenesulfonic acid fluorescence emission were monitored at 500 nm (excitation 395 nm, slit widths 5.0/10.0 nm). The fraction unfolded of three to four independent experiments for wild-type, R68S, and 104–427 and seven to eight independent experiments for V106A without L-Phe (solid line) and with 1 mM L-Phe (dashed line) were determined (top panel; wild-type (black), R68S (blue), V106A (green), and 103–427 (red)), and the respective transition midpoints were calculated using the Boltzmann sigmoidal equation. For comparison of the transition midpoints, a paired  $t$  test, two-tailed, was used. Transition midpoints for wild-type and variant PAH, with (○) and without (●) L-Phe preincubation were plotted and compared (bottom panel) (ns, not significant; \*,  $p < 0.05$ ; \*\*,  $p < 0.01$ ; \*\*\*,  $p < 0.001$ ). C, enzyme activity measured for the wild-type PAH and the preactivated variants R68S, V106A, and 103–427 without preincubation (●) and with preincubation of the enzyme (○) with 1 mM L-Phe before initiation of the reaction by the addition of BH<sub>4</sub>. Data obtained for the non-preincubated and preincubated enzymes followed the Hill kinetic model as shown for the activated wild-type PAH. For all enzyme activity measurements, fluorescence intensity was recorded and after subtraction of the blank reaction converted to enzyme activity units (nmol of L-Tyr/min  $\times$  mg protein) using the standard curve obtained by L-Tyr concentration measurements. Values are given as the mean  $\pm$  S.E. of three independent experiments.

PAH Cooperativity for BH<sub>4</sub>

TABLE 5

Comparison of BH<sub>4</sub>-dependent enzyme kinetic parameters of variant PAH proteins with and without L-Phe preincubation

Steady state kinetic parameters of variant MBP-PAH fusion proteins were determined by direct in-well activity measurements. Apparent affinities for BH<sub>4</sub> (C<sub>0.5</sub>) and the Hill-coefficient (*h*) as a measure of cooperativity are shown. Enzyme kinetic parameters determined at variable BH<sub>4</sub> concentrations (0–125 μM) and standard L-Phe concentrations (1 mM) with and without preincubation of the enzyme with L-Phe (1 mM).

	Without L-Phe preincubation				With L-Phe preincubation			
	V <sub>max</sub> <sup>a</sup>	K <sub>m</sub>	C <sub>0.5</sub> <sup>a</sup>	h <sub>BH<sub>4</sub></sub>	V <sub>max</sub> <sup>a</sup>	C <sub>0.5</sub> <sup>a</sup>	h <sub>BH<sub>4</sub></sub>	Activation fold <sup>b</sup>
	nmol L-Tyr/min × mg protein	μM	μM		nmol L-Tyr/min × mg protein	μM		
WT	2277 ± 84	8 ± 1	—	1.0	7288 ± 282	33 ± 2	2.2	2.8
R68S	7928 ± 232	—	29 ± 1	1.8	6940 ± 225	34 ± 2	1.8	0.9
V106A	9041 ± 489	—	40 ± 3	1.6	9773 ± 534	43 ± 4	1.8	1.0
103–427	1980 ± 100	—	16 ± 2	2.1	2421 ± 73	19 ± 1	2.6	1.3

<sup>a</sup> Values are given as the mean ± S.E. of three independent measurements.

<sup>b</sup> Fold increase in PAH activity by L-Phe preincubation calculated at the standard L-Phe (1 mM) and BH<sub>4</sub> (75 μM) concentrations.

the activated enzyme, where the kinetic model does not rely on the presence of L-Phe but is determined by activating conformational rearrangements.

**Evaluation of Model Fitting**—To validate the experimental data on conditions that determine PAH cooperativity, an extended evaluation of model fitting by nonlinear regression analysis of BH<sub>4</sub>-dependent kinetics was performed. The test parameters goodness of fit (*R*<sup>2</sup>), root mean square (*S*<sub>y,x</sub>), runs test, and residuals of values were compared, and an F-test was run to discriminate between the two nested kinetic models Michaelis-Menten and Hill for activated and non-activated PAH, respectively.

First we analyzed non-activated PAH. A simple calculation of goodness of fit (*R*<sup>2</sup>) did not allow for distinction between the two models used for data analyses (*R*<sup>2</sup><sub>MM</sub> 0.97; *R*<sup>2</sup><sub>H</sub> 0.97) (supplemental Table 1). The residuals of values (supplemental Fig. 2) and, thus, the S.D. of the residuals also showed no marked improvement of data description by the more complicated Hill equation. Although the runs test showed a marginally significant deviation of the data from the Michaelis-Menten model (*p* = 0.048), the F-test proved the simpler Michaelis-Menten kinetics to be the correct model for data analysis of BH<sub>4</sub>-dependent kinetics of non-activated PAH (F ratio 2.86; *p* = 0.125) (Table 6). This was confirmed by refined analysis of BH<sub>4</sub>-dependent kinetics in the limits of 0–50 μM. As before, *R*<sup>2</sup>, *S*<sub>y,x</sub>, and the residuals of values did not allow for a clear distinction between the two models (supplemental Table 1). However, no significant deviation of the data from any of the two equations could be determined by the runs test. Yet again, the F-test revealed that the data were best described by the simpler Michaelis-Menten kinetic model (F ratio 0.58; *p* = 0.463) (Table 6).

In contrast to non-activated PAH, enzyme activation by L-Phe now resulted in marked differences of the two models even by goodness of fit (*R*<sup>2</sup><sub>MM</sub> 0.96; *R*<sup>2</sup><sub>H</sub> 0.99) (supplemental Table 1) (Table 6). In addition, evaluation of the data by the Hill equation revealed a decrease of *S*<sub>y,x</sub> by ~2-fold, and the residuals of values showed less fluctuation (supplemental Fig. 2). The runs test showed no significant deviation from any of the two models used, but comparison by the F-test resulted in a highly significant *p* value (F ratio 274.28; *p* < 0.0001) (Table 6) favoring Hill kinetics. Detailed analysis at low BH<sub>4</sub> concentrations (0–50 μM) additionally uncovered a significant deviation of the data from Michaelis-Menten kinetics in the runs test (*p* = 0.024) (Table 6) (supplemental Table 1 and Fig. 2). Taken

TABLE 6

## Comparison of two nested non-linear regression models

F-test for two nested models after measurement of wild-type PAH kinetics without and with preincubation of the enzyme with L-Phe. Enzyme kinetics were measured with L-Phe (1 mM) and BH<sub>4</sub> (0–125 μM and 0–50 μM). The F-test assumes that the Michaelis-Menten equation is a simpler case of the Hill equation. If the simpler model is correct, the F ratio is near 1.0. To verify the correctness of the more complicated model (if the F ratio is >1.0), the *p* value is calculated. If the *p* value is less than the traditional significance level of 5%, it can be concluded that the data do not randomly fit to the more complicated model but fit significantly better to Hill than to Michaelis-Menten kinetics.

BH <sub>4</sub>	F-test		
	L-Phe preincubation	F ratio	<i>p</i> value
μM			
0–125	—	2.86	0.125
0–125	+	274.28	<0.0001
0–50	—	0.58	0.463
0–50	+	62.79	<0.0001

together, the evaluation of model fitting provided clear evidence for BH<sub>4</sub>-dependent positive cooperativity of activated PAH, whereas the BH<sub>4</sub>-dependent kinetics of the non-activated enzyme followed the non-cooperative Michaelis-Menten model.

Next, we aimed to learn whether the presence of the L-Phe substrate has an impact on the kinetic model beyond L-Phe induced conformational changes upon PAH activation. To validate structural preactivation of R68S, V106A, and of the dimeric double-truncated 103–427 PAH, we first analyzed whether BH<sub>4</sub>-dependent kinetic data would fit significantly better to the more complex Hill equation even without L-Phe preincubation. Indeed, we identified an increase in *R*<sup>2</sup>, a more than 2-fold decrease in *S*<sub>y,x</sub>, and a significant deviation of the Michaelis-Menten model in the runs test for the variants R68S and V106A (supplemental Table 2). Only the dimeric 103–427 showed a less pronounced reduction in *S*<sub>y,x</sub> and no discrimination between the two models in the runs test. In all cases fluctuation of the residuals of values was lower using the Hill equation (supplemental Fig. 2). This was in line with the results obtained by the F-test (*p* < 0.01) (Table 7). Hence, the kinetic data fit significantly better to the more complicated Hill equation, indicating substrate-independent structural preactivation. Second, model fitting of the structurally activated variants was compared with and without prior incubation with L-Phe in the next step. All in all, the presence of L-Phe only negligibly changed the test results. Only for the dimeric 103–427, *S*<sub>y,x</sub> was markedly lower upon evaluation by sigmoidal kinetics, and the runs test classified Michaelis-Menten as an incorrect

**TABLE 7**  
**Comparison of two nested non-linear regression models with and without preincubation of preactivated variants**

F-test for two nested models after measurement of enzyme kinetics without and with preincubation of the enzyme with L-Phe. Enzyme kinetics were measured with L-Phe (1 mM) and BH<sub>4</sub> (0–125 μM). The F-test assumes that the Michaelis-Menten equation is a simpler case of the Hill equation. If the simpler model is correct, the F ratio is near 1.0. To verify the correctness of the more complicated model (if the F ratio is >1.0), the *p* value is calculated. If the *p* value is less than the traditional significance level of 5%, it can be concluded that the data do not randomly fit to the more complicated model but fit significantly better to Hill than to Michaelis-Menten kinetics.

	F-test		
	L-Phe preincubation	F ratio	<i>p</i> value
R68S	–	58.02	<0.0001
R68S	+	69.63	<0.0001
V106A	–	24.00	<0.001
V106A	+	35.44	<0.001
103–427	–	10.66	<0.01
103–427	+	40.23	<0.001

model (supplemental Table 2). Again, all data provided evidence for a correct data description by the Hill kinetic model (supplemental Table 2 and Fig. 2) (Table 7).

In summary, extended analysis and comparison of the two non-linear regression models Michaelis-Menten and Hill revealed non-cooperative kinetics of the non-activated enzyme, whereas activation of the enzyme clearly induced cooperativity. Moreover, L-Phe preincubation did not have a significant impact on the kinetic model of structurally activated variant PAH.

## DISCUSSION

In this study we established a new method for the evaluation of PAH kinetic parameters, allowing for real-time detection of enzyme activity. Continuous assays are the safest means of determining reaction velocity from the slope of a plot of signal versus time (23). However, many assays used for the evaluation of PAH enzyme kinetics are discontinuous due to chromatographic separation of the substrate from the product before product detection. We aimed to establish the measurement of L-Tyr production without separation from the substrate L-Phe. The spectral properties of the aromatic amino acids and differences in quantum yield allowed for direct detection of L-Tyr uninfluenced by L-Phe concentrations. However, the IFE of BH<sub>4</sub> at the excitation and emission maxima of L-Tyr (274 and 304 nm, respectively) had to be taken into account. By analyzing the IFE of BH<sub>4</sub> on L-Tyr fluorescence in the entire range of concentrations used in the assay, a concentration-dependent correction factor was defined (27, 28). This facilitated accurate and precise quantification of L-Tyr product formation inside the assay reaction mixture. In addition, all substances required to perform the activity assay were applied by means of an integrated injection system. Although equally precise, this led to marked time reduction in sample preparation. Furthermore, sequential duplicate measurements subsequent to sample injections of up to four different PAH proteins in a 96-well format substantially increased the throughput of enzyme kinetics analyses. The addition of various substrate and cofactor concentrations as well as their injection at different time-points proved this method to be very flexible, allowing for numerous assay conditions in one single run.

By applying the new technique, we observed burst-phase kinetics of preactivated and lag-phase kinetics of non-activated PAH. The discontinuous assays used previously measured product formation from the initiation of the reaction to a defined end point, and burst- and lag-phase kinetics were not taken into consideration. However, pre-steady state kinetics should not be ignored as they may lead to erroneous interpretations regarding the existence of cooperativity (50). A complete model describing the enzyme reaction is a prerequisite for comprehensive understanding of the mechanisms involved in pre-steady state kinetics. Assumptions to approach such a model have been made using a prokaryotic monomeric PAH (51). Yet this enzyme lacks the regulatory properties of the oligomeric multidomain human protein and is, therefore, not applicable to human PAH. Therefore, we decided to assess steady state kinetics at a 1-min time frame after the burst-phase and provided a linear rate of reaction velocity for the non-activated and the activated enzyme while remaining within 10% of substrate turnover.

The data of continuous measurements were compared with our results obtained previously by the discontinuous assay as well as to data described in the literature. Differences in  $V_{\max}$  between the discontinuous and the continuous assay were found. These variations may be due to the different methods used, yet additional aspects such as different time frames for measurement of steady state kinetics and the improvement of protein purification methods in our laboratory within the last years play an important role and may further explain these findings. Notably, large differences in enzyme activities, ranging up to 7-fold, can also be found in the literature (16, 37, 52, 53). However, kinetic parameters describing apparent affinity and enzyme allostery ( $S_{0.5}$ ,  $K_m/C_{0.5}$ , Hill coefficient (*h*), and activation-fold) were similar to results obtained using discontinuous assays and to results previously described (17, 37), confirming the accuracy of our newly developed continuous assay. Furthermore, calculation of the coefficient of variation proved the new assay to be as precise as the standard discontinuous assays applied.

Interestingly, data points did not fit to the Michaelis-Menten kinetic model when the method was applied to determine BH<sub>4</sub>-dependent enzyme kinetics. Instead, a good fit was found applying the Hill kinetic model. All previous studies using different methods had shown hyperbolic non-cooperative binding kinetics of the cofactor to PAH (17, 19, 25, 53). When applying the continuous assay, BH<sub>4</sub>-dependent kinetics of wild-type PAH revealed positive cooperativity. However, our experiments were performed with an L-Phe-preincubated (activated) enzyme, whereas in most of the previous studies the non-activated enzyme had been used. To elucidate whether PAH activation determines cofactor dependent cooperativity, we compared enzyme kinetics of non-activated and of activated PAH. In agreement with previous findings, the continuous assay without L-Phe preincubation resulted in hyperbolic binding kinetics of BH<sub>4</sub>. Together with the observed BH<sub>4</sub>-dependent cooperativity of activated PAH, these results suggested that cooperativity of BH<sub>4</sub> depends on an activated state of the enzyme.

Thus, we investigated whether the shift in enzyme kinetics from Michaelis-Menten to the Hill kinetic model depends on

## PAH Cooperativity for BH<sub>4</sub>

the presence of the L-Phe substrate itself or on structural attributes of the activated enzyme. This was dissected by means of conformationally preactivated genetic variants of PAH (R68S, V106A, dimeric 103–427). Using two different spectroscopic techniques we analyzed local and global effects on protein structure by mutation/truncation or by L-Phe, respectively, and correlated this with enzyme kinetic parameters. Preincubation of wild-type PAH with L-Phe leads to a series of structural and functional changes resulting in enzyme activation (16, 37, 41–45). On the structural level these include a red-shifted and enhanced tryptophan emission and a right-shifted thermal denaturation profile. On the functional level an increase in  $V_{\max}$ , a decreased apparent affinity, and a switch from non-cooperative to positive cooperative kinetics accounted for activation. All three variants displayed characteristics of structural and functional preactivation but to varying degrees. Preactivation of the variants was reflected by the activation-fold with values ranging from 0.9 to 1.3. Furthermore, all variants displayed clear positive cooperativity without prior incubation with the substrate. In the presence of L-Phe some selective structural changes for single variants were observed, *i.e.* a minor shift in tryptophan emission for R68S and a significantly enhanced transition midpoint of the thermal denaturation for 103–427. However, no variant showed decisive changes in enzyme kinetic parameters upon L-Phe preincubation. This observation held true irrespective of whether the parameter was at the same level as activated wild-type PAH. These data provide evidence that the variants are activated at a structural level and that L-Phe does not have any additional effect on their activity and cooperativity. We conclude that the conformation associated with preactivation accounts for positive cooperativity where L-Phe induces activating conformational changes that in turn lead to allostery. The addition of the substrate to the assay, however, does not induce cooperativity by itself.

Mathematical analyses of the data obtained by enzyme kinetic measurements were used to substantiate our findings on the comparison of the kinetic models (29, 34, 54–58). A simple calculation of best-fit parameters for enzyme kinetic data ( $R^2$ , root mean square, runs test) did not always allow for a clear distinction between the Michaelis-Menten and the Hill model. However, the application of an F-test made evident to which biological mechanism the kinetic data are linked with highest probability (29–32). Even though a more complex model like the Hill equation would always fit the experimental data better than a simpler model, the F-test revealed that kinetics of non-preincubated wild-type PAH were not described significantly better by this model. However, analysis of the L-Phe-activated enzyme gave a significant  $p$  value in the F-test for the Hill equation and, thus, proved positive cooperativity. These findings were corroborated when enzyme kinetic analyses were focused on the area of distinct sigmoidality, *i.e.* on the range of 0 to 50  $\mu\text{M}$  BH<sub>4</sub>. Statistical analyses of model fitting for preactivated PAH variants verified BH<sub>4</sub>-dependent cooperativity even without prior incubation with L-Phe. Taken together, mathematical analyses of the cofactor-dependent enzyme kinetic data confirmed that the non-activated enzyme follows

Michaelis-Menten kinetics, whereas the activated enzyme shows cooperativity.

Cooperativity of PAH to the L-Phe substrate is reflected by a Hill coefficient of  $>3.0$  and has previously been described to be propagated throughout the whole tetramer (59). Alterations in the orientation of the oligomerization domain transfer cooperative activating conformational changes from one to the other dimer. This requires a switch between a low affinity “T-state” conformation to a high affinity “R-state” conformation at elevated L-Phe concentrations following the model proposed by Monod, Wyman, and Changeux. The Hill coefficients of BH<sub>4</sub>-dependent kinetics determined for the L-Phe preincubated (activated) wild-type PAH and the preactivated variants in this study were  $\sim 2.0$ . The current study may, thus, allow speculating that enzyme activation leads to positive cooperativity in BH<sub>4</sub> binding. The dissimilar Hill coefficients for substrate and cofactor binding may also show that cooperative binding of BH<sub>4</sub> follows different conformational alterations propagating cooperativity than found for L-Phe binding. This may explain that positive cooperativity was not only observed for the tetrameric enzyme but also for the truncated PAH 103–427 that lacks the regulatory and the oligomerization domain and, thus, only exists in dimeric form. However, whether there is cooperative behavior of PAH upon BH<sub>4</sub> binding in the strict mechanistic sense or hysteresis leading to cooperative kinetics could not be fully elucidated. Further crystallization and NMR studies are needed for a thorough understanding of the impact of L-Phe and BH<sub>4</sub> binding on cooperative allosteric changes in PAH structure.

In conclusion, the development of a novel method for real-time measurement of PAH activity provided accurate, fast, and efficient PAH enzyme kinetic measurements in a 96-well format. Application of this method for wild-type PAH revealed BH<sub>4</sub>-dependent positive cooperativity previously not described. Spectroscopic assessment of activating conformational changes and statistical evaluation of model-fitting disclosed PAH activation as a prerequisite for BH<sub>4</sub>-dependent positive cooperativity. BH<sub>4</sub> has recently been approved as a pharmacological chaperone drug in the treatment of phenylketonuria. We showed that the presence of L-Phe affects the BH<sub>4</sub>-dependent kinetic properties of PAH. These findings may, thus, have implications for an individualized therapy, as they support the hypothesis that patient metabolic state may have a more significant effect on the interplay of the drug and the conformation and function of the target protein than currently appreciated.

*Acknowledgment*—We are indebted to Christoph Siegel for excellent technical assistance.

## REFERENCES

1. Zschocke, J. (2003) *Hum. Mutat.* **21**, 345–356
2. Fiege, B., and Blau, N. (2007) *J. Pediatr.* **150**, 627–630
3. Muntau, A. C., Röschinger, W., Habich, M., Demmelmair, H., Hoffmann, B., Sommerhoff, C. P., and Roscher, A. A. (2002) *N. Engl. J. Med.* **347**, 2122–2132
4. Levy, H. L., Milanowski, A., Chakrapani, A., Cleary, M., Lee, P., Trefz, F. K., Whitley, C. B., Feillet, F., Feigenbaum, A. S., Bebchuk, J. D., Christ-

- Schmidt, H., and Dorenbaum, A. (2007) *Lancet* **370**, 504–510
5. Trefz, F. K., Burton, B. K., Longo, N., Casanova, M. M., Gruskin, D. J., Dorenbaum, A., Kakkis, E. D., Crombez, E. A., Grange, D. K., Hartz, P., Lipson, M. H., Milanowski, A., Randolph, L. M., Vockley, J., Whitley, C. B., Wolff, J. A., Bechuk, J., Christ-Schmidt, H., and Hennermann, J. B. (2009) *J. Pediatr.* **154**, 700–707
6. Shiman, R., Gray, D. W., and Hill, M. A. (1994) *J. Biol. Chem.* **269**, 24637–24646
7. Shiman, R., Xia, T., Hill, M. A., and Gray, D. W. (1994) *J. Biol. Chem.* **269**, 24647–24656
8. Xia, T., Gray, D. W., and Shiman, R. (1994) *J. Biol. Chem.* **269**, 24657–24665
9. Shiman, R., and Gray, D. W. (1980) *J. Biol. Chem.* **255**, 4793–4800
10. Shiman, R., Jones, S. H., and Gray, D. W. (1990) *J. Biol. Chem.* **265**, 11633–11642
11. Shiman, R., Mortimore, G. E., Schworer, C. M., and Gray, D. W. (1982) *J. Biol. Chem.* **257**, 11213–11216
12. Mitnaul, L. J., and Shiman, R. (1995) *Proc. Natl. Acad. Sci. U.S.A.* **92**, 885–889
13. Andersen, O. A., Stokka, A. J., Flatmark, T., and Hough, E. (2003) *J. Mol. Biol.* **333**, 747–757
14. Solstad, T., Stokka, A. J., Andersen, O. A., and Flatmark, T. (2003) *Eur. J. Biochem.* **270**, 981–990
15. Andersen, O. A., Flatmark, T., and Hough, E. (2002) *J. Mol. Biol.* **320**, 1095–1108
16. Stokka, A. J., Carvalho, R. N., Barroso, J. F., and Flatmark, T. (2004) *J. Biol. Chem.* **279**, 26571–26580
17. Gersting, S. W., Kemter, K. F., Staudigl, M., Messing, D. D., Danecka, M. K., Lagler, F. B., Sommerhoff, C. P., Roscher, A. A., and Muntau, A. C. (2008) *Am. J. Hum. Genet.* **83**, 5–17
18. Waters, P. J., Parniak, M. A., Akerman, B. R., and Scriver, C. R. (2000) *Mol. Genet. Metab.* **69**, 101–110
19. Erlandsen, H., Pey, A. L., Gámez, A., Pérez, B., Desviat, L. R., Aguado, C., Koch, R., Surendran, S., Tying, S., Matalon, R., Scriver, C. R., Ugarte, M., Martínez, A., and Stevens, R. C. (2004) *Proc. Natl. Acad. Sci. U.S.A.* **101**, 16903–16908
20. Bailey, S. W., and Ayling, J. E. (1980) *Anal. Biochem.* **107**, 156–164
21. Ledley, F. D., Grenett, H. E., and Woo, S. L. (1987) *J. Biol. Chem.* **262**, 2228–2233
22. Martínez, A., Knappskog, P. M., Olafsdottir, S., Døskeland, A. P., Eiken, H. G., Svebak, R. M., Bozzini, M., Apold, J., and Flatmark, T. (1995) *Biochem. J.* **306**, 589–597
23. Copeland, R. A. (2000) *Enzymes: A Practical Introduction to Structure, Mechanism, and Data Analysis*, 2nd Ed., Wiley-VCH, New York, NY
24. Fisher, D. B., and Kaufman, S. (1973) *J. Biol. Chem.* **248**, 4345–4353
25. Flatmark, T., Stokka, A. J., and Berge, S. V. (2001) *Anal. Biochem.* **294**, 95–101
26. Pey, A. L., and Martínez, A. (2005) *Mol. Genet. Metab.* **86**, S43–S53
27. Liu, Y., Kati, W., Chen, C. M., Tripathi, R., Molla, A., and Kohlbrenner, W. (1999) *Anal. Biochem.* **267**, 331–335
28. Palmier, M. O., and Van Doren, S. R. (2007) *Anal. Biochem.* **371**, 43–51
29. Reissmann, S., Parnot, C., Booth, C. R., Chiu, W., and Frydman, J. (2007) *Nat. Struct. Mol. Biol.* **14**, 432–440
30. Hutt, D. M., Baltz, J. M., and Ngsee, J. K. (2005) *J. Biol. Chem.* **280**, 20197–20203
31. Brock, D. A., Ehrenman, K., Ammann, R., Tang, Y., and Gomer, R. H. (2003) *J. Biol. Chem.* **278**, 52262–52272
32. De Koninck, P., and Schulman, H. (1998) *Science* **279**, 227–230
33. James, J. R., Oliveira, M. L., Carmo, A. M., Iaboni, A., and Davis, S. J. (2006) *Nat. Methods* **3**, 1001–1006
34. Miller, W. L., Matewish, M. J., McNally, D. J., Ishiyama, N., Anderson, E. M., Brewer, D., Brisson, J. R., Berghuis, A. M., and Lam, J. S. (2008) *J. Biol. Chem.* **283**, 3507–3518
35. Bailey, S. W., and Ayling, J. E. (1978) *J. Biol. Chem.* **253**, 1598–1605
36. Kaufman, S. (1993) *Adv. Enzymol. Relat. Areas Mol. Biol.* **67**, 77–264
37. Knappskog, P. M., Flatmark, T., Aarden, J. M., Haavik, J., and Martínez, A. (1996) *Eur. J. Biochem.* **242**, 813–821
38. Bjørge, E., de Carvalho, R. M., and Flatmark, T. (2001) *Eur. J. Biochem.* **268**, 997–1005
39. Pérez, B., Desviat, L. R., Gómez-Puertas, P., Martínez, A., Stevens, R. C., and Ugarte, M. (2005) *Mol. Genet. Metab.* **86**, S11–S16
40. Gersting, S. W., Lagler, F. B., Eichinger, A., Kemter, K. F., Danecka, M. K., Messing, D. D., Staudigl, M., Domdey, K. A., Zsifkovits, C., Fingerhut, R., Glossmann, H., Roscher, A. A., and Muntau, A. C. (2010) *Hum. Mol. Genet.* **19**, 2039–2049
41. Kappock, T. J., Harkins, P. C., Friedenber, S., and Caradonna, J. P. (1995) *J. Biol. Chem.* **270**, 30532–30544
42. Davis, M. D., Parniak, M. A., Kaufman, S., and Kempner, E. (1997) *Proc. Natl. Acad. Sci. U.S.A.* **94**, 491–495
43. Chehin, R., Thorólfsson, M., Knappskog, P. M., Martínez, A., Flatmark, T., Arrondo, J. L., and Muga, A. (1998) *FEBS Lett.* **422**, 225–230
44. Teigen, K., Frøystein, N. A., and Martínez, A. (1999) *J. Mol. Biol.* **294**, 807–823
45. Thórolfsson, M., Ibarra-Molero, B., Fojan, P., Petersen, S. B., Sanchez-Ruiz, J. M., and Martínez, A. (2002) *Biochemistry* **41**, 7573–7585
46. Monod, J., Wyman, J., and Changeux, J. P. (1965) *J. Mol. Biol.* **12**, 88–118
47. Koshland, D. E., Jr., Némethy, G., and Filmer, D. (1966) *Biochemistry* **5**, 365–385
48. Knappskog, P. M., and Haavik, J. (1995) *Biochemistry* **34**, 11790–11799
49. Shiman, R., Gray, D. W., and Pater, A. (1979) *J. Biol. Chem.* **254**, 11300–11306
50. Cornish-Bowden, A., and Cárdenas, M. L. (1987) *J. Theor. Biol.* **124**, 1–23
51. Volner, A., Zoidakis, J., and Abu-Omar, M. M. (2003) *J. Biol. Inorg. Chem.* **8**, 121–128
52. Erlandsen, H., Bjørge, E., Flatmark, T., and Stevens, R. C. (2000) *Biochemistry* **39**, 2208–2217
53. Pey, A. L., Pérez, B., Desviat, L. R., Martínez, M. A., Aguado, C., Erlandsen, H., Gámez, A., Stevens, R. C., Thórolfsson, M., Ugarte, M., and Martínez, A. (2004) *Hum. Mutat.* **24**, 388–399
54. Lee, J., Johnson, J., Ding, Z., Paetzel, M., and Cornell, R. B. (2009) *J. Biol. Chem.* **284**, 33535–33548
55. Velloso, L. M., Bhaskaran, S. S., Schuch, R., Fischetti, V. A., and Stebbins, C. E. (2008) *EMBO Rep.* **9**, 199–205
56. Sawicki, A., and Willows, R. D. (2008) *J. Biol. Chem.* **283**, 31294–31302
57. Isin, E. M., and Guengerich, F. P. (2006) *J. Biol. Chem.* **281**, 9127–9136
58. Pauwels, F., Vergauwen, B., Vanrobaeys, F., Devreese, B., and Van Beeumen, J. J. (2003) *J. Biol. Chem.* **278**, 16658–16666
59. Thórolfsson, M., Teigen, K., and Martínez, A. (2003) *Biochemistry* **42**, 3419–3428

## SUPPLEMENTAL MATERIALS AND METHODS

*Real-time multi-well kinetic analysis.* The application of the enzyme reaction mixture to a 96-well plate with varying substrate concentrations was automated using a multi-well fluorescence detection device with integrated injection system (FLUOstar OPTIMA, BMG Labtech). The reaction was initiated by sequential injection of BH<sub>4</sub> with and without simultaneous injection of L-Phe, allowing the determination of L-Tyr production in all wells after the following scheme. Following the injection of BH<sub>4</sub>, L-Phe and a final mixture of the samples, 2 rows consisting of 24 wells were measured in repeated cycles over a time period of 60 seconds (Fig. 1F), the time frame evaluated to be within the linear range of action for the enzyme concentration used (Fig. 1E).

*Defining the protein concentration.* Enzyme activity was measured using the assay described under standard conditions with 1 mM L-Phe and 75 μM BH<sub>4</sub>, with varying protein concentrations (0.005-3 mg/ml). Production of L-Tyr was measured directly over a time period of 10 minutes. Initial velocity was determined as the time period in which less than 10 % of the substrate is utilized. For all protein concentrations, steady state kinetics occurred 30 seconds after initiation of the reaction and burst-phase kinetics. With decreasing protein concentrations, steady state kinetics were linear over increasing periods of time, yet sensitivity for the measurement of L-Tyr production decreased. All measurements were assayed as triplicates and all concentrations refer to a final volume of 204 μl. A final protein concentration of 0.01 mg/ml with an optimal time range of 60 seconds for linear range of reaction was chosen for all activity assays (Fig. 1E).

## FIGURE LEGENDS

**SUPPLEMENTAL FIGURE 1. Verifying spectral separation and the inner filter effect of BH<sub>4</sub>.** *A*, To verify spectral separation needed for the direct in-well fluorescence detection of enzymatic L-Tyr production, 190 μM L-Tyr were measured at the L-Tyr excitation wavelength 304 nm as a function of increasing L-Phe concentrations. L-Tyr fluorescence signal intensities uninfluenced by increasing L-Phe concentrations are shown. *B*, A decrease in L-Tyr fluorescence intensity with increasing BH<sub>4</sub> concentrations, as applied in the BH<sub>4</sub>-dependent enzyme activity assay, is shown. Specific correction factors were determined on the basis of the factorial decrease of signal intensity for every BH<sub>4</sub> concentration added to the reaction mixture to account for its inner filter effect.

**SUPPLEMENTAL FIGURE 2. Comparison of non-linear regression model fitting by the Michaelis-Menten and the Hill kinetic model.** Residuals of values calculated using the Michaelis-Menten and Hill-equation for non-linear regression analysis of the enzyme kinetic data obtained for the wild-type PAH, R68S, V106A and the dimeric PAH 103-427, without (-) and with (+) preincubation of the enzyme with 1 mM L-Phe, are shown. Enzyme kinetics were determined with varying BH<sub>4</sub> concentrations (0-50 and 0-125 μM) and one L-Phe concentration (1 mM). The residuals of values were used as the primary criteria for selecting one model over the other. In case of indifferent residuals of values, the simpler Michaelis-Menten kinetic model was chosen for data-fitting because a more complex model like the Hill equation would always fit the experimental data better than a simpler model. A good model fitting reduces the residuals to zero. The model best describing the enzyme kinetic data obtained is shown in green. While BH<sub>4</sub>-dependent enzyme kinetics of the non-activated wild-type PAH were best described by the Michaelis-Menten equation, the activated wild-type PAH and the preactivated variants followed the Hill kinetic model.

**SUPPLEMENTAL TABLE 1. Comparison of two nested non-linear regression models**

[BH <sub>4</sub> ] $\mu$ M	L-Phe preincubation	Henri-Michaelis-Menten-Equation			Hill-Equation		
		R <sup>2</sup>	Sy.x	Runs	R <sup>2</sup>	Sy.x	Runs
0-125	-	0.9660	127.5	3 <sup>§</sup> (P = 0.048)	0.9742	117.8	8 n.s.
0-125	+	0.9609	559.2	5 n.s.	0.9943	225.6	7 n.s.
0-50	-	0.9802	46.60	6 n.s.	0.9813	47.75	10 n.s.
0-50	+	0.9806	287.0	3 <sup>§</sup> (P = 0.024)	0.9973	112.1	6 n.s.

Analysis of goodness of fit, Sy.x and runs test for two nested models after measurement of wild-type PAH kinetics without and with preincubation of the enzyme with L-Phe. Enzyme kinetics were measured with L-Phe (1 mM) and BH<sub>4</sub> (0-125  $\mu$ M and 0-50  $\mu$ M).

<sup>§</sup> If the data were randomly scattered above and below the curve, there is less than 5% chance of observing so few runs. The data systematically deviate from the curve. Most likely, the data were fit to the wrong equation. P < 0.05

**SUPPLEMENTAL TABLE 2. Comparison of two nested non-linear regression models with and without preincubation of preactivated variants**

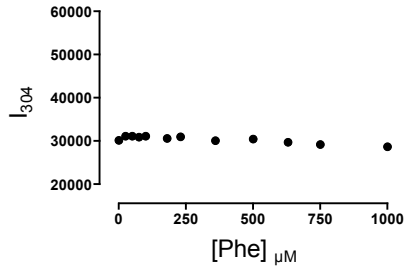
	L-Phe preincubation	Henri-Michaelis-Menten-Equation			Hill-Equation		
		R <sup>2</sup>	Sy.x	Runs	R <sup>2</sup>	Sy.x	Runs
R68S	-	0.9788	412.4	3 <sup>§</sup> (P = 0.048)	0.9972	160.3	5 n.s.
R68S	+	0.9762	385.1	3 <sup>§</sup> (P = 0.047)	0.9973	138.2	9 n.s.
V106A	-	0.9850	341.4	3 <sup>§</sup> (P = 0.024)	0.9956	195.2	9 n.s.
V106A	+	0.9790	454.7	3 <sup>§</sup> (P = 0.024)	0.9954	224.9	7 n.s.
103-427	-	0.9231	197.4	5 n.s.	0.9628	144.8	7 n.s.
103-427	+	0.9177	265.0	3 <sup>§</sup> (P = 0.033)	0.9836	124.6	7 n.s.

Analysis of goodness of fit, Sy.x and runs test for two nested models after measurement of enzyme kinetics without and with preincubation of the enzyme with L-Phe. Enzyme kinetics were measured with L-Phe (1 mM) and BH<sub>4</sub> (0-125  $\mu$ M).

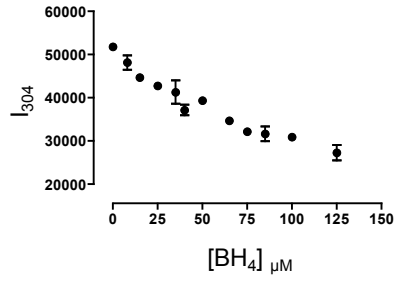
<sup>§</sup> If the data were randomly scattered above and below the curve, there is less than 5% chance of observing so few runs. The data systematically deviate from the curve. Most likely, the data were fit to the wrong equation. P < 0.05

# SUPPLEMENTAL FIGURE 1

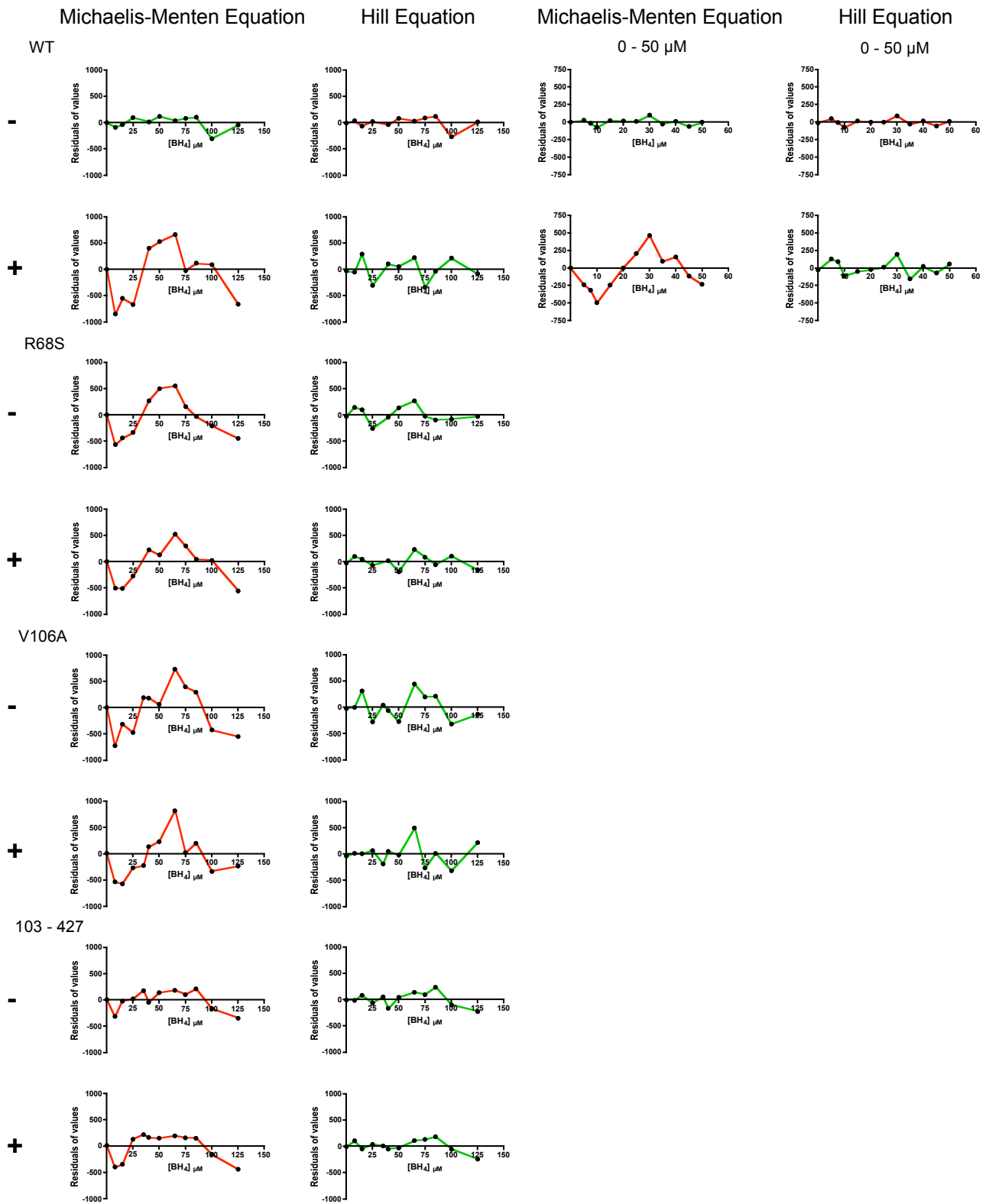
**A**



**B**



## SUPPLEMENTAL FIGURE 2



# The interplay between genotype, metabolic state and cofactor treatment governs phenylalanine hydroxylase function and drug response

Michael Staudigl<sup>1,†</sup>, Søren W. Gersting<sup>1,†</sup>, Marta K. Danecka<sup>1</sup>, Dunja D. Messing<sup>1</sup>,  
Mathias Woidy<sup>1</sup>, Daniel Pinkas<sup>1</sup>, Kristina F. Kemter<sup>1,‡</sup>, Nenad Blau<sup>2,3</sup> and Ania C. Muntau<sup>1,\*</sup>

<sup>1</sup>Department of Molecular Pediatrics, Dr von Hauner Children's Hospital, Ludwig-Maximilians-University, 80337 Munich, Germany, <sup>2</sup>Division of Clinical Chemistry and Biochemistry, University Children's Hospital, Zürich, Switzerland and <sup>3</sup>Zürich Center for Integrative Human Physiology (ZIHP), Zürich, Switzerland

Received March 7, 2011; Revised and Accepted April 12, 2011

The discovery of a pharmacological treatment for phenylketonuria (PKU) raised new questions about function and dysfunction of phenylalanine hydroxylase (PAH), the enzyme deficient in this disease. To investigate the interdependence of the genotype, the metabolic state (phenylalanine substrate) and treatment (BH<sub>4</sub> cofactor) in the context of enzyme function *in vitro* and *in vivo*, we (i) used a fluorescence-based method for fast enzyme kinetic analyses at an expanded range of phenylalanine and BH<sub>4</sub> concentrations, (ii) depicted PAH function as activity landscapes, (iii) retraced the analyses in eukaryotic cells, and (iv) translated this into the human system by analyzing the outcome of oral BH<sub>4</sub> loading tests. PAH activity landscapes uncovered the optimal working range of recombinant wild-type PAH and provided new insights into PAH kinetics. They demonstrated how mutations might alter enzyme function in the space of varying substrate and cofactor concentrations. Experiments in eukaryotic cells revealed that the availability of the active PAH enzyme depends on the phenylalanine-to-BH<sub>4</sub> ratio. Finally, evaluation of data from BH<sub>4</sub> loading tests indicated that the patient's genotype influences the impact of the metabolic state on drug response. The results allowed for visualization and a better understanding of PAH function in the physiological and pathological state as well as in the therapeutic context of cofactor treatment. Moreover, our data underscore the need for more personalized procedures to safely identify and treat patients with BH<sub>4</sub>-responsive PAH deficiency.

## INTRODUCTION

Phenylketonuria (PKU; OMIM #261600), the most common inborn error of amino acid metabolism, is an autosomal recessive disorder caused by phenylalanine hydroxylase (PAH) deficiency (PAH; EC 1.14.16.1) (1). Currently, 627 different disease-causing mutations in the *PAH* gene are known ([www.pahdb.mcgill.ca](http://www.pahdb.mcgill.ca); [www.hgmd.org](http://www.hgmd.org)) and some of these were shown to lead to protein misfolding with loss of function (2–4).

Pharmacological doses of 6R-L-erythro-5,6,7,8-tetrahydrobiopterin (BH<sub>4</sub>), the enzyme's natural cofactor, can reduce blood phenylalanine concentrations (5–10) and increase phenylalanine oxidation rates *in vivo* (11) in patients with

PAH deficiency without any evidence of cofactor deficiency. The compound was shown to rescue the biochemical phenotype by correcting PAH misfolding and was thus classified as a pharmacological chaperone (4,12). Following these studies, sapropterin dihydrochloride, the synthetic form of the natural PAH cofactor, was approved as an orphan drug to alleviate or even replace burdensome dietary treatment in a significant share of patients with PKU due to PAH deficiency (13–16).

However, not all patients show BH<sub>4</sub> responsiveness. Since the introduction of sapropterin dihydrochloride as a pharmacological treatment, many attempts to predict BH<sub>4</sub> responsiveness from a patient's genotype were made (17–19).

\*To whom correspondence should be addressed. Tel: +49 8951602746; Fax: +49 8951607952; Email: [ania.muntau@med.lmu.de](mailto:ania.muntau@med.lmu.de)

<sup>†</sup>The authors wish it to be known that, in their opinion, the first two authors should be regarded as joint First Authors.

<sup>‡</sup>Present address: Leukocare AG, Am Klopferspitz 19, 82152 Planegg, Germany.

Combined evidence seems to support the view that residual enzyme activity of individual mutations may be a parameter that—to some extent—allows for discrimination of responders and non-responders (19–22). In two studies performed on Croatian and Turkish populations, calculation of mean *in vitro* residual enzyme activity of the two PAH variants arising from both alleles led to the identification of some responders with high accuracy, whereas patients with two fully inactive alleles were found to be always non-responders (19,22). Yet, in many instances, no clear genotype–phenotype correlation is found pointing to contributing factors such as the patient's age or initial blood phenylalanine concentrations (17,19). Marked inconsistencies as to BH<sub>4</sub> responsiveness were observed for two of the most common PKU mutations associated with this particular phenotype, R261Q and Y414C (17) and for R252W, L48S and R241C homozygous genotypes (22). In addition, interpretation of genotype effects is hampered by the fact that >80% of BH<sub>4</sub> responders are compound heterozygous (17).

Hydroxylation of the substrate L-phenylalanine to the product L-tyrosine with the use of the natural cofactor BH<sub>4</sub> and molecular oxygen is a complexly regulated catalytic mechanism. While L-phenylalanine induces activating conformational rearrangements, BH<sub>4</sub> leads to the formation of an inactive dead-end PAH–BH<sub>4</sub> complex (23–26). Recent studies unraveled new aspects concerning the interplay of phenylalanine and BH<sub>4</sub> having an impact on enzyme kinetics as well as on drug response. Adoption of an enzyme activity assay using a newly developed fluorescence-based real-time PAH activity assay revealed cooperativity of recombinant PAH towards the BH<sub>4</sub> cofactor. This was restricted to the phenylalanine substrate-activated state of the enzyme indicating that conformational rearrangements of the PAH protein induce cooperative binding (27). Moreover, investigations of the BH<sub>4</sub> effect in two different mouse models for BH<sub>4</sub>-responsive PAH deficiency provided evidence that the response to BH<sub>4</sub> in terms of rescue of enzyme function by increasing the effective intracellular PAH amount also depends on phenylalanine concentrations and on the underlying genotype (12). These results suggested that the influence of substrate and cofactor concentrations in the presence of a certain genotype on enzyme function and on the response to the pharmacological chaperone BH<sub>4</sub> might be of even more functional and therapeutic relevance than previously estimated. In addition, the BH<sub>4</sub> loading test routinely used worldwide to assess BH<sub>4</sub> responsiveness in PAH deficiency (28,29) was shown to result in a number of inconsistencies that are still not well understood. In some but not all cases, this may be due to inadequate BH<sub>4</sub> dosage or to initial blood phenylalanine concentrations near to the physiological state. Unfortunately, this may lead to false negative results precluding cofactor treatment and thus increasing burden of treatment in some BH<sub>4</sub>-responsive patients.

To address these issues, (i) we adapted our new fluorescence-based method for fast enzyme kinetic analyses to cover an expanded range of phenylalanine and BH<sub>4</sub> concentrations when compared with previous analytical setups enabling the investigation of the mutual impact of substrate and cofactor on PAH enzyme kinetics, (ii) we depicted these data as activity landscapes uncovering the optimal working

range of recombinant wild-type and mutated PAH, (iii) we retraced these analyses in a eukaryotic cell culture system, revealing that the availability of the active PAH enzyme depends on both the metabolic state and drug dosage, and (iv) we translated this into the human system by analyzing the effect of the genotype, phenylalanine concentrations and the BH<sub>4</sub> dosage applied on the results of oral BH<sub>4</sub> loading tests from PAH-deficient patients.

## RESULTS

### Expanded insights into wild-type PAH kinetics unraveling the mutual impact of substrate and cofactor concentrations

In order to investigate the interdependence of L-phenylalanine and BH<sub>4</sub> in PAH enzyme kinetics, we adapted a newly developed fluorescence-based real-time activity assay (27) to simultaneously analyze the effect of a wide range of substrate and cofactor concentrations on PAH activity. Process automation now allowed for continuous measurement of tyrosine product formation over time in one single operation consisting of six sequential runs for all 96 wells (Fig. 1A). The assay was expanded to cover the space of 0 to 4000 μM L-phenylalanine and 0–500 μM BH<sub>4</sub> (Fig. 1B). First, we validated the data obtained with the new method by comparison with previous findings using a standard high-performance liquid chromatography (HPLC) based discontinuous assay (2). Data points determined at either varying L-phenylalanine concentrations (0–1000 μM) and one BH<sub>4</sub> concentration (75 μM) or at one L-phenylalanine concentration (1000 μM) and varying BH<sub>4</sub> concentrations (0–125 μM), respectively, were used to calculate enzyme kinetic parameters. Prior to calculation, an *F*-test was used to decide whether the Michaelis–Menten or the Hill kinetic model was more appropriate (27). Both L-phenylalanine and BH<sub>4</sub>-dependent PAH enzyme kinetics showed clear data-fitting to the Hill equation (Fig. 1C), as previously described for the L-phenylalanine-activated enzyme (27). Although  $V_{\max}$  values for L-phenylalanine and BH<sub>4</sub>-dependent kinetics were higher in the new assay, allosteric parameters, i.e. apparent substrate affinity, the Hill coefficient and apparent cofactor affinity, were similar in both assays (Table 1).

We depicted the data analyzed by non-linear and polynomial regression fitting as three-dimensional landscapes of enzyme activity (30). This enabled a visual representation of the mutual impact of substrate (*x*-axis) and cofactor concentrations (*y*-axis) on PAH kinetics (color code) representing functional conditions of the PAH enzyme. Wild-type PAH showed a peak maximum enzyme activity at 575 μM L-phenylalanine and 125 μM BH<sub>4</sub>, respectively (Fig. 1D). The analysis of PAH enzyme kinetics at BH<sub>4</sub> and L-phenylalanine concentrations extended to supraphysiological levels led to a number of interesting observations. High PAH enzyme activity was determined at a surprisingly wide range of substrate and cofactor concentrations. The optimal working range reflected by PAH enzyme activity in the boundaries of  $[S]_{0.5}$  to  $K_i$  for the substrate and  $[C]_{0.5}$  to  $K_i$  for the cofactor spanned from 252 to 2026 μM L-phenylalanine and from 44 to 306 μM BH<sub>4</sub> (Table 2). At L-phenylalanine concentrations above 561 μM, we observed the well-known substrate inhibition of enzyme activity (30,31). Notably, at cofactor

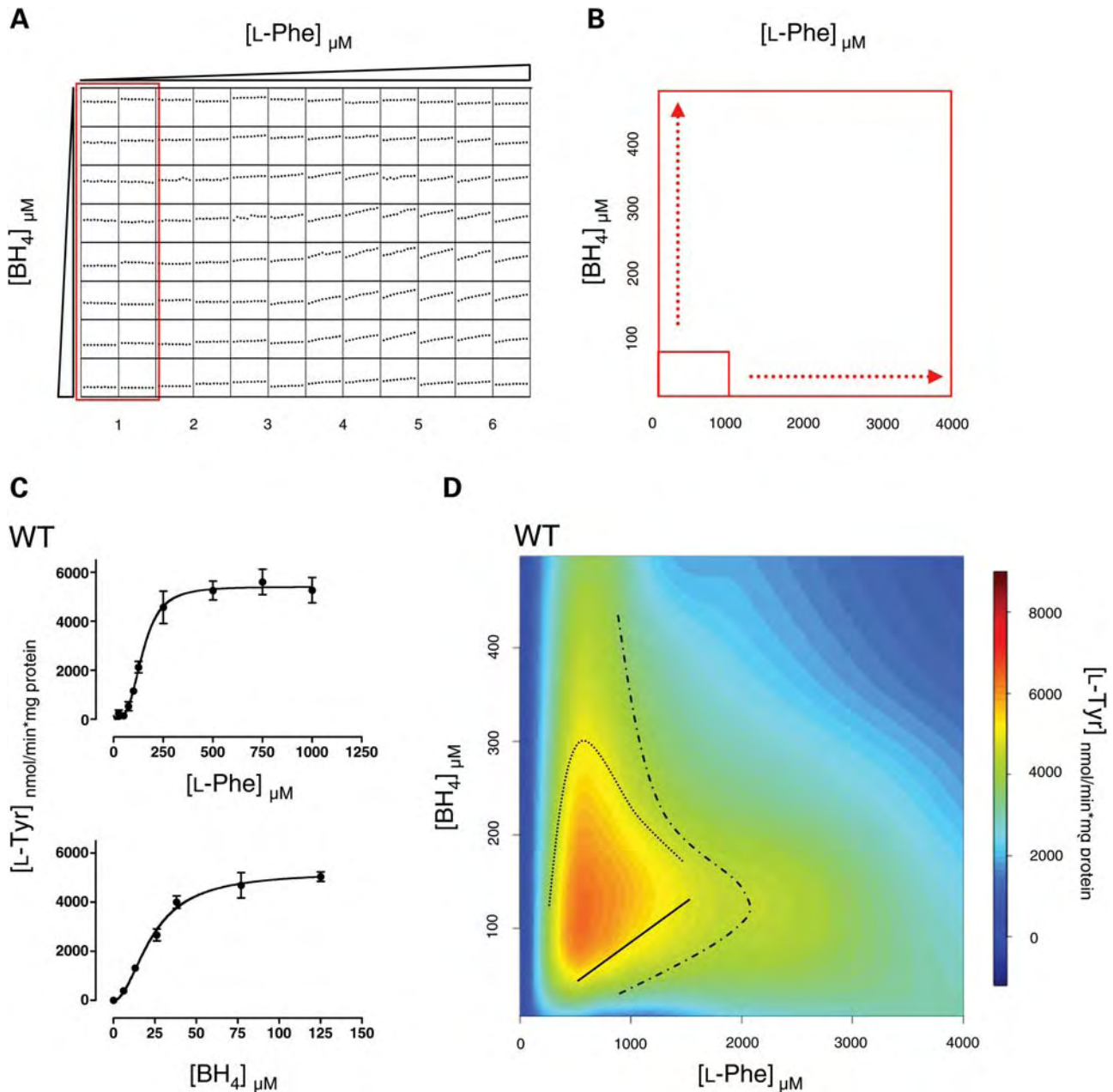


**Figure 1.** Optimal working range of wild-type PAH activity. (A) Scheme of sequential measurements of PAH enzyme kinetics in a 96-well plate. One sequence consists of two columns (red box). In each column, cofactor concentrations (0–500  $\mu\text{M}$ ) were varied at a fixed substrate concentration (0–4000  $\mu\text{M}$ ), respectively. Repeated cycles allowed for kinetic measurements of 16 wells over a time period of 90 s. (B) Extension of substrate and cofactor concentrations. The range of L-phenylalanine and BH<sub>4</sub> concentrations was expanded from standard conditions (BH<sub>4</sub>, 75  $\mu\text{M}$ ; L-phenylalanine 1000  $\mu\text{M}$ , red box) to 500  $\mu\text{M}$  BH<sub>4</sub> and 4000  $\mu\text{M}$  L-phenylalanine (arrows), respectively. (C) Cooperativity of PAH towards substrate and cofactor. Pre-activated PAH showed sigmoidal behavior for L-phenylalanine- (upper panel) and BH<sub>4</sub>-dependent (lower panel) PAH enzyme kinetics. (D) Activity landscape of human wild-type PAH. Data for PAH enzyme activity assayed at varying L-phenylalanine and BH<sub>4</sub> concentrations were interpolated and depicted by a color code. The dot-and-dash line represents  $K_i$  for substrate inhibition at varying cofactor concentrations, the dotted line represents  $K_i$  for cofactor inhibition at varying substrate concentrations. With increasing substrate concentrations, more BH<sub>4</sub> is needed to maintain the same level of enzyme activity (solid line).

concentrations above 108  $\mu\text{M}$  cofactor inhibition occurred. In addition, a mutual interdependence of both inhibitory events was found. These observations represent previously unknown findings. Over and above that, at L-phenylalanine concentrations within the range naturally occurring in the pathological state (500–1500  $\mu\text{M}$ ), the enzyme requires more

BH<sub>4</sub> with increasing L-phenylalanine concentrations to maintain the same level of enzyme activity.

Taken together, the considerable extension of analysis conditions and the evaluation of data by compiling activity landscapes provided new insights into PAH kinetics. It allowed for a precise evaluation of peak PAH enzyme activity and the

**Table 1.** Comparison of enzyme kinetic parameters of human wild-type MBP-PAH at standard L-phenylalanine (1000  $\mu\text{M}$ ) and BH<sub>4</sub> (75  $\mu\text{M}$ ) concentrations

	L-phenylalanine <sup>a</sup> $V_{\text{max}}$ (nmol L-tyrosine/min $\times$ mg protein)	[S] <sub>0.5</sub> ( $\mu\text{M}$ )	$h_{\text{Phe}}$	BH <sub>4</sub> <sup>b</sup> $V_{\text{max}}$ (nmol L-tyrosine/min $\times$ mg protein)	[C] <sub>0.5</sub> ( $\mu\text{M}$ )	$K_{\text{m}}$ ( $\mu\text{M}$ )	$h_{\text{BH}_4}$
Continuous assay	5407 $\pm$ 210	145 $\pm$ 11	3.3	5222 $\pm$ 286	23 $\pm$ 2		2.0
Discontinuous assay	3470 $\pm$ 75	155 $\pm$ 6	3.0	3425 $\pm$ 139		24 $\pm$ 3	

Steady-state kinetic parameters of wild-type MBP-PAH fusion proteins.  $V_{\text{max}}$  and the apparent affinities for L-phenylalanine ( $S_{0.5}$ ) and BH<sub>4</sub> ( $C_{0.5}$ ,  $K_{\text{m}}$ ) as well as the Hill coefficient ( $h$ ) as a measure of cooperativity are shown. Enzyme kinetic parameters were determined from enzyme activities measured using the newly developed fluorescence-based continuous assay and compared with enzyme activities measured by the standard HPLC-based discontinuous assay (2). Data were analyzed using the  $F$ -test for model comparison and the kinetic parameters of the best-fitting model (cooperative versus non-cooperative) were calculated. Values are given as mean  $\pm$  SEM of three independent measurements.

<sup>a</sup>Enzyme kinetic parameters determined at variable L-phenylalanine concentrations (0–1000  $\mu\text{M}$ ) and standard BH<sub>4</sub> concentration (75  $\mu\text{M}$ ) with pre-incubation of the enzyme by L-phenylalanine (1000  $\mu\text{M}$ ).

<sup>b</sup>Enzyme kinetic parameters determined at variable BH<sub>4</sub> concentrations (0–125  $\mu\text{M}$ ) and standard L-phenylalanine concentration (1000  $\mu\text{M}$ ) with pre-incubation of the enzyme by L-phenylalanine (1000  $\mu\text{M}$ ).

**Table 2.** Peak enzyme activity and range of substrate and cofactor concentrations of wild-type and variant PAH

	Peak activity (nmol L-tyrosine/min $\times$ mg protein)	Residual activity (%)	L-phenylalanine concentration at peak activity ( $\mu\text{M}$ )	[S] <sub>0.5</sub> - $K_{\text{i}}^{\S}$	BH <sub>4</sub> concentration at peak activity ( $\mu\text{M}$ )	[C] <sub>0.5</sub> - $K_{\text{i}}$ or $K_{\text{m}}-K_{\text{i}}^{\S}$
WT	6370	100	561	252–2026	108	44–306
F39L	5865	92	622	187–2275	143	35–331
I65T	3533	55	612	254–2075	135	29–322
R261Q	2654	42	842	344–2825	149	41–321
P275L	5215	82	1293	238–1980	334	71–435
P314S	1956	31	612	76–1043	80	42–218
V388M	6355	100	591	201–1933	105	47–296
Y414C <sup>a</sup>	3106	49	591	124–1048 <sup>a</sup>	105	43–274
Y417H	5206	82	471	147–1501	92	63–262

Peak enzyme activity of variant tetrameric MBP-PAH fusion proteins measured by direct in-well activity measurements. The apparent affinities for L-phenylalanine ( $S_{0.5}$ ) and BH<sub>4</sub> ( $C_{0.5}/K_{\text{m}}$ ) as well as  $K_{\text{i}}$  for substrate and cofactor inhibition were calculated based on non-linear regression analysis at L-phenylalanine and BH<sub>4</sub> concentrations of peak enzyme activity.

<sup>\S</sup> $K_{\text{i}}$  calculated at peak L-phenylalanine and BH<sub>4</sub> concentrations using the Boltzman-sigmoidal equation.

<sup>a</sup>Calculation of  $K_{\text{i}}$  at a range of L-phenylalanine 0–1624  $\mu\text{M}$ .

optimal working range spanning a wide area of substrate and cofactor concentrations. Moreover, cofactor inhibition as well as a mutual impact of substrate and cofactor concentrations on PAH activity have been identified.

### Activity landscapes: the effect of PAH mutations on PAH enzyme kinetics

Variant PAH proteins harboring mutations mapping to the regulatory (F39L, I65T), the catalytic (R216Q, P275L, P314S, V388M) and the dimerization motif of the oligomerization domain (Y414C, Y417H) of the enzyme were analyzed. The results from kinetic measurements were depicted as activity landscapes and compared with those from wild-type PAH (Fig. 2). For each variant analyzed, enzyme kinetic parameters and peak enzyme activities with their corresponding L-phenylalanine or BH<sub>4</sub> concentrations were determined (Tables 2 and 3). The area of optimal enzyme activity defined as the range  $[S]_{0.5}$  to  $K_{\text{i}}$  for the substrate and  $[C]_{0.5}$  to  $K_{\text{i}}$  for the cofactor, respectively, was calculated (Table 2).

The variant proteins bearing the mutation F39L or I65T, both located in the regulatory domain, showed at first glance a landscape pattern comparable with that of the wild-type.

Besides enzyme activity (F39L, 92%; I65T, 55%), the variants displayed unaffected enzyme kinetic parameters as well as similar effects of substrate and cofactor inhibition as found for the wild-type enzyme. However, a more detailed analysis revealed that peak PAH activities were found at similar substrate concentrations, but at  $\sim 1.3$ -fold higher cofactor concentrations when compared with the wild-type. This indicates that in the presence of these mutations, more cofactor is needed to achieve optimal PAH function.

All mutations mapping to the catalytic domain induced marked alterations of activity landscapes. For the variant R261Q, the area of substantial PAH activity was much larger than for the wild-type, but residual enzyme activity was reduced to 42%. The concentrations of substrate and cofactor needed to achieve peak PAH activity were shifted to higher values (L-phenylalanine, 1.5-fold; BH<sub>4</sub>, 1.4-fold). We observed reduced affinity to the substrate by a factor of 0.5 ( $[S]_{0.5}$  282  $\mu\text{M}$ ). Binding of BH<sub>4</sub> followed Michaelis-Menten kinetics representing a loss of cooperativity that occurred with reduced affinity ( $K_{\text{m}}$  66  $\mu\text{M}$ ). Broadening of the landscape resulted from a significant shift of enzyme inhibition. Notably, the variant did not display cooperative binding of BH<sub>4</sub> when activated. Taken together, the unique feature of

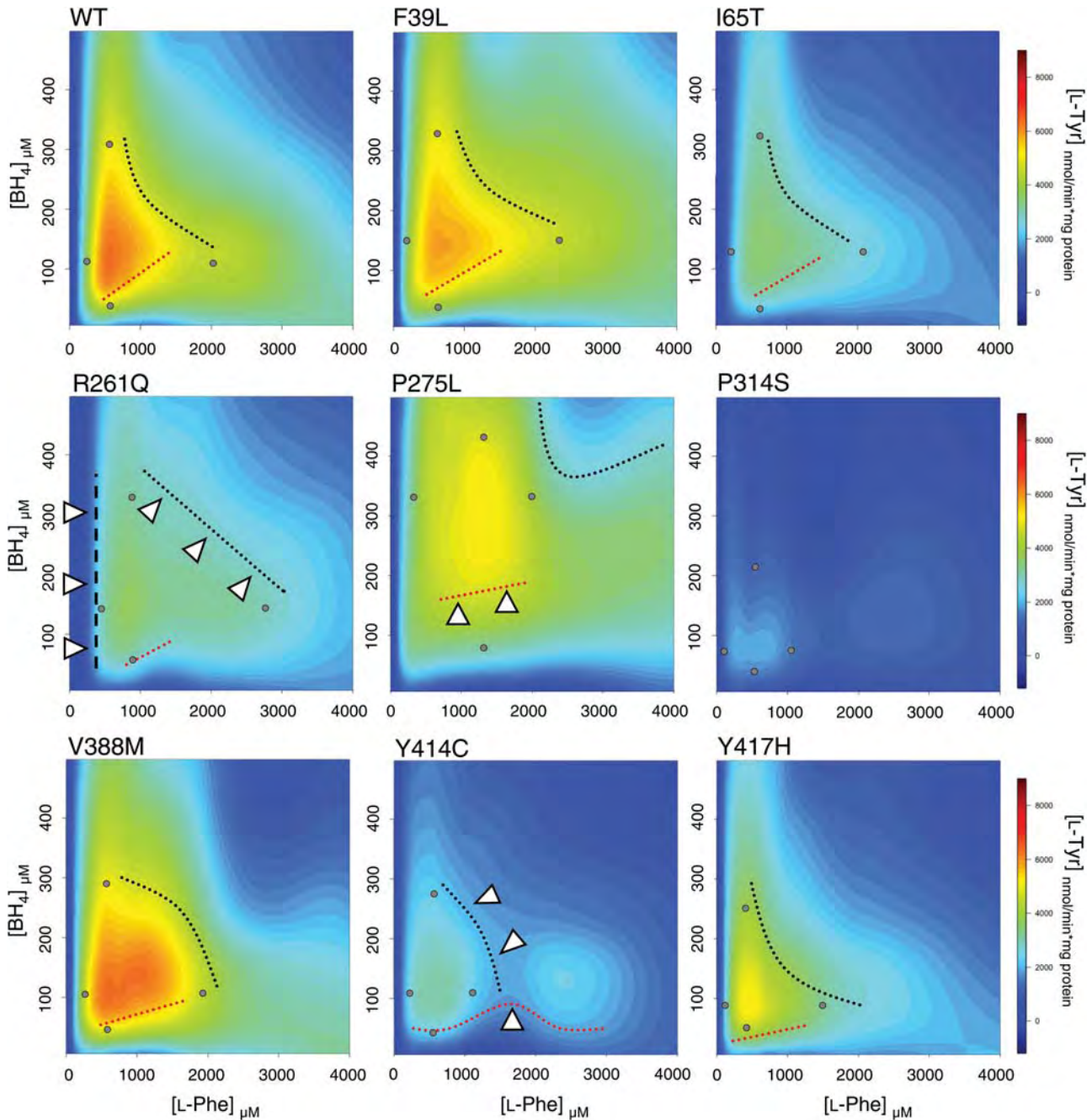


**Figure 2.** Activity landscapes of recombinant wild-type and variant PAH. The interpolated specific enzyme activities are color-coded and given as a function of different *L*-phenylalanine and BH<sub>4</sub> concentrations. Substrate and cofactor inhibition are depicted as a summation line (black dotted line). Positions of  $S_{0.5}$  and  $K_i$  for *L*-phenylalanine and  $C_{0.5}$  and  $K_i$  for BH<sub>4</sub>, respectively, are indicated at peak enzyme activities (open circles). Marked changes in the activity landscape of variant PAH when compared with the wild-type (WT) are highlighted (open triangles) and BH<sub>4</sub> concentrations needed to maintain the same enzyme activity with increasing *L*-phenylalanine concentrations are shown (red dotted line).

the R261Q variant was the right shift of PAH enzyme activity towards higher *L*-phenylalanine concentrations indicating a reduced affinity of this variant to its substrate and that the enzyme displays low activity at *L*-phenylalanine concentrations below 600  $\mu\text{mol/l}$ . At these substrate concentrations, even very high BH<sub>4</sub> doses would not produce any response in PAH activity. The presence of the mutation P275L resulted in an enzyme with overall high residual enzyme activity

(82%), yet with a shift of peak enzyme activity to 2.3-fold higher *L*-phenylalanine and 3-fold higher BH<sub>4</sub> concentrations (*L*-phenylalanine 1293  $\mu\text{M}$ , BH<sub>4</sub> 334  $\mu\text{M}$ ) than the wild-type. In comparison to the wild-type, the enzyme had a substantially higher need for BH<sub>4</sub> to achieve the optimal working range. As a consequence, substrate and cofactor inhibition was almost abolished. The variant protein bearing the mutation P314S showed a severe loss in residual enzyme activity (31%) with

**Table 3.** Enzyme kinetic parameters at standard L-phenylalanine (1000  $\mu\text{M}$ ) and BH<sub>4</sub> (75  $\mu\text{M}$ ) concentrations calculated from activity landscapes

	L-phenylalanine <sup>a</sup> $V_{\text{max}}$ (nmol L-tyrosine/min $\times$ mg protein)	[S] <sub>0.5</sub> ( $\mu\text{M}$ )	$h_{\text{Phe}}$	BH <sub>4</sub> <sup>b</sup> $V_{\text{max}}$ (nmol L-tyrosine/min $\times$ mg protein)	[C] <sub>0.5</sub> ( $\mu\text{M}$ )	$K_{\text{m}}$ ( $\mu\text{M}$ )	$h_{\text{BH}_4}$
WT	5407 $\pm$ 210	145 $\pm$ 11	3.3	5222 $\pm$ 286	23 $\pm$ 2		2.0
F39L	4961 $\pm$ 342	115 $\pm$ 15	2.7	5669 $\pm$ 311	36 $\pm$ 3		1.7
I65T	3166 $\pm$ 96	161 $\pm$ 10	2.7	3277 $\pm$ 196	27 $\pm$ 3		1.7
R261Q	3041 $\pm$ 128	282 $\pm$ 18	3.4	4693 $\pm$ 598		66 $\pm$ 17	
P275L	3204 $\pm$ 126	112 $\pm$ 8	2.6	3022 $\pm$ 179	36 $\pm$ 3		2.8
P314S	1650 $\pm$ 91	76 $\pm$ 9	1.8	991 $\pm$ 25	24 $\pm$ 1		5.2
V388M	5639 $\pm$ 112	140 $\pm$ 6	2.7	5895 $\pm$ 236	26 $\pm$ 2		1.8
Y414C	2895 $\pm$ 206	120 $\pm$ 17	2.4	2148 $\pm$ 203	28 $\pm$ 4		2.6
Y417H	4434 $\pm$ 247	111 $\pm$ 10	3.6	3011 $\pm$ 93	23 $\pm$ 1		2.5

Steady-state kinetic parameters of variant tetrameric MBP-PAH fusion proteins determined by direct in-well activity measurements. Data were analyzed using the *F*-test for model comparison and the kinetic parameters of the best-fitting model (cooperative versus non-cooperative) were calculated.  $V_{\text{max}}$  and the apparent affinities for L-phenylalanine ( $S_{0.5}$ ) and BH<sub>4</sub> ( $C_{0.5}$ ,  $K_{\text{m}}$ ) as well as the Hill coefficient ( $h$ ) as a measure of cooperativity are shown. Values are given as mean  $\pm$  SEM of three independent measurements.

<sup>a</sup>Enzyme kinetic parameters determined at variable L-phenylalanine concentrations (0–1000  $\mu\text{M}$ ) and standard BH<sub>4</sub> concentration (75  $\mu\text{M}$ ) with pre-incubation of the enzyme by L-phenylalanine (1000  $\mu\text{M}$ ).

<sup>b</sup>Enzyme kinetic parameters determined at variable BH<sub>4</sub> concentrations (0–125  $\mu\text{M}$ ) and standard L-phenylalanine concentration (1000  $\mu\text{M}$ ) with pre-incubation of the enzyme by L-phenylalanine (1000  $\mu\text{M}$ ).

a narrow optimal working range that was shifted towards lower L-phenylalanine as well as BH<sub>4</sub> concentrations. In addition, enzyme kinetics revealed a significantly increased apparent affinity to the substrate with marked reduction in cooperativity. In contrast to previous findings (3,32), where the variant protein V388M was described as a  $K_{\text{m}}$  variant with reduced affinity to the cofactor, we detected high residual enzyme activity over an expanded range of substrate and cofactor concentrations. Residual PAH activity was 100% and peak catalysis (L-phenylalanine 591  $\mu\text{M}$ , BH<sub>4</sub> 105  $\mu\text{M}$ ) as well as effects of substrate and cofactor inhibition were similar to that of the wild-type enzyme.

Mutations mapping to the oligomerization domain, Y414C and Y417H, showed a narrowed optimal working range that was shifted to lower substrate concentrations. However, this was less pronounced for the milder mutation Y417H (82% residual enzyme activity) when compared with Y414C (49%). On the other hand, Y417H needed less BH<sub>4</sub> to achieve the area of optimal function. Interestingly, different to all variants analyzed, Y414C showed two peaks of high enzyme activity.

Taken together, we identified many similarities between the activity landscapes of the wild-type and variant PAH proteins, showing generally high residual enzyme activity as well as substrate and cofactor inhibition. However, these activity landscapes also revealed important differences in the regulation of PAH activity by BH<sub>4</sub> and L-phenylalanine and helped to visualize the interdependence of substrate and cofactor concentrations on variant PAH enzyme activity.

### Cofactor action on PAH function in respect of kinetic behavior and the chaperone effect

We used two different approaches to analyze different aspects of cofactor action on the wild-type, R261Q and Y414C PAH enzyme in HEK293 cells. First, we in part retraced the activity landscapes analyzing the kinetic behavior by assaying enzyme activity of cell lysates at different L-phenylalanine

concentrations (0–1000  $\mu\text{M}$ ) while keeping the BH<sub>4</sub> concentration constant (75  $\mu\text{M}$ ) (Fig. 3A). Secondly, we analyzed the chaperone effect of the BH<sub>4</sub> cofactor at different phenylalanine and BH<sub>4</sub> concentrations after a 72 h incubation.

As expected, the wild-type protein showed the highest enzyme activity of all three proteins analyzed with a peak activity at about 250  $\mu\text{M}$  L-phenylalanine. The latter finding differed from the peak activity observed for recombinant PAH at  $\sim$ 500  $\mu\text{M}$ . As seen for prokaryotic PAH, a further increase in L-phenylalanine concentrations resulted in substrate inhibition. The variant R261Q displayed  $\sim$ 50% residual enzyme activity and a lower slope of the curve that leveled off at a plateau. Reduced enzyme function, which was shifted toward higher substrate concentrations with a broadened working range, substantiated results from activity landscapes. Residual enzyme activity of eukaryotic Y414C was substantially lower than the specific activity of the corresponding recombinant variant. In addition to peak activity at 180  $\mu\text{M}$  L-phenylalanine, a second slight incline of activity was observed at high L-phenylalanine concentrations (1000  $\mu\text{M}$ ). Although generally shifted toward lower substrate concentrations, this is in line with the two peaks observed in the activity landscape.

Next, we aimed to elucidate the long-term chaperone effect of varying intracellular phenylalanine and BH<sub>4</sub> concentrations on PAH function. The determination of enzyme activity at standard conditions after previous incubation of cells with different substrate and cofactor concentrations assays the availability of functionally active PAH. For this purpose, stably transfected cells were cultivated with L-phenylalanine concentrations of 91, 500 or 1200  $\mu\text{M}$  and BH<sub>4</sub> concentrations of 0, 40 or 75  $\mu\text{M}$  for 72 h. First, cells were cultivated at L-phenylalanine levels representing the physiological state (91  $\mu\text{M}$ ), mild PKU (500  $\mu\text{M}$ ) or classical PKU (1200  $\mu\text{M}$ ) without the addition of BH<sub>4</sub> to the medium (Fig. 3B). Wild-type PAH activity showed a trend towards an increase only at clearly pathological L-phenylalanine concentrations. For R261Q, a steady but statistically not significant increase in enzyme activity was seen

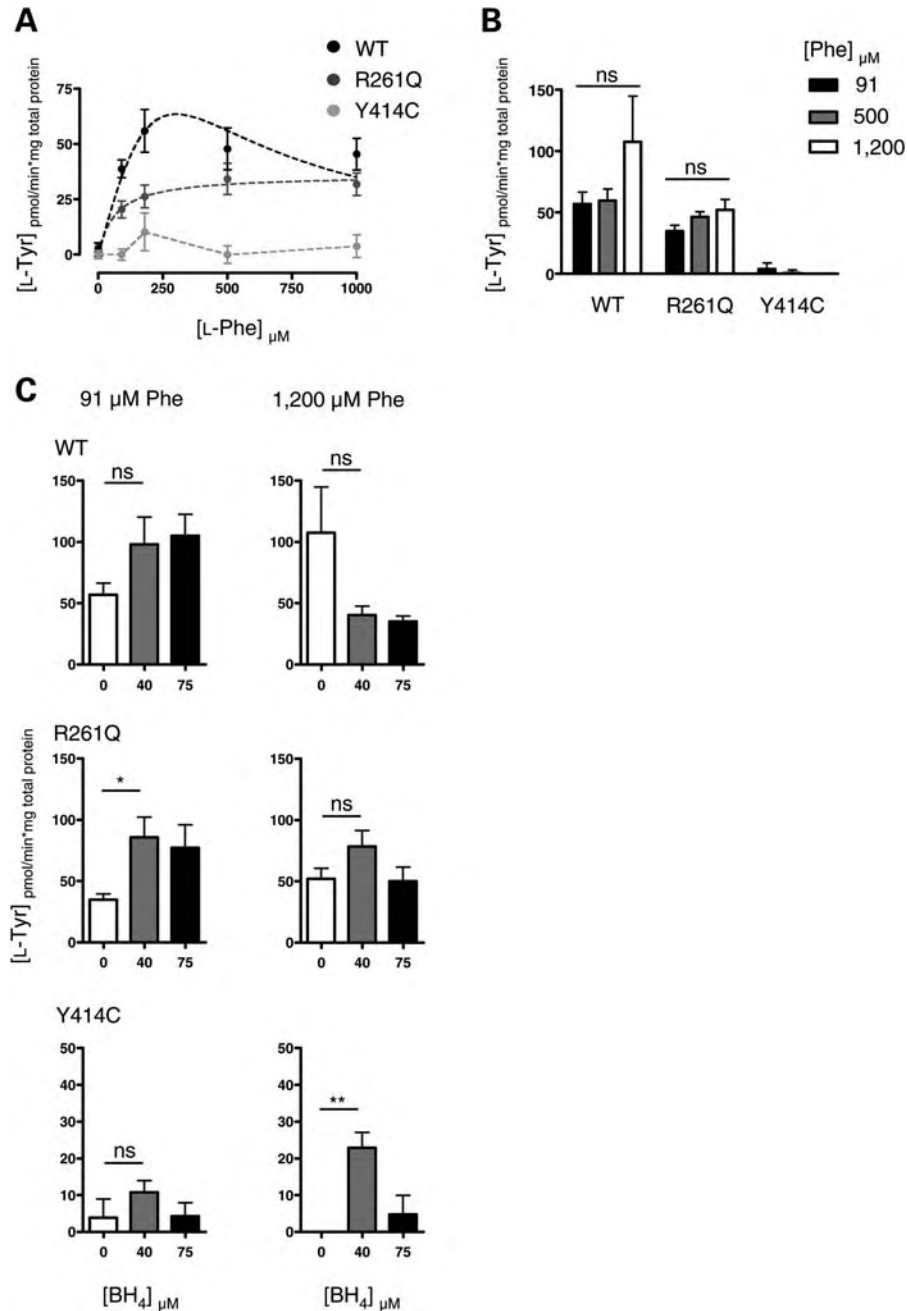


**Figure 3.** Cofactor action on PAH function in respect of kinetic behavior and the chaperone effect. **(A)** Enzyme activity of eukaryotic expressed PAH assayed at varying substrate concentrations. Enzyme activities in cell lysates of HEK293 cells stably transfected with wild-type PAH, R261Q or Y414C were determined at varying L-phenylalanine concentrations (0–1000  $\mu\text{M}$ ) and a fixed BH<sub>4</sub> concentration (75  $\mu\text{M}$ ). **(B)** Effect of varying intracellular phenylalanine concentrations on functionally active PAH. PAH enzyme activity in HEK293 cell lysates expressing wild-type PAH, R261Q or Y414C was determined at standard assay concentrations (1000  $\mu\text{M}$  L-phenylalanine and 75  $\mu\text{M}$  BH<sub>4</sub>) after prior incubation with different L-phenylalanine concentrations (black, 91  $\mu\text{M}$ ; dark gray, 500  $\mu\text{M}$ ; white, 1200  $\mu\text{M}$ ) for 72 h. **(C)** Mutual impact of varying substrate and cofactor concentrations on functionally active PAH. Cells stably expressing wild-type PAH, R261Q or Y414C were cultivated at different phenylalanine (left column, 91  $\mu\text{M}$ ; right column, 1200  $\mu\text{M}$ ) and BH<sub>4</sub> concentrations (white, 0; dark gray, 40  $\mu\text{M}$ ; and black, 75  $\mu\text{M}$ ). PAH enzyme activities were analyzed at standard assay conditions. PAH activities are given as mean  $\pm$  SEM of three independent experiments. Significant differences in enzyme activities were calculated using one-way ANOVA and Dunnett's multiple comparison test (ns, not significant; \* $P$  < 0.05; \*\* $P$  < 0.01).

upon increasing substrate concentrations in the medium ( $35 \pm 5$  to  $52 \pm 9$  pmol L-tyrosine/min  $\times$  mg total protein). For Y414C, residual activity was very low without any effect of increasing L-phenylalanine concentrations.

To further evaluate the mutual impact of the substrate and the cofactor on enzyme activity in the eukaryotic system, 40 or 75  $\mu\text{M}$  BH<sub>4</sub> were added to the medium at L-phenylalanine concentrations of 91 or 1200  $\mu\text{M}$ , respectively (Fig. 3C).

Interestingly, at physiological L-phenylalanine concentrations (91  $\mu\text{M}$ ), the addition of 40 and 75  $\mu\text{M}$  BH<sub>4</sub> induced a trend towards increased enzyme activity of wild-type PAH (57  $\pm$  9 to 98  $\pm$  22 and 105  $\pm$  18 pmol L-tyrosine/min  $\times$  mg total protein), whereas the opposite effect was observed at elevated L-phenylalanine concentrations (1200  $\mu\text{M}$  L-phenylalanine, 108  $\pm$  37 to 40  $\pm$  7 and 35  $\pm$  5 pmol L-tyrosine/min  $\times$  mg total protein). For the variant R261Q, the addition of 40  $\mu\text{M}$  BH<sub>4</sub> at physiological L-phenylalanine concentrations resulted in a significant increase in enzyme activity (35  $\pm$  5 to 86  $\pm$  17 pmol L-tyrosine/min  $\times$  mg total protein), but the inhibitory effect at elevated L-phenylalanine concentrations as seen for the wild-type was not observed. At physiological L-phenylalanine concentrations, the variant Y414C showed low residual enzyme activity with only a minor increase upon the addition of 40  $\mu\text{M}$  BH<sub>4</sub>. Interestingly, at high L-phenylalanine concentrations (1200  $\mu\text{M}$ ), the addition of 40 but not 75  $\mu\text{M}$  BH<sub>4</sub> led to a significant increase in residual enzyme activity (23  $\pm$  4 pmol L-tyrosine/min  $\times$  mg total protein) achieving as much as 40% of the wild-type level.

Taken together, findings from the prokaryotic system depicted by activity landscapes were substantiated in the eukaryotic environment. Also in this system probing lysates of cultured cells, the mutual impact of different L-phenylalanine and BH<sub>4</sub> concentrations on enzyme activity varied among different PAH variants with substrate inhibition for the wild-type as well as constant activity levels for R261Q also at very high L-phenylalanine concentrations. Residual enzyme activity of Y414C was substantially lower in cell culture when compared with the specific activity of the recombinant protein, but enzyme function was rescued by the addition of BH<sub>4</sub>. This may point to impaired protein stability in the eukaryotic environment and a stabilizing pharmacological chaperone effect by BH<sub>4</sub>.

### The mutual impact of substrate and cofactor concentrations on results from BH<sub>4</sub> loading tests performed in PAH deficient patients

So far, data pointed to a simultaneous dependency of PAH function from available substrate and cofactor concentrations. After having confirmed results from the prokaryotic system in the eukaryotic system, we aimed to investigate whether our observations may be transferred to the human situation by analyzing data from BH<sub>4</sub>-loading tests performed in patients with PAH deficiency. To address this issue, we collected data of patients homozygous or functionally hemizygous for the mutations F39L, I65T, R261Q or Y414C, that underwent a BH<sub>4</sub>-loading test with a dose of 20 mg/kg body weight and a duration of at least 24 h from the literature (19,33–37) and from the BIOPKU database (www.biopku.org). First, we compiled the course of blood phenylalanine values within 24 h after a single dose of BH<sub>4</sub> as a function of initial blood phenylalanine concentrations. For all mutations analyzed, different blood phenylalanine concentrations at the beginning of the test led to differences in the extent of BH<sub>4</sub> responsiveness, i.e. the percent decrease in blood phenylalanine after drug administration. Patients carrying the mutations F39L, I65T and Y414C showed a peak level of BH<sub>4</sub> responsiveness below an initial blood phenylalanine concentration of 500  $\mu\text{M}$  (Fig. 4A).

In the presence of F39L and I65T increasing initial blood phenylalanine concentrations were associated with a decrease in BH<sub>4</sub> responsiveness. While patients with F39L still displayed positive response at 1000  $\mu\text{M}$  phenylalanine (>30% decrease in blood phenylalanine), those carrying I65T did not show a drug response when initial blood phenylalanine concentrations were >800  $\mu\text{M}$ . The mutation Y414C led to inconsistent response to BH<sub>4</sub> with maximum responsiveness at initial blood phenylalanine concentrations up to 750  $\mu\text{M}$  phenylalanine and at 1000  $\mu\text{M}$  phenylalanine. In general, patients bearing the mutation Y414C showed a high degree in BH<sub>4</sub> responsiveness with the lowest response remaining within the range of 30% decrease in blood phenylalanine.

Patients bearing the mutation R261Q showed strong inconsistencies in BH<sub>4</sub> responsiveness with some patients displaying high levels of responsiveness (>60% decrease of blood phenylalanine) and others no response at all (Fig. 4B). To investigate the basis of these inconsistencies, we analyzed the impact of both the genotype on BH<sub>4</sub> response and of phenylalanine concentrations on different genotypes comprising the R261Q mutation. The decrease in blood phenylalanine concentrations was significantly stronger in individuals carrying the R261Q mutation in the homozygous state (median, 37.5%) than those carrying it in the functional hemizygous state (median, 6.5%). However, among homozygous patients, some were responders and some were not, whereas all functionally hemizygous patients had to be classified as non-responders. Interestingly, the level of initial blood phenylalanine did not allow differentiating either homozygous responders from homozygous non-responders or homozygotes from functional hemizygotes.

In addition to the influence of initial blood phenylalanine concentrations on BH<sub>4</sub> response, we analyzed the impact of the genotype on BH<sub>4</sub> dose response to investigate the optimal PAH working range *in vivo*. Literature data providing information on BH<sub>4</sub> dosage revealed clear differences for patients homozygous for R261Q, patients homozygous for Y414C and those compound heterozygous for these two mutations (Fig. 4C). In the presence of the mutation R261Q, the percent decrease in blood phenylalanine levels remained nearly unchanged for the range of BH<sub>4</sub> dosages between 10 and 30 mg/kg body weight. In contrast, patients bearing the mutation Y414C showed a gain in BH<sub>4</sub> response with increasing BH<sub>4</sub> doses (5–20 mg/kg body weight). Interestingly, patients compound heterozygous for R261Q and Y414C showed an intermediate response with respect to the BH<sub>4</sub> dosage administered (10–20 mg/kg body weight) when compared with patients homozygous for these mutations.

As a conclusion, *in vivo* PAH activity is a function of the phenylalanine substrate and the BH<sub>4</sub> cofactor as well as the patient's genotype. Hence, enzyme function in the individual patient at a given time point is the resultant of the metabolic state and the dosage of cofactor treatment both in turn determined by the underlying mutations.

## DISCUSSION

Regulation of PAH activity is essentially governed by the abundance of the phenylalanine substrate and the BH<sub>4</sub>

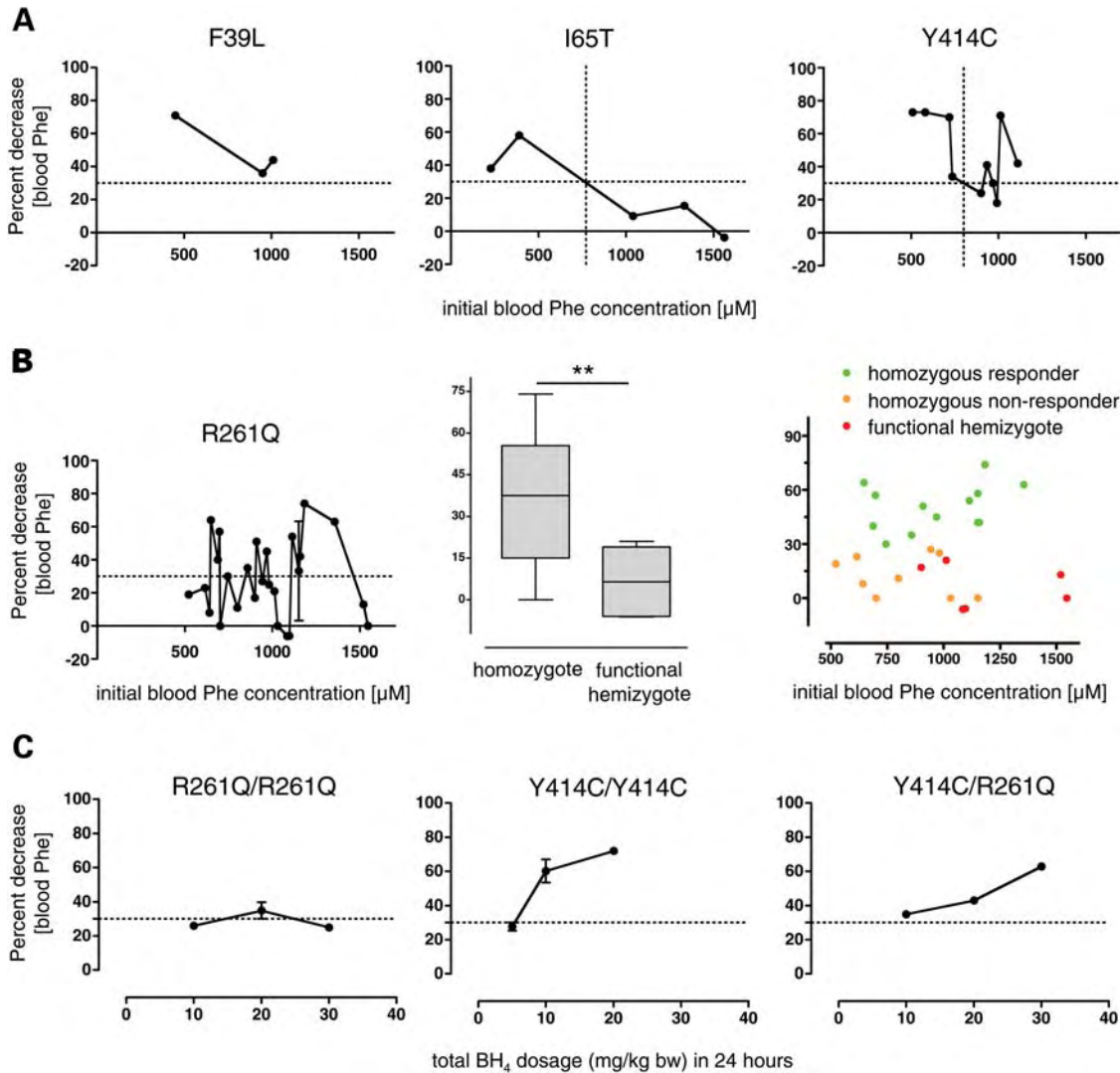


**Figure 4.** Evaluation of BH<sub>4</sub> responsiveness in PAH-deficient patients. (A) The impact of the genotype and of initial blood phenylalanine concentrations on BH<sub>4</sub> response. The graphs show the percent decrease in blood phenylalanine levels 24 h after a single dose of BH<sub>4</sub> (20 mg/kg bw) in patients homozygous or functional hemizygous for the mutations F39L ( $n = 3$ ), I65T ( $n = 5$ ) or Y414C ( $n = 10$ ) as a function of different blood phenylalanine values at the beginning of the test. The horizontal dashed line indicates 30% decrease in blood phenylalanine concentrations, the arbitrary criterion of BH<sub>4</sub> responsiveness. The vertical dashed line shows the initial blood phenylalanine concentration, above which BH<sub>4</sub> leads to a blood phenylalanine decrease of <30%. (B) BH<sub>4</sub> responsiveness in patients carrying the mutation R261Q ( $n = 28$ ). (Left) Percent decrease in blood phenylalanine 24 h after a single dose of BH<sub>4</sub> (20 mg/kg bw) as a function of initial blood phenylalanine values in patients homozygous or functional hemizygous for the R261Q mutation. (Middle) Percent decrease in blood phenylalanine 24 h after a single dose of BH<sub>4</sub> (20 mg/kg bw) in patients carrying the R261Q mutation in the homozygous state ( $n = 22$ ) in comparison to functional hemizygotes ( $n = 6$ ). The boxes show the interquartile ranges (25th to 75th percentiles), the horizontal black bars represent the median, the bars indicate the range. Significance is indicated (\*\* $P < 0.01$ , unpaired Student's  $t$ -test). (Right) Percent decrease in blood phenylalanine concentrations in function of initial blood phenylalanine values in homozygous responders ( $n = 13$ ) and non-responders ( $n = 9$ ) as well as functional hemizygous patients ( $n = 6$ ) displaying the mutation R261Q. (C) The impact of the genotype on BH<sub>4</sub> dose response. Percent decrease in blood phenylalanine 24 h after a single application of BH<sub>4</sub> in different dosages in patients homozygous for R261Q ( $n = 24$ ) (left), homozygous for Y414C ( $n = 10$ ) (middle) or compound heterozygous for R261Q/Y414C ( $n = 3$ ) (right).

cofactor. The supply of substrate, e.g. upon food intake, induces enzyme activation and subsequently full catalytic activity. In contrast, at low blood phenylalanine levels, e.g. under fasting conditions, BH<sub>4</sub>-induced PAH inhibition prevents from undue elimination of the essential amino acid phenylalanine. Thus, it is the ratio of phenylalanine to BH<sub>4</sub> that determines activation and inhibition of the enzyme. However, the concentration of BH<sub>4</sub> in the liver cell is held rather constant, whereas phenylalanine levels undergo

substantial fluctuations in function of the metabolic state and—in the presence of PAH deficiency—of the underlying genotype. While treating patients with BH<sub>4</sub> we intervene in this system without disposing of profound knowledge concerning the effect of shifts of the substrate-to-cofactor ratio. In the work presented here, we first wanted to apply the newly developed real-time fluorescence-based PAH enzyme activity assay to identify the optimal working range of the enzyme with respect to these substances. Secondly, we aimed to analyze

the influence of changes in the phenylalanine-to-BH<sub>4</sub> ratio on PAH function of the wild-type and variant enzymes.

Analyses of wild-type PAH revealed two interesting new findings. In addition to the well-known enzyme inhibition by the substrate, cofactor inhibition was identified by the extension of the enzyme activity assay to much higher cofactor concentrations. Moreover, we learned that with increasing phenylalanine concentrations, more BH<sub>4</sub> is needed to maintain the same level of PAH activity. Still, it has to be considered that the full range of substrate and cofactor concentrations applied in our novel assay provided new insights into theoretical aspects of PAH enzymology, but it is well beyond physiological levels. However, our approach allowed for detailed visualization and better understanding of conditions corresponding to those occurring at the edges of classical pathological situations in PKU patients and in the therapeutic context upon cofactor treatment.

The optimal working range of the wild-type enzyme occurred at phenylalanine concentrations of 250–500 μM. From a physiological point of view, this appears reasonable, since upon food intake liver phenylalanine concentrations are expected to reach levels up to 500 μM rather than around 1000 μM, the phenylalanine concentration at which standard PAH enzyme activity assays are performed (2,38). Our results showed that the optimal BH<sub>4</sub> concentration for PAH enzyme activity is ~100 μM, while standard PAH activity assays are run at 75 μM BH<sub>4</sub> (2,38). In any case, the physiological cellular BH<sub>4</sub> concentration in the liver is by far lower (~8.5 μM) (26), implying that the cell has always to be considered BH<sub>4</sub> deficient in view of the enzymatic task. Yet, in light of the inhibitory potential of BH<sub>4</sub> on the enzyme, a cellular cofactor concentration significantly below the  $K_m$  value of 23 μM reduces inhibition when activity is needed, i.e. at phenylalanine concentrations above the physiological range. The trade-off between these two tasks is balanced by a 6-fold higher affinity of the enzyme toward the cofactor ( $K_m$ , 23 μM) than toward the substrate ( $S_{0.5}$ , 145 μM). As a consequence, PAH binds BH<sub>4</sub> and phenylalanine at a ratio of 0.5 at 100 μM blood phenylalanine (inhibition) when compared with 0.09 at 561 μM blood phenylalanine (no inhibition). These theoretical assumptions are corroborated by previous *in vivo* <sup>13</sup>C-phenylalanine oxidation tests performed in a PKU mouse model (39). In the euphenylalaninemic state, a hypothetical BH<sub>4</sub> deficiency is overruled by an inhibitory effect following the application of BH<sub>4</sub> in wild-type animals. However, in hyperphenylalaninemia phenotypes, the administration of BH<sub>4</sub> leads to an immediate increase in <sup>13</sup>C-phenylalanine oxidation. In view of a time to effect of <5 min, this has to be considered independent of a pharmacological chaperone effect and rather points to compensation of BH<sub>4</sub> deficiency in this metabolic state. Comparable studies in humans addressing phenylalanine concentrations, BH<sub>4</sub> concentrations, the effect of BH<sub>4</sub> in healthy individuals, time to onset of action and effect duration would be of interest, but have not yet been performed.

Next, we investigated the effect of selected missense mutations in the *PAH* gene on the optimal working range of the enzyme. In general, activity landscapes of the wild-type and variant PAH proteins displayed comparable patterns with rather high residual enzyme activity and a limited area

of maximum activity. More detailed analyses, however, revealed various alterations with respect to the extension and position of the optimal working range in the coordinates of substrate and cofactor concentrations. Most variant proteins were in need of more BH<sub>4</sub> to achieve peak activity (F39L, I65T, R261Q, P275L, Y417H, Y414C). For two variants (R261Q and P275L), maximum activity was determined at markedly higher phenylalanine concentrations (842 and 1293 μM). In contrast, three variants (P314S, Y414C and Y417H) presented a narrowed optimal working range that was shifted to lower phenylalanine concentrations when compared with the wild-type.

Two of these mutations, R261Q and Y414C, are frequent, but inconsistently associated with BH<sub>4</sub> responsiveness (17,34–37). The analysis of activity landscapes provided first evidence for an impact of the metabolic state on variant PAH function. R261Q displayed marked reduction in enzyme activity at phenylalanine concentrations in the therapeutic range below 240 μM giving rise to the hypothesis that patients bearing this mutation in the homozygous or functional hemizygous state would not benefit from a restrictive dietary regime. On the other hand, the mutation Y414C that induces a shift of activity to lower phenylalanine concentrations would require a rather strict metabolic adjustment with low blood phenylalanine values to achieve optimized PAH activity. Thus, observations from the analysis of activity landscapes could be of importance for a deeper understanding of inconsistent results from BH<sub>4</sub> loading tests or some disappointing experiences upon BH<sub>4</sub> treatment of our patients. To perform a further step in this direction, we carried out cell culture experiments and analyzed data from BH<sub>4</sub> loading tests performed in PKU patients.

Data extracted from activity landscapes were reproduced in the setting of stably transfected cells. Having gained insights into the mutual impact of varying substrate and cofactor concentrations on PAH activity, we were then interested in answering the question of how changes in the metabolic state would affect the effective PAH concentration, that is, the intracellular amount of functional PAH enzyme available for phenylalanine conversion. Since BH<sub>4</sub> has been classified as a pharmacological chaperone, i.e. a stabilizing compound that helps to overcome PAH degradation in the cell, it is expected to raise the amount of PAH in cell culture. In addition, we had previously shown that the effective PAH concentration is influenced by changes in the phenylalanine-to-BH<sub>4</sub> ratio in the mouse (12). To address these issues in cell culture, we mimicked physiological (euphenylalaninemic) and pathologic (hyperphenylalaninemic) conditions representing classical PKU. The supplementation of BH<sub>4</sub> induced diverse results in the presence of R261Q and Y414C, respectively. BH<sub>4</sub> was beneficial for catalytic PAH function of the R261Q variant particularly at low phenylalanine levels, whereas a significant increase in PAH enzyme activity reflecting an increase in the effective PAH amount was observed for Y414C under PKU conditions. Interestingly, the therapeutic range for BH<sub>4</sub> was narrow for Y414C, a finding confirming the observations from the activity landscapes.

As a next step, we aimed to verify the clinical relevance of our findings and analyzed the effect of different substrate

and cofactor concentrations on the outcome of single dose BH<sub>4</sub>-loading tests in individuals carrying different *PAH* genotypes. In clinical routine, the initial phenylalanine concentration at the beginning of the BH<sub>4</sub>-loading test is not expected to significantly affect the outcome of the test. In general, only a minimum phenylalanine concentration of 400 μM is considered to be required for reliable test results. Surprisingly, data from BH<sub>4</sub> loading tests available in the BIOPKU database and in the literature (19,33–37,40) does not confirm this view. We learned that patients carrying one of the mutations F39L, I65T or Y414C in either a homozygous or a functional hemizygous state show substantially different responses to the BH<sub>4</sub>-loading test in function of the phenylalanine concentration at the beginning of the test. For example, in presence of the mutation I65T, the response may vary from 60% at 500 μM phenylalanine to 0% at 1500 μM blood phenylalanine. This is a new finding that may undermine our trust in current BH<sub>4</sub>-loading test protocols. Our results may, for instance, allow for the hypothesis that patients carrying the I65T mutation are at risk to show false negative test results at phenylalanine concentrations >750 μM. In the case of the R261Q mutation, phenylalanine concentrations did not significantly influence test results (Fig. 4B). However, the kind of genotype significantly affected BH<sub>4</sub> responsiveness with carriers of the R261Q mutation in the homozygous state showing a higher response (37.5% decrease in phenylalanine after BH<sub>4</sub> loading) than individuals with the mutation in the functional hemizygous state (6.5% decrease). Further analysis revealed that none of the patients carrying the R261Q mutation in combination with a null mutation met the criterion of BH<sub>4</sub> responsiveness of 30% decrease of phenylalanine concentrations, whereas 12 out of 21 patients with a homozygous genotype did and 9 out of 21 patients did not. Similar observations were recently reported in 27 Turkish PKU patients with a homozygous R261Q genotype and variable clinical phenotypes (11% mild hyperphenylalaninemia, 67% mild PKU, 22% classic PKU), from which only 39.1% were BH<sub>4</sub> responsive (22). Taken together, our results show that the outcome of a BH<sub>4</sub>-loading test may much more vary in function of individual test circumstances than previously assumed. Unfortunately, it has to be expected that this is true for a number of mutations and in view of the lifelong consequences for our patients arising from the initial classification of being a responder or not it has to be emphasized that with the knowledge available today results from single-loading tests are not sufficient to determine BH<sub>4</sub> responsiveness in patients with *PAH* deficiency.

Last, we analyzed the effect of BH<sub>4</sub> dosage on the results of single BH<sub>4</sub>-loading tests. Since ~10 years, a dosage of 20 mg/kg body weight is internationally recommended (11,28,29,41). However, in some centers and countries, this recommendation may not be followed. In homozygous R261Q patients, the dosage of BH<sub>4</sub> (10, 20 and 30 mg/kg body weight) did not seem to influence test results (26, 27 and 25% decrease, respectively). In presence of the Y414C mutation, increasing BH<sub>4</sub> dosages increased BH<sub>4</sub> responsiveness in terms of percent decrease of blood phenylalanine after BH<sub>4</sub> application.

Interestingly, compound heterozygous patients carrying both the R261Q and the Y414C mutation also showed a dose dependency of response, but to a lower extent than homozygous Y414C patients.

In summary, we developed a rapid *PAH* enzyme activity assay allowing for a much higher throughput than previous assays and for detailed analysis of a broad range of substrate and cofactor concentrations on *PAH* enzyme kinetics. This enabled new insights into optimal *PAH* working range at physiological, pathological and therapeutic conditions. As to enzyme kinetics, two main conclusions can be drawn from our experimental work: phenylalanine concentrations for optimal working range of *PAH* are lower, whereas BH<sub>4</sub> concentrations for optimal *PAH* activity are higher than previously assumed. The validity of our observations was substantiated and expanded by the fact that we were able to translate data from the prokaryotic system into the eukaryotic cell culture system and into patient data. Of relevance for the clinical context, we revealed a significant impact of the genotype, substrate concentrations and BH<sub>4</sub> dosage on the assessment of BH<sub>4</sub> responsiveness.

Since the discovery of the pharmacological effect of BH<sub>4</sub> in patients with *PAH* deficiency (5), the scientific community discusses possible mechanisms of BH<sub>4</sub> responsiveness in PKU. The initial concept was kinetic action, in particular the hypothesis that *PAH* gene mutations lead to decreased affinity of the variant protein to the cofactor, that is overcome by the administration of pharmacological doses of BH<sub>4</sub>. Kinetic studies using the recombinant *PAH* protein revealed that this is true only in rare instances (2,32,42). Subsequent work moved the concept away from kinetic effects toward the view of BH<sub>4</sub> acting as a molecular chaperone by increasing the stability of partially misfolded *PAH* proteins and by this the effective intracellular concentration of functional *PAH* enzyme (3,4,12). A deeper view into *PAH* enzyme kinetics using a technology that allows for the analysis of a broad range of substrate and cofactor concentrations on *PAH* activity now showed that besides the indubitable chaperone effect, kinetic aspects also have to be taken into account. Thus, we may now put forward the view of both concepts being of relevance for the diagnosis and the treatment of patients with *PAH* deficiency. The diagnostic loading test with BH<sub>4</sub> or long-term BH<sub>4</sub> treatment has to be seen in the light of the fact that short-term supply of BH<sub>4</sub> can compensate for latent BH<sub>4</sub> deficiency as to optimal catalytic function (kinetic effect), whereas long-term treatment with pharmacological doses of BH<sub>4</sub> increases the stability of *PAH* and by this the amount of metabolically active enzyme (chaperone effect). In addition, individual mutations may shift the impact of one or the other therapeutic effect.

For daily clinical routine, this underscores the need for even more standardized and at the same time individualized test procedures including detailed documentation of phenylalanine concentrations before the BH<sub>4</sub> load and the awareness that the metabolic status of the patient will influence the outcome of the test. In non-responders with suggestive genotypes, repetition of the loading test at different initial phenylalanine concentrations may help rule out false negative results. Moreover, we suggest to combine short-term BH<sub>4</sub> loading tests (assessment of kinetic effects) and long-term BH<sub>4</sub> treatment

tests (assessment of chaperone effects) with *in vivo*  $^{13}\text{C}$ -phenylalanine oxidation tests (assessment of the effect of  $\text{BH}_4$  on *in vivo* PAH enzyme activity) (11,43). The test is non-invasive, innocuous, easy to perform and may add important information about an individual's response to the drug at a functional level.

In conclusion, our work pinpoints the importance of genotyping PKU patients even in clinical routine and underscores the need for more personalized testing procedures addressing individual patient characteristics, the metabolic state and the dosage of the test compound to safely identify  $\text{BH}_4$  responsiveness in PAH-deficient patients.

## MATERIALS AND METHODS

### Patients and mutations

Mutations previously identified in  $\text{BH}_4$  responsive patients (4,11) were analyzed in terms of the effect of various substrate (L-phenylalanine) and cofactor ( $\text{BH}_4$ ) concentrations on PAH enzyme activity. The mutations mapped to the regulatory domain (F39L, I65T), the catalytic domain (R261Q, P275L, P314S, V388M) or to the dimerization motif of the oligomerization domain (Y414C, Y417H). Forty-six patients homozygous and functional hemizygous for the mutations F39L ( $n = 3$ ), I65T ( $n = 5$ ), R261Q ( $n = 28$ ) and Y414C ( $n = 10$ ) were identified performing a comprehensive literature survey and by extracting data from the BIOPKU database ([www.biopku.org](http://www.biopku.org)). Patients were included in the analysis, when data on a  $\text{BH}_4$ -loading test using 20 mg/kg body weight and blood phenylalanine concentrations over a period of at least 24 h were available. In addition, the effect of different  $\text{BH}_4$  dosages, ranging from 5 to 30 mg/kg body weight, on the course of blood phenylalanine concentrations was analyzed (16,19,34,35,37).

### Expression and purification of recombinant PAH proteins

The cDNA of human PAH (EST clone obtained from imaGenes, formerly RZPD, Germany) was cloned into the prokaryotic expression vector pMAL-c2E (New England Biolabs) encoding an N-terminal maltose-binding protein (MBP) tag. PAH mutants were constructed by site-directed mutagenesis as previously described (2). Expression plasmids containing the wild-type PAH and variants were transformed to *Escherichia coli* DH5 $\alpha$ . Expressed proteins were purified by affinity chromatography (MBPTrap, GE Healthcare) followed by size-exclusion chromatography using a HiLoad 26/60 Superdex 200 column (GE Healthcare) on an ÄKTExpress system (2). Obtained tetramers of the fusion proteins were collected and protein concentrations were determined spectrophotometrically using  $\epsilon_{280}$  (1mg/ml) = 1.63.

### PAH activity assay

*Enzyme activity of the recombinantly expressed PAH.* The multi-well PAH activity assay and data evaluation were performed as previously described (27) with modifications. L-phenylalanine and 22.35 mM Na HEPES, pH 7.3, were added to all wells of a 96-well plate with different volumes.

This resulted in 12 columns of varying L-phenylalanine concentrations (0–4000  $\mu\text{M}$ ). A reaction buffer containing 1 mg/ml catalase (Sigma-Aldrich), 10  $\mu\text{M}$  ferrous ammonium sulfate (Sigma-Aldrich) and the tetrameric MBP–PAH fusion protein (0.01 mg/ml) was prepared and injected in all 96 wells. After pre-incubation with L-phenylalanine for 5–20 min, the reaction was initiated by the addition of variable concentrations of  $\text{BH}_4$  (6*R*-L-erythro-5,6,7,8-tetrahydrobiopterin, Cayman Chemical) (0–500  $\mu\text{M}$ ) stabilized in 100 mM dithiothreitol (DTT; Fluka Chemie). PAH activity was determined at 25°C and 90 s measurement time per well. Using sets of 16 wells and 10 measurement cycles per set, total measurement time for all 96 wells was 22 min. Substrate production was measured by the detection of the increase in L-tyrosine fluorescence intensity, at an excitation wavelength of 274 nm and an emission wavelength of 304 nm, using a fluorescence photometer (FLUOstar OPTIMA, BMG Labtech) and assayed as triplicates. Measured fluorescence intensity signals were corrected by the inner filter effect of  $\text{BH}_4$  for every  $\text{BH}_4$  concentration added. Enzyme activity measurements were quantified by the measurement of L-tyrosine standards (0–200  $\mu\text{M}$ ) before each experiment, and fluorescence intensity was converted to enzyme activity units (nmol L-tyrosine/min  $\times$  mg protein). Data were analyzed by non-linear regression analysis using the Michaelis–Menten or the Hill kinetic model after comparison of model-fitting using the *F*-test (GraphPad Prism 4.0c) (27). All concentrations mentioned refer to the final concentration in a 202  $\mu\text{l}$  reaction mixture.

*Standard PAH activity assay of eukaryotic expressed PAH.* PAH enzyme activity was determined as previously described (2,39) with modifications. Twenty microliters of total lysates obtained from cell culture were pre-incubated with 1000  $\mu\text{M}$  L-phenylalanine and 1 mg/ml catalase (Sigma-Aldrich) for 5 min (25°C) in 15 mM Na HEPES pH 7.3, followed by 1 min incubation with 10  $\mu\text{M}$  ferrous ammonium sulfate (Sigma-Aldrich). The reaction was initiated by the addition of 75  $\mu\text{M}$   $\text{BH}_4$  stabilized in 2 mM DTT, carried out for 60 min at 25°C and stopped by acetic acid followed by 10 min incubation at 95°C. All concentrations mentioned refer to the final concentration in a 100  $\mu\text{l}$  reaction mixture. The amount of L-tyrosine production was measured and quantified by HPLC, assayed as duplicates. Three independent experiments were performed.

### PAH activity landscapes

The data set of multi-well enzyme activity assayed in a 12  $\times$  8 matrix corresponding to 12 different L-phenylalanine concentrations ranging from 0 to 4000  $\mu\text{M}$  (columns) at 8  $\text{BH}_4$  concentrations ranging from 0 to 500  $\mu\text{M}$  (rows) was loaded into non-linear regression analysis software (GraphPad Prism 4.0c). A non-linear regression analysis was performed for each column of the data matrix in order to extend the sparse data set for  $\text{BH}_4$  concentrations from 8 measured to 400 newly calculated values following a substrate inhibition curve. This resulted in a 12  $\times$  400 matrix of activity values. For further calculation of the data and for the creation of landscapes, this data matrix was exported to the free software

package R ([www.r-project.org](http://www.r-project.org)). In order to draw a smooth surface of the landscape, we used the function *interp.loess* from additional R package *tgp* (<http://cran.r-project.org/web/packages/tgp/index.html>), which interpolates between two data points by using local polynomial regression fitting to find a function between them. This resulted in an increase in data from an originally measured  $12 \times 8$  (96-well format) over a  $12 \times 400$  to a  $400 \times 400$  data set. This grid was then depicted as a smooth landscape plot using the function *image.plot* from package *fields* (<http://cran.r-project.org/web/packages/fields/index.html>). To facilitate calculation of landscapes, a script was written accepting comma-separated files and automatically coloring landscapes depending on the measured and interpolated fluorescence intensities.

### Stable expression of PAH in HEK293

Stably transfected cells were generated using the Flp-In system (Invitrogen) according to the manufacturer's protocol. The Flp-In-293 cell line was maintained in basic DMEM (PAA Laboratories) supplemented with L-glutamine, high glucose (4.5 g/l), 10% fetal bovine serum (GIBCO), 1% antibiotics (Antibiotic-Antimycotic; PAA) and 100 µg/ml Zeocin (Invitrogen). Cells were stably transfected with pEF5/FRT/V5-DEST cDNA constructs coding for the wild-type, R261Q or Y414C PAH, respectively. Positive clones were selected and maintained in medium containing 150 µg/ml hygromycin B (Invitrogen).

For all further experiments, cells were cultured for 72 h under three different conditions: (i) basic RPMI 1640 medium (91 µM phenylalanine, PAA Laboratories) supplemented with stable glutamine, 10% fetal bovine serum (GIBCO), 1% antibiotics (Antibiotic-Antimycotic; PAA) and 150 µg/ml of hygromycin B, (ii) basic medium (as described above) with 500 µM phenylalanine, and (iii) basic medium with 1200 µM phenylalanine. Additionally, culture conditions were modified by adding 40 or 75 µM BH<sub>4</sub>, respectively. Culture medium was changed every 24 h. Cells were harvested and lysed by three freeze-thaw cycles in a Tris-KCl lysis buffer (0.03 M Tris, 0.2 M KCl, pH 7.2) containing protease inhibitors (Roche), followed by 20 min centrifugation at 3000 rcf, 4°C. Recovered supernatants were subsequently used for activity assays.

### Statistics

Group mean values were compared by Student's unpaired two-tailed *t*-test. Eukaryotic PAH activities following BH<sub>4</sub> treatment were analyzed by one-way ANOVA and Dunnett's post-test. Statistical analyses were performed using GraphPad Prism 4.0c (GraphPad Software).

### ACKNOWLEDGEMENTS

The authors wish to thank Professor Christian Sommerhoff for support and discussion concerning the development of the automated enzyme activity assay and Heike Preisler and Christoph Siegel for excellent technical assistance. This

article is part of an M.D. thesis to be submitted by M.S. at Ludwig-Maximilians-University, Munich, Germany.

**Conflict of Interest statement.** A.C.M. is a member of Merck Serono advisory boards and is currently conducting research sponsored by this company. S.W.G. is currently conducting research sponsored by Merck Serono. The research presented in this specific manuscript was not sponsored by the company.

### FUNDING

This work was supported and funded by the Bavarian Genome Research Network (BayGene) and in part by the Swiss National Science Foundation grant no. 3100A0-119982/2 (to N.B.).

### REFERENCES

1. Scriver, C. and Kaufman, S. (2001) *Hyperphenylalaninemia: Phenylalanine Hydroxylase Deficiency in the Metabolic & Molecular Bases of Inherited Disease*. McGraw-Hill, New York, NY.
2. Gersting, S.W., Kemter, K.F., Staudigl, M., Messing, D.D., Danecka, M.K., Lagler, F.B., Sommerhoff, C.P., Roscher, A.A. and Muntau, A.C. (2008) Loss of function in phenylketonuria is caused by impaired molecular motions and conformational instability. *Am. J. Hum. Genet.*, **83**, 5–17.
3. Erlandsen, H., Pey, A.L., Gamez, A., Pérez, B., Desviat, L.R., Aguado, C., Koch, R., Surendran, S., Tying, S., Matalon, R. *et al.* (2004) Correction of kinetic and stability defects by tetrahydrobiopterin in phenylketonuria patients with certain phenylalanine hydroxylase mutations. *Proc. Natl Acad. Sci. USA*, **101**, 16903–16908.
4. Pey, A.L., Pérez, B., Desviat, L.R., Martínez, M.A., Aguado, C., Erlandsen, H., Gámez, A., Stevens, R.C., Thörólfsson, M., Ugarte, M. *et al.* (2004) Mechanisms underlying responsiveness to tetrahydrobiopterin in mild phenylketonuria mutations. *Hum. Mutat.*, **24**, 388–399.
5. Kure, S., Hou, D.C., Ohura, T., Iwamoto, H., Suzuki, S., Sugiyama, N., Sakamoto, O., Fujii, K., Matsubara, Y. and Narisawa, K. (1999) Tetrahydrobiopterin-responsive phenylalanine hydroxylase deficiency. *J. Pediatr.*, **135**, 375–378.
6. Spaapen, L.J., Bakker, J.A., Velter, C., Loots, W., Rubio-Gozalbo, M.E., Forget, P.P., Dorland, L., De Koning, T.J., Poll-The, B.T., Ploos van Amstel, H.K. *et al.* (2001) Tetrahydrobiopterin-responsive phenylalanine hydroxylase deficiency in Dutch neonates. *J. Inher. Metab. Dis.*, **24**, 352–358.
7. Trefz, F.K., Aulela-Scholz, C. and Blau, N. (2001) Successful treatment of phenylketonuria with tetrahydrobiopterin. *Eur. J. Pediatr.*, **160**, 315.
8. Weglage, J., Grenzebach, M., von Teeffelen-Heithoff, A., Marquardt, T., Feldmann, R., Denecke, J., Godde, D. and Koch, H.G. (2002) Tetrahydrobiopterin responsiveness in a large series of phenylketonuria patients. *J. Inher. Metab. Dis.*, **25**, 321–322.
9. Steinfeld, R., Kohlschütter, A., Zschocke, J., Lindner, M., Ullrich, K. and Lukacs, Z. (2002) Tetrahydrobiopterin monotherapy for phenylketonuria patients with common mild mutations. *Eur. J. Pediatr.*, **161**, 403–405.
10. Lindner, M., Steinfeld, R., Burgard, P., Schulze, A., Mayatepek, E. and Zschocke, J. (2003) Tetrahydrobiopterin sensitivity in German patients with mild phenylalanine hydroxylase deficiency. *Hum. Mutat.*, **21**, 400.
11. Muntau, A.C., Röschinger, W., Habich, M., Demmelmair, H., Hoffmann, B., Sommerhoff, C.P. and Roscher, A.A. (2002) Tetrahydrobiopterin as an alternative treatment for mild phenylketonuria. *N. Engl. J. Med.*, **347**, 2122–2132.
12. Gersting, S.W., Lagler, F.B., Eichinger, A., Kemter, K.F., Danecka, M.K., Messing, D.D., Staudigl, M., Domdey, K.A., Zsifkovits, C., Fingerhut, R. *et al.* (2010) Pahenu1 is a mouse model for tetrahydrobiopterin-responsive phenylalanine hydroxylase deficiency and promotes analysis of the pharmacological chaperone mechanism in vivo. *Hum. Mol. Genet.*, **19**, 2039–2049.

13. Levy, H.L., Milanowski, A., Chakrapani, A., Cleary, M., Lee, P., Trefz, F.K., Whitley, C.B., Feillet, F., Feigenbaum, A.S., Bechuk, J.D. *et al.* (2007) Efficacy of sapropterin dihydrochloride (tetrahydrobiopterin, 6R-BH4) for reduction of phenylalanine concentration in patients with phenylketonuria: a phase III randomised placebo-controlled study. *Lancet*, **370**, 504–510.
14. Trefz, F.K., Burton, B.K., Longo, N., Casanova, M.M., Gruskin, D.J., Dorenbaum, A., Kakkis, E.D., Crombez, E.A., Grange, D.K., Harmatz, P. *et al.* (2009) Efficacy of sapropterin dihydrochloride in increasing phenylalanine tolerance in children with phenylketonuria: a phase III, randomized, double-blind, placebo-controlled study. *J. Pediatr.*, **154**, 700–707.
15. Lee, P., Treacy, E.P., Crombez, E., Wasserstein, M., Waber, L., Wolff, J., Wendel, U., Dorenbaum, A., Bechuk, J., Christ-Schmidt, H. *et al.* (2008) Safety and efficacy of 22 weeks of treatment with sapropterin dihydrochloride in patients with phenylketonuria. *Am. J. Med. Genet. A*, **146A**, 2851–2859.
16. Burton, B.K., Grange, D.K., Milanowski, A., Vockley, G., Feillet, F., Crombez, E.A., Abadie, V., Harding, C.O., Cederbaum, S., Dobbelaere, D. *et al.* (2007) The response of patients with phenylketonuria and elevated serum phenylalanine to treatment with oral sapropterin dihydrochloride (6R-tetrahydrobiopterin): a phase II, multicentre, open-label, screening study. *J. Inherit. Metab. Dis.*, **30**, 700–707.
17. Zurflüh, M.R., Zschocke, J., Lindner, M., Feillet, F., Chery, C., Burlina, A., Stevens, R.C., Thöny, B. and Blau, N. (2008) Molecular genetics of tetrahydrobiopterin-responsive phenylalanine hydroxylase deficiency. *Hum. Mutat.*, **29**, 167–175.
18. Guldberg, P., Rey, F., Zschocke, J., Romano, V., Francois, B., Michiels, L., Ullrich, K., Hoffmann, G.F., Burgard, P., Schmidt, H. *et al.* (1998) A European multicenter study of phenylalanine hydroxylase deficiency: classification of 105 mutations and a general system for genotype-based prediction of metabolic phenotype. *Am. J. Hum. Genet.*, **63**, 71–79.
19. Karacic, I., Meili, D., Sarnavka, V., Heintz, C., Thöny, B., Ramadza, D.P., Fumic, K., Mardesic, D., Baric, I. and Blau, N. (2009) Genotype-predicted tetrahydrobiopterin (BH4)-responsiveness and molecular genetics in Croatian patients with phenylalanine hydroxylase (PAH) deficiency. *Mol. Genet. Metab.*, **97**, 165–171.
20. Blau, N. and Erlandsen, H. (2004) The metabolic and molecular bases of tetrahydrobiopterin-responsive phenylalanine hydroxylase deficiency. *Mol. Genet. Metab.*, **82**, 101–111.
21. Elsas, L.J., Greto, J. and Wierenga, A. (2010) The effect of blood phenylalanine concentration on Kuvan response in phenylketonuria. *Mol. Genet. Metab.*, **102**, 407–412.
22. Dobrowolski, S.F., Heintz, C., Miller, T., Ellingson, C., Ozer, I., Gökçay, G., Baykal, T., Thöny, B., Demirkol, M. and Blau, N. (2011) Molecular genetics and impact of residual in vitro phenylalanine hydroxylase activity on tetrahydrobiopterin responsiveness in Turkish PKU population. *Mol. Genet. Metab.*, **102**, 116–121.
23. Shiman, R. and Gray, D.W. (1980) Substrate activation of phenylalanine hydroxylase. A kinetic characterization. *J. Biol. Chem.*, **255**, 4793–4800.
24. Shiman, R., Jones, S.H. and Gray, D.W. (1990) Mechanism of phenylalanine regulation of phenylalanine hydroxylase. *J. Biol. Chem.*, **265**, 11633–11642.
25. Shiman, R., Mortimore, G.E., Schworer, C.M. and Gray, D.W. (1982) Regulation of phenylalanine hydroxylase activity by phenylalanine in vivo, in vitro, and in perfused rat liver. *J. Biol. Chem.*, **257**, 11213–11216.
26. Mitnaul, L.J. and Shiman, R. (1995) Coordinate regulation of tetrahydrobiopterin turnover and phenylalanine hydroxylase activity in rat liver cells. *Proc. Natl Acad. Sci. USA*, **92**, 885–889.
27. Gersting, S.W., Staudigl, M., Truger, M.S., Messing, D.D., Danecka, M.K., Sommerhoff, C.P., Kemter, K.F. and Muntau, A.C. (2010) Activation of phenylalanine hydroxylase induces positive cooperativity towards the enzyme's natural cofactor. *J. Biol. Chem.*, **285**, 30686–30697.
28. Blau, N., Bélanger-Quintana, A., Demirkol, M., Feillet, F., Giovannini, M., MacDonald, A., Trefz, F.K. and van Spronsen, F.J. (2009) Optimizing the use of sapropterin (BH(4)) in the management of phenylketonuria. *Mol. Genet. Metab.*, **96**, 158–163.
29. Levy, H., Burton, B., Cederbaum, S. and Scriver, C. (2007) Recommendations for evaluation of responsiveness to tetrahydrobiopterin (BH(4)) in phenylketonuria and its use in treatment. *Mol. Genet. Metab.*, **92**, 287–291.
30. Pey, A.L. and Martínez, A. (2005) The activity of wild-type and mutant phenylalanine hydroxylase and its regulation by phenylalanine and tetrahydrobiopterin at physiological and pathological concentrations: an isothermal titration calorimetry study. *Mol. Genet. Metab.*, **86**(Suppl. 1), S43–S53.
31. Copeland, R.A. (2000) *Enzymes: A Practical Introduction to Structure, Mechanism, and Data Analysis*. Wiley-VCH, New York.
32. Leandro, P., Rivera, I., Lechner, M.C., de Almeida, I.T. and Konecki, D. (2000) The V388M mutation results in a kinetic variant form of phenylalanine hydroxylase. *Mol. Genet. Metab.*, **69**, 204–212.
33. Matalon, R., Koch, R., Michals-Matalon, K., Moseley, K., Surendran, S., Tyring, S., Erlandsen, H., Gámez, A., Stevens, R.C., Romstad, A. *et al.* (2004) Biopterin responsive phenylalanine hydroxylase deficiency. *Genet. Med.*, **6**, 27–32.
34. Lindner, M., Gramer, G., Garbade, S.F. and Burgard, P. (2009) Blood phenylalanine concentrations in patients with PAH-deficient hyperphenylalaninaemia off diet without and with three different single oral doses of tetrahydrobiopterin: assessing responsiveness in a model of statistical process control. *J. Inherit. Metab. Dis.*, **32**, 514–522.
35. Nielsen, J.B., Nielsen, K.E. and Guttler, F. (2010) Tetrahydrobiopterin responsiveness after extended loading test of 12 Danish PKU patients with the Y414C mutation. *J. Inherit. Metab. Dis.*, **33**, 9–16.
36. Leuzzi, V., Carducci, C., Chiarotti, F., Artiola, C., Giovanniello, T. and Antonozzi, I. (2006) The spectrum of phenylalanine variations under tetrahydrobiopterin load in subjects affected by phenylalanine hydroxylase deficiency. *J. Inherit. Metab. Dis.*, **29**, 38–46.
37. Feillet, F., Chery, C., Namour, F., Kimmoun, A., Favre, E., Lorentz, E., Battaglia-Hsu, S.F. and Gueant, J.L. (2008) Evaluation of neonatal BH4 loading test in neonates screened for hyperphenylalaninemia. *Early Hum. Dev.*, **84**, 561–567.
38. Martínez, A., Knappskog, P.M., Olafsdottir, S., Døskeland, A.P., Eiken, H.G., Svebak, R.M., Bozzini, M., Apold, J. and Flatmark, T. (1995) Expression of recombinant human phenylalanine hydroxylase as fusion protein in *Escherichia coli* circumvents proteolytic degradation by host cell proteases. Isolation and characterization of the wild-type enzyme. *Biochem. J.*, **306**, 589–597.
39. Lagler, F.B., Gersting, S.W., Zsifkovits, C., Steinbacher, A., Eichinger, A., Danecka, M.K., Staudigl, M., Fingerhut, R., Glossmann, H. and Muntau, A.C. (2010) New insights into tetrahydrobiopterin pharmacodynamics from Pah(enu1/2), a mouse model for compound heterozygous tetrahydrobiopterin-responsive phenylalanine hydroxylase deficiency. *Biochem. Pharmacol.*, **80**, 1563–1571.
40. Pérez-Duenas, B., Vilaseca, M.A., Mas, A., Lambruschini, N., Artuch, R., Gómez, L., Pineda, J., Gutiérrez, A., Mila, M. and Campistol, J. (2004) Tetrahydrobiopterin responsiveness in patients with phenylketonuria. *Clin. Biochem.*, **37**, 1083–1090.
41. Blau, N. (2008) Defining tetrahydrobiopterin (BH4)-responsiveness in PKU. *J. Inherit. Metab. Dis.*, **31**, 2–3.
42. Knappskog, P.M., Eiken, H.G., Martínez, A., Bruland, O., Apold, J. and Flatmark, T. (1996) PKU mutation (D143G) associated with an apparent high residual enzyme activity: expression of a kinetic variant form of phenylalanine hydroxylase in three different systems. *Hum. Mutat.*, **8**, 236–246.
43. Treacy, E.P., Delente, J.J., Elkas, G., Carter, K., Lambert, M., Waters, P.J. and Scriver, C.R. (1997) Analysis of phenylalanine hydroxylase genotypes and hyperphenylalaninemia phenotypes using L-[1-<sup>13</sup>C]phenylalanine oxidation rates in vivo: a pilot study. *Pediatr. Res.*, **42**, 430–435.

## 9. Danksagung

An dieser Stelle möchte ich mich bei einigen sehr wichtigen Menschen bedanken, die mich während des Studiums und während meiner Promotionsarbeit stets unterstützt haben und ohne deren Hilfe diese Promotion nicht zustande gekommen wäre.

Zunächst möchte ich mich bei meiner Doktormutter und Mentorin Frau Professor Dr. med. Ania C. Muntau für eine unglaublich lehrreiche Zeit bedanken. Natürlich danke ich ihr für zahlreiche, zeitintensive Diskussionen über Ergebnisse, Daten und Grafiken, die im Rahmen dieser Arbeit entstanden sind. Ich möchte mich auch dafür bedanken, die Möglichkeit erhalten zu haben, meine Arbeit auf internationalen Kongressen präsentieren zu dürfen und Kontakte mit international anerkannten Kollegen auf dem Gebiet der Stoffwechselmedizin knüpfen zu können. Zusätzlich wurde ich stets im Rahmen meiner klinischen Tätigkeit als Arzt unterstützt und gefördert. Am wichtigsten erscheint mir jedoch die Tatsache, von Frau Professor Dr. med. Ania C. Muntau gelernt zu haben, was es bedeutet naturwissenschaftliche Forschung auf hohem Niveau zu betreiben, mit dem Ziel, die gewonnenen Erkenntnisse für Patienten und zukünftige Therapiemöglichkeiten anzuwenden.

Während der Promotion wurde ich außerdem immer durch meinen Betreuer und Freund Dr. med. Søren W. Gersting unterstützt. Seine aufopferungsvolle Hingabe Doktoranden in unserer Arbeitsgruppe zu leiten und zu fördern war beispielhaft. Dank seiner Unterstützung wurden Methoden entwickelt, Daten diskutiert, Vorträge gemeistert und zahlreiche Publikationen geschrieben.

Natürlich möchte ich mich bei allen Mitarbeitern der Arbeitsgruppe für Molekulare Pädiatrie bedanken. In den letzten Jahren ergaben sich immer wieder Möglichkeiten des Wissensaustausches zwischen Chemikern, Biologen, technischen Assistenten und Medizinerinnen. Gleichzeitig wurden langjährige Freundschaften geschlossen. Ein besonderes Dankeschön gilt dabei Dunja Reiß, Marta Danecka, Amelie Lotz, Mathias Woidy, Kristina Kemter, Doris Bruer, Anja Schultze, Heike Preisler, Anna Heckel-Pompey und Christoph Siegl.

Außerdem möchte ich mich bei Prof. Dr. med. Christian Sommerhoff für seine Ideen und wichtige Diskussionen zu Enzymatik und Methodenentwicklung bedanken.

Diese Arbeit wäre auch nie ohne die vielseitige Unterstützung und der Geduld meiner Eltern Rudolf und Brigitte Staudigl entstanden. Sie gaben mir immer die Möglichkeit meinen Wünschen, Vorstellungen und Träumen nachzugehen. Bei meinen beiden Schwestern Bettina und Andrea sowie ihren beiden Ehemännern John Hunter und Alexander möchte ich mich ebenfalls bedanken. Trotz meiner sporadischen Anwesenheit und Wortmeldungen unterstützten sie mich in meinem Werdegang und waren bereit sich zahlreiche Geschichten über Qualen und Freuden der naturwissenschaftlichen Forschung anzuhören.

Hiermit möchte ich mich auch bei meiner Lebensgefährtin Christine Wagner bedanken. Ihre ausdauernde Liebe, Unterstützung, Verständnis und Akzeptanz für meine Arbeit haben diese Promotion und den Beginn meiner klinischen Tätigkeit erst ermöglicht.

Nicht zuletzt möchte ich mich bei meinen Freunden bedanken, die, obwohl ich sie gerade wegen meiner Arbeit häufig vernachlässigt habe stets zu mir gestanden haben und für die erforderliche Abwechslung sorgten. Dadurch haben sie mir immer wieder die Kraft gegeben haben meine Arbeit mit der gleichen Begeisterung fortzusetzen.

## 10. Lebenslauf

### Michael Staudigl

Kurfürstenstr. 20  
80801 München  
Tel.: 089/35894756  
Mobil: 0177/3306794  
E-mail: Michael.Staudigl@med.uni-muenchen.de

### Zur Person

---

Geburtsdatum	19.03.1980
Geburtsort	München
Familienstand	ledig
Staatsangehörigkeit	deutsch

### Ausbildung und berufliche Laufbahn

---

seit 2010	Ausbildung zum Facharzt für Pädiatrie sowie Spezialisierung auf dem Gebiet der pädiatrischen Stoffwechselmedizin unter der Leitung von Frau Prof. Dr. A. C. Muntau im Dr. von Haunerschen Kinderspital der Ludwig-Maximilians-Universität (LMU), München
2007-2010	Wissenschaftlicher Mitarbeiter in der Abteilung für Molekulare Pädiatrie am Dr. von Haunerschen Kinderspital der LMU München (Prof. Dr. A. C. Muntau)  Betreuung medizinischer Doktoranden und biologischer Diplomanden  Befundung der Mutationsanalyse bei Verdacht auf Phenylketonurie
2007	Approbation als Arzt
2006 – 2007	Praktisches Jahr: 1. Terial: Innere Medizin an der Harvard Medical School in Boston, USA 2. Terial: Chirurgie in der Chirurgischen Klinik Innenstadt, LMU, München 3. Terial: Pädiatrie am Dr. von Haunerschen Kinderspital, LMU, München
2000 – 2007	Studium der Humanmedizin an der LMU, München
1999	Abitur am Aventinus-Gymnasium, Burghausen
1993 – 1999	Aventinus-Gymnasium, Burghausen
1989 – 1993	Middle School an der Oregon Episcopal School, Portland, Oregon, USA
1986 – 1989	Grundschule, Emmerting

## Stipendien und Auszeichnungen

---

2010	Auszeichnung für Best Oral Presentation in Basic Research, 2 <sup>nd</sup> Phenylketonuria Group (EPG) Symposium, „Advances and Challenges in PKU“, München
2008	<i>Travel Scholarship</i> der <i>Society for the Study of Inborn Errors of Metabolism</i> , Lisboa 2008
März bis August 2006	Stipendiat der <i>Munich-Harvard Alliance</i> an der <i>Harvard Medical School</i> in Boston, USA

## Lehrtätigkeit

---

seit 2008	Mentor im MeCuM-Mentor-Programm für Studierende
seit 2007	Tutor im Vorbereitungskurs der PJ-Stipendiaten der <i>Munich-Harvard Alliance</i> an der LMU in München, Deutschland
2006	Mitentwicklung des Konzeptes „Skills Lab“: Zentrum für Unterricht und Studium (ZeUS) an der LMU in München, Deutschland in Zusammenarbeit mit der <i>Harvard Medical School</i> in Boston, USA